Synthesis of cyclic azobenzene analogues for incorporation into oligonucleotides, peptides and polymers

DHRUVAL KUMAR JOSHI

Department of Chemistry

A thesis submitted to the Department of Chemistry

in partial fulfillment of the requirements for the degree of

Master of Science

Faculty of Mathematics and Science, Brock University

St. Catharines, Ontario

October, 2013

Abstract

(A) In recent years, considerable amount of effort has contributed towards enhancing our understanding of the new photoswitch, cyclic azobenzene, particularly from the theoretical point of view. However, the challenging part with this system was poor efficiency of its synthesis from 2,2'- dinitrodibenzyl and lack of effective methods for further modification which would be useful to incorporate this system into biomolecules as a photoswitch. We report the synthesis of cyclic azobenzene and analogues from 2,2'-dinitrodibenzyl, which would allow for further incorporation of this cyclic azobenzene into biomolecules. Reaction of 2,2'-dinitrodibenzyl with zinc metal powder in the presence of triethylammonium formate buffer (pH-9.5) gave a cyclic azoxybenzene, 11,12-dihydrodibenzo[c,g][1,2]diazocine-5-oxide. The latter compound was converted into cyclic azobenzene analogues (bromo-, chloro-, cyano-, and carboxyl) through subsequent transformations. The carboxylic acid analogue was reacted with D-threoninol to give the corresponding amide, which readily undergoes photo-isomerization upon illumination with light. Upon illumination with light at 400 nm, approximately 70% of *cis*- isomer of amide was isomerized to *trans*- isomer. It was observed that *cis*- to *trans*- isomerization reached the maximum steady state of light transmission after approximately 40 min, whereas the *trans*- to *cis*- isomerization approximately acquired in 2 h to regain full recovery of light transmission. Cyclic azobenzene phosphoramidite was synthesized from DMT-protected D-threoninol linked cyclic azobenzene.

(B) In recent years, there has been considerable interest invested towards the synthesis of azobenzene analogues for incorporation into proteins. Among the many azobenzene analogues, the synthesis of bi-functional cyclic azobenzene analogues for the incorporation into proteins is relatively new. In this thesis, we report the synthesis of a cyclic azobenzene biscarboxylic acid from 4-(bromomethyl)benzonitrile.

(C) Azobenzene has been widely used in the field of polymer science to study the surface morphology and surface properties of polymers. In this thesis, we report the incorporation of cyclic azobenzene into a commercial polymer 2-(hydroxyethyl)methacrylate. Samples collected after 24 h from the reaction solution showed approximately 9% of incorporation of cyclic azobenzene into polymer compared to samples collected after 10 h, which showed approximately 6% incorporation.

Acknowledgements

I would like to acknowledge the following members whose advice and guidance have made this possible. First and foremost I would like to thank my supervisor and mentor Professor Tony Yan for his guidance and supervision throughout my graduate studies. He treated me with great patience and his words of encouragement and support has truly changed me as a student and as a researcher. I could not have imagined having a better mentor and supervisor for my graduation study.

I would also like to thank my supervisory committee members, Professor Atkinson and Professor Heather Gordon for their valuable discussions and advice throughout the years. Their insight and suggestions during our progress meetings allowed me to view my strategies and objectives in a different prospective. I would like to thank Professor Christopher Wilds, Concordia University, Quebec, Canada for accepting to be my external examiner.

I would like to extend my humble gratitude to my fellow labmates: Ningzhang Zhou, Qiang Wang, Jia Li, Viola, Ravi, Nazanin, Christopher, Emily, Ben, Rameez, and Sukhmani, and Parthajit for their friendship and support. My sincere thanks to Tim Jones and Razvan Simionesu for their assistance in collecting data for mass spectrometry and NMR spectroscopy.

Lastly, I would like to thank the Natural Sciences and Engineering Research Council of Canada for funding this work and Research Cooperation.

Table of contents

Chapter 1-Nucleic Acids and Photoresponsive Molecules

Chapter 2- Photoisomerization and Synthesis of Azobenzenes

List of Figures

List of Schemes

List of Abbreviations

A	adenine
AcOH	acetic acid
AcONa	sodium acetate
Ac_2O	acetic anhydride
Al	aluminium
$AlCl_3$	aluminium chloride
$AlBr_3$	aluminium bromide
$B(OH)_3$	boric acid
Br_2	bromine
C	cytosine
CS_2	carbon disulfide
CuBr	copper bromide
$CuSO_4$	copper sulphate
CH_2Cl_2	methylene chloride
$CHCl_3$	chloroform
CuCN	copper cyanide
DMF	dimethylformamide

DMT-Cl	dimethoxytrityl chloride
d	doublet
D	dextrorotatory
DNA	deoxyribose nucleic acid
EtOH	ethanol
EI	electro impact
FRET	Förster resonance energy transfer
g	gram
G	guanine
h	hour
HPLC	high performance liquid chromatograpy
HCl	hydrochloric acid
Hz	Hertz
HgO	mercuric oxide
HBr	hydrogen bromide
H_2O_2	hydrogen peroxide
H_2SO_4	sulfuric acid
HR-MS	high resolution mass spectroscopy

Kcal	kilocalories
$KMnSO_4$	potassium permanganate
KNO_3	potassium nitrate
KOH	potassium hydroxide
LED	liquid emitting diode
Li	lithium
L	levorotatory
mg	milligram
ml	millilitre
mM	millimolar
$MnCl_2$	manganese chloride
MHz	mega Hertz
$MgSO_4$	magnesium sulfate
M.P.	Melting point
MeCN	acetonitrile
mRNA	messenger ribonucleic acid
min	minute
M	molar

mol	moles
MnO_2	manganese dioxide
MeOH	methanol
$MoCl_2O_2$	molybdenum dioxo dichloride
NH_2NH_2	hydrazine
NMR	nuclear magnetic resonance
NaOH	sodium hydroxide
$NiCl_2$	nickel chloride
nm	nanometer
n-	non-bonding
OH	hydroxyl
o-	ortho
OMe	methoxy
ODN	oligo deoxynucleotide
PCl_3	phosphorus chloride
Ph	phenyl
$Py^+ Br_3^-$	pyridinium tribromide
PPh_3	triphenylphosphine

Pd/C	palladium on carbon
Py	pyridine
Pb	lead
R_f	retention factor
RNA	ribonucleic acid
r.t.	room temperature
siRNA	short interfering ribonucleic acid
ssDNA	single stranded deoxyribose nucleic acid
t	triplet
T	thymine
TMG	tetra methyl guanidine
t-BuOCl	*tert*-butyl hypochloridite
THF	tetrahydrofuran
tBuOK	potassium *tert*-butoxide
$TiCl_3$	titanium trichloride
UV-Vis	ultraviolet-visible
Zn	zinc
Å	Angstrom

α	alpha
β	beta
λ	lambda
π	pi bonding
π^*	pi anti-bonding
$^\circ C$	degrees in Celsius

CHAPTER 1- Nucleic acids and photoresponsive molecules

1.1 Introduction to nucleic acids

Nucleic acids, first discovered by Friedrich Miescher in 1869,[1, 2] are high molecular weight biopolymers essential for all known forms of life. Nucleic acids are composed of mainly three components, a nucleobase (purine and pyrimidine), a sugar unit (pentose sugar), and a phosphate group (Figure 1).

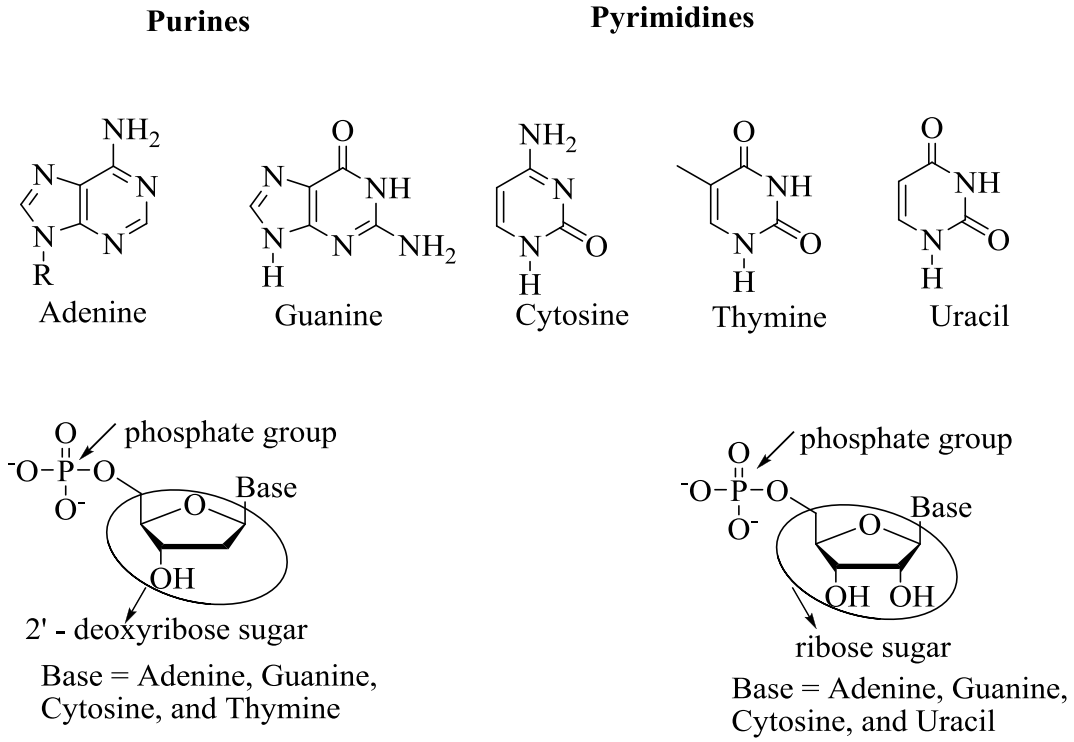

Figure 1. Structures of purine and pyrimidines and sugar-phosphate group in nucleic acids.

Adenine and guanine form the purines whereas cytosine and thymine form the pyrimidines in DNA. The nucleobase and a sugar (2′-deoxyribose or ribose sugar) moiety together form a nucleoside.

A nucleotide is formed if a phosphate group is attached to the 5′-OH of the sugar. Nucleotides are connected through phosphodiester linkages between 5′-OH and 3′-OH on two adjacent nucleosides, which essentially form the backbone of the nucleic acids (Figure 2). Two basic kinds of nucleic acids are deoxyribonucleic acid (DNA) and ribonucleic acid (RNA). DNA and RNA are made up of deoxyribose and ribose sugar, respectively. In addition, thymine in DNA is replaced with uracil in RNA; uracil lacks a methyl group on its heterocyclic ring.

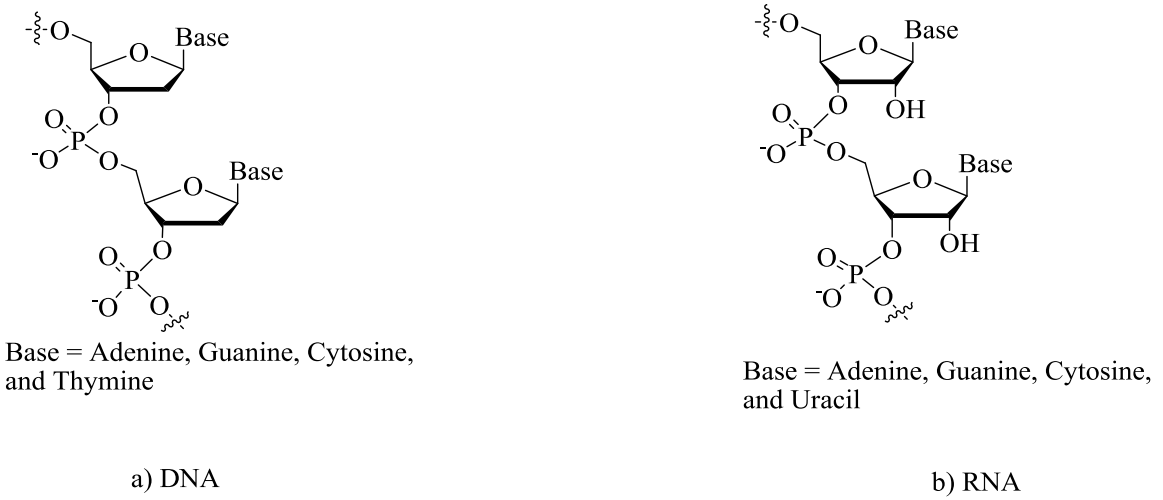

Figure 2. Chemical structures of a) DNA and b) RNA.

Nucleic acids are involved in encoding, transfer, and expression of genetic information via replication, transcription and translation. The DNA acts as repository of genetic information which is transcribed into RNA.[3] The encoded genetic information from RNA is then used to guide protein synthesis through a process known as translation.[4]

The order of the specific sequence in which the four DNA nucleobases are connected constitutes the genetic information, the blueprint for the construction of the essential building blocks of life, proteins.

In nature, most DNA molecules are double stranded, and RNAs are single-stranded. DNA duplexes consist of two anti-parallel strands brought together by base pairing as a result of hydrogen bonding. It follows that, in the canonical Watson-Crick base pairing, guanine forms three sets of hydrogen bonds with cytosine and adenine forms two sets of hydrogen bonds with thymine (Figure 3).

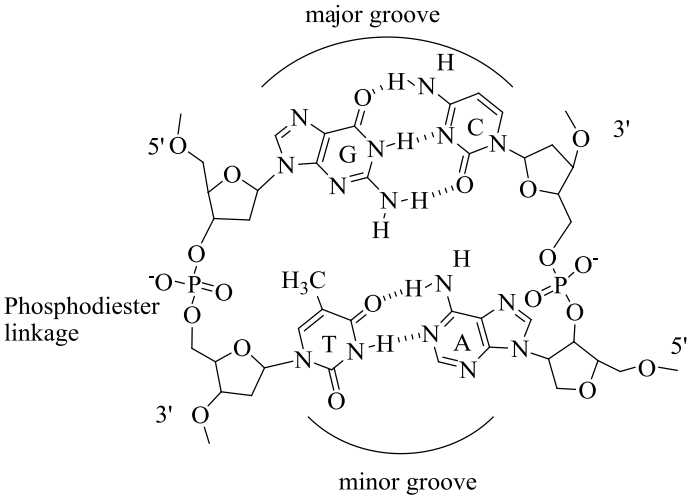

Figure 3. Base-pairing pattern in DNA.

In DNA duplexes, the two strands run antiparallel to each other, i.e., one strand runs in 5′-3′ direction whereas the other strand runs in 3′-5′ direction (Figure 3). One of the strands in the DNA duplex acts as the template strand, while the other acts as the replicating strand. The replicating strand is self-duplicated using the template strand in the DNA duplex. DNA can exist in three different conformations, A-, B-, and Z-forms, of which B-DNA is the most common form. In this form, the phosphodiester backbone of DNA is twisted around its longitudinal axis to form a right-handed double helix with a hydrophilic backbone of alternating 2′-deoxyribose groups and negatively charged phosphate groups situated on the outer part of the helix.

Two distinct grooves are formed and run along the side of the helix. The major groove is wide and deep, while the minor groove is narrow and deep.

The DNA duplex is 22 to 26 Å wide and the rise per nucleotide residue is approximately 3.3 Å in B-DNA.[5] In chromosomes, DNA is packed into coiled structures. These chromosomes are replicated in a process called DNA replication. In eukaryotic organisms (animals, plants, fungi, and protists), DNA is stored inside the cell nucleus. In contrast, prokaryotes store their DNA in the cytoplasm.[6]

All the necessary information required for the development of an organism (prokaryotes and eukaryotes) throughout life is encoded in DNA, although, in some viruses, RNA stores genetic information. Therefore study of biological processes, such as hybridization, transcription, and translation will provide insight on biochemical roles of nucleic acids. In addition, studying the interactions of DNA with proteins will confer more insight into various biomolecular functions such as gene expression, replication and repair mechanisms.

1.2 Photoregulation of functions of biomolecules

Recently, much attention has been focused on understanding the etiology and pathophysiology of various diseases such as Alzheimer's disease, as well as the involvement of molecules in over- and under- expression of proteins and genes.

There has been a great amount of work over the past two decades in artificially controlling gene expression and protein functions. Functional regulation of various biomolecules, such as DNA, RNA, proteins, and enzymes, has been achieved by different methods such as small molecules, gene therapy, antisense oligonucleotides, and small interfering RNA (siRNA).

The above methods are effective but often lack selectivity as well as spatio-temporal control. One approach to achieve selectivity and spatio-temporal control is by regulating a particular cellular function by placing the system of interest under the control of internal or external stimuli. For nucleic acids, external stimuli such as light could play very crucial roles in regulating the functions of nucleic acids. This approach can provide insight into the mechanisms vital for DNA recognition and DNA-mediated bioprocess.

Light works best as an external stimulus and has several advantages over other external stimuli such as heat: 1) no contamination from light to the reaction system, 2) control of excitation wavelength can be achieved through the design of photoresponsive molecules, and 3) ease of controlling irradiation time and local excitation.[7] Indeed light has been used clinically, for example, in treating patients or blood samples from patients suffering with cutaneous T-cell lymphoma, where 8-methoxypsoralen (8-MOP) in combination with UV-A irradiation was used as a treatment therapy.[8]

There are various examples of naturally occurring light-dependent and light-responsive molecules, for example phototropins, a class of light-activated kinases which upon photoactivation converts the noncovalent protein-flavin mononucleotide (FMN) complex into a covalent protein-FMN adduct within the Per-Arnt-Sim (PAS) domain.[9] As another example, photolyases are involved in the repair mechanism of UV-induced DNA lesions in the genome of various organisms such as *Escherichia coli, Bacillus firmus, and Saccharomyces cerevisae*.[10]

1.3 Irreversible photoregulation of functions of biomolecules

Photoregulation of DNA properties is usually achieved by covalently attaching a photoresponsive molecule to the DNA. Photosensitive molecules, such as caged molecules (irreversible photocontrol), and photoswitchable molecules, such as azobenzene, spiropyrans, and diarylarenes (reversible photocontrol), have been employed as tools to regulate the functions of various biomacromolecules such as DNA, RNA, and proteins.

1.3.1 Caged photosensitive molecules

Caged molecules are particularly widely used in photo-control of nucleic acids. J.F. Hoffman was the first person to coin the term "caging" in 1978.[11] Among the classes of other photosensitive or photocleavable molecules, the class of caged molecules emerges as one of the most compelling approaches in achieving spatio-temporal control with light as a conditional trigger. Caged molecules are photolabile, and are irreversibly cleaved with light, releasing the functional molecule.[12] In 1971 Martinek *et al*. performed a series of studies on peptidase *α*-chymotrypsin (CT).[13] Reaction of CT **2** with *cis*-cinnamoyl imidazole **1** resulted in *cis*-acylated product **3** (Scheme 1). *α*-Chymotrypsin was temporarily deactivated by the formation of *cis*-cinnamoylated adduct and this effect persisted for several hours in dark. Upon irradiation with light, the *cis*-product isomerises to *trans*-adduct **5**, regenerating the active enzyme **2**, thereby cleaving the substrate, tyrosine ester to tyrosine which is then converted to melanin by the enzyme tyrosinase. Since only *trans*- product is cleaved by the enzyme, the *cis*-cinnamoyl product could be called caged.[13]

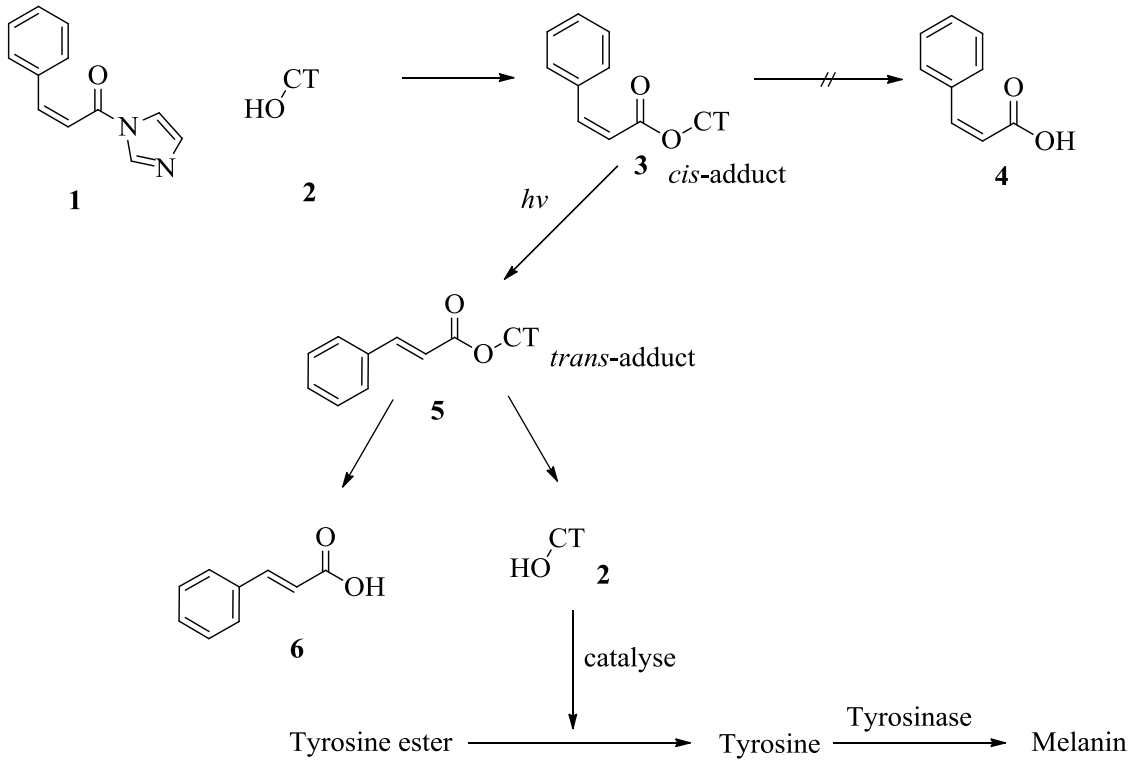

Scheme 1. Photoreaction of peptidase α-chymotrypsin.[13]

Engels and his group synthesized caged cyclic adenosine monophosphate **7** (cAMP, Scheme 2) to investigate the triester's reactivity towards photolysis in the presence of a photolabile group (*o*-nitrobenzyl group) blocking the terminal phosphate group in cAMP.[14] The caged cAMP showed lower affinity towards protein kinase degradation (protein kinase converts cAMP to ADP), however, upon photoirradiation at 366 nm, release of *o*-nitrobenzyl group due to photolysis transforms caged cAMP into active cAMP with high affinity for protein kinase. The rate of production of cAMP upon photolysis of caged cAMP was estimated by liquid chromatography through the hydrolysis of the triester. A good separation between cAMP and open-chain alkyl esters was obtained.

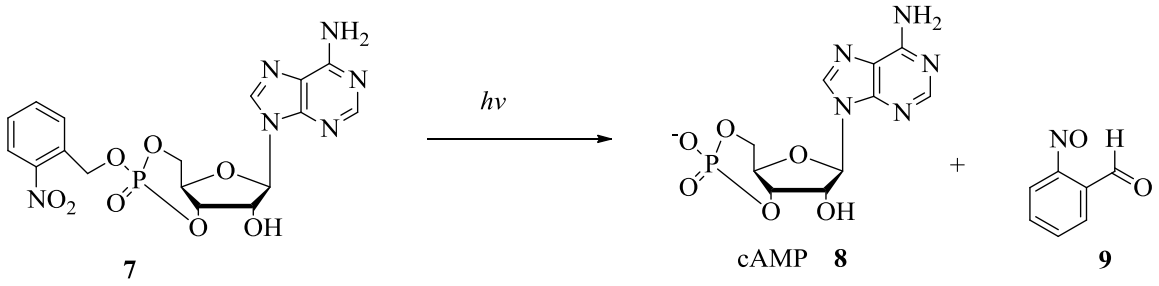

7 cAMP **8** **9**

Scheme 2. Light-responsive cAMP derivative.[14]

In 1978, Hoffman *et al*. synthesized the first, caged adenosine triphosphate derivative **10** in which the terminal phosphate (Scheme 3) was masked with a photolabile *o*-nitrobenzyl group.[11] The caged ATP **10**, upon irradiation at 340 nm, underwent photolysis, releasing adenosine 5'-triphosphate **11**. Prior to irradiation, the caged ATP was found to be neither a substrate nor an inhibitor of purified renal Na, K-ATPase. Upon illumination at 340 nm, 70% of ATP was liberated in 30 s, which was readily hydrolysed to adenosine diphosphate (ADP) and a phosphate group (Pi) by Na, K-ATPase. Rapid release of ATP upon photolysis from stable precursor renders caged ATP as a stable source of ATP resistant to intracellular ATPases until the ATP is released following photolytic irradiation.[11]

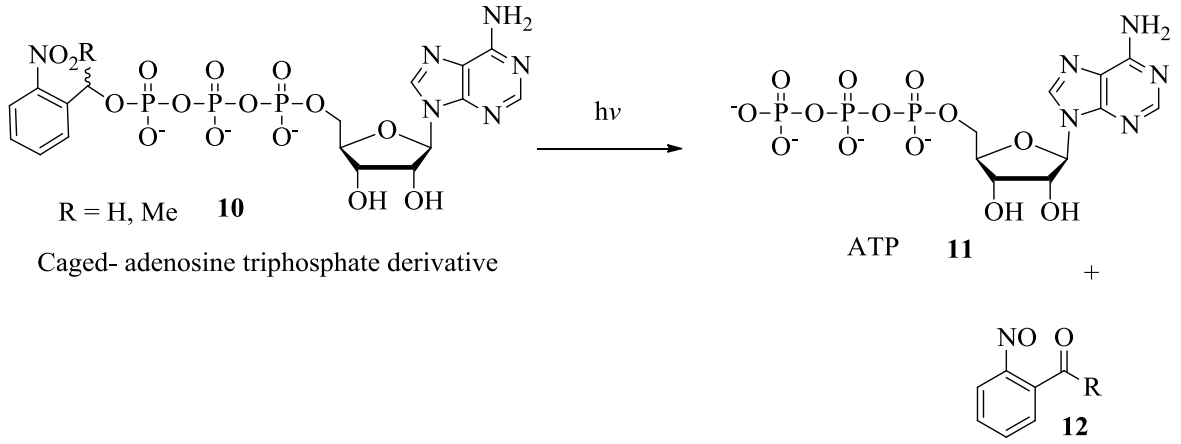

Scheme 3. The first light-responsive molecule **10** to be called caged.[11]

A number of caging chemistries have been used in photoregulation of nucleic acids. Among these caging groups, *o*-nitrobenzyl group (ONB **13**, R = H, Figure 4) and its derivatives are mostly preferred. ONB is one of the most widely explored protecting groups in solid phase reactions as a photocleavable linker.[15] Despite its wide application as a photolabile group, the use in living systems as a caging group is hampered due to the formation of a nitrosoaldehyde byproduct of ONB, which is found to be harmful to the body.[16, 17]

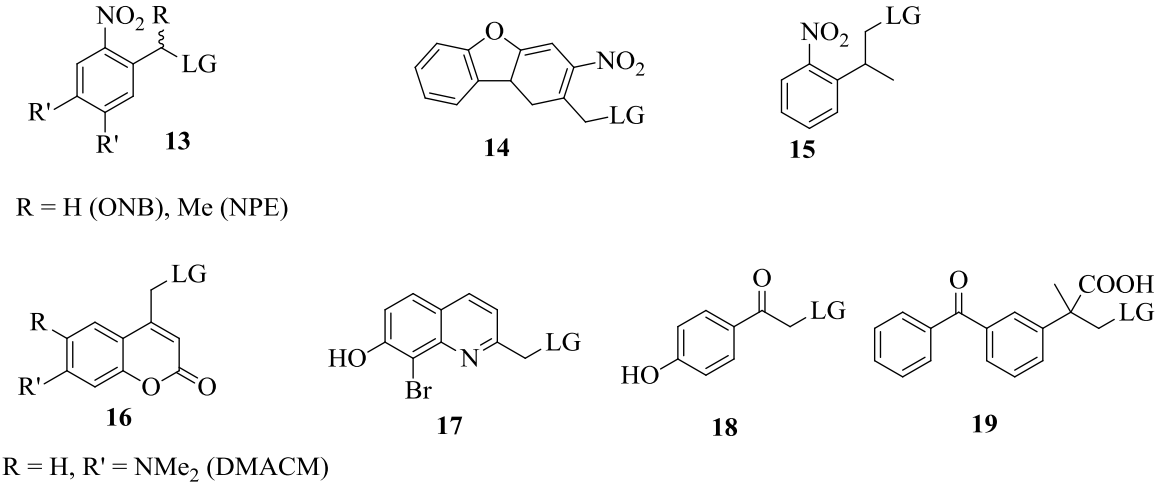

Figure 4. List of photo-labile molecules used as caging groups. (LG= leaving group, carbonate or carbamate linker).[15, 18-24]

Figure 4 shows examples of photolabile groups, such as nitrophenylethyl (NPE) **13** (R = Me),[18] nitrodibenzofurane chromophore **14**,[19] 2-(2-nitrophenyl) propyl (NPP, less harmful nitrostyryl species) **15**,[20] coumarin derivative in [7-(dimethylamino) coumarin-4-yl] methyl (DMACM) **16**,[21] 8-bromo-7-hydroxyquinoline (BHQ) **17**,[22] *p*-hydroxyphenacyl (pHP) **18**,[23] and ketoprofen **19**.[24] These caging groups have been employed in several studies, to regulate the functions of nucleic acids and gene expression.[15]

1.3.1.1 Regulation of second messenger and nucleotide cofactor functions by caged molecules

Naturally occurring cyclic nucleotides such as cAMP and cGMP (cyclic guanine monophosphate) are secondary messengers involved in crucial roles, relaying signals from the receptors found on the surface of various cells to the target site inside the cell, such as the nucleus.[7] In addition, cCMP (cyclic cytidine monophosphate) is involved in eukaryotic

messaging, whereas the role of cyclic uridine monophosphate (cUMP) is still not clear. cAMP was found to play an important role in regulating the turning of growth cones,[25(i)] which are the terminal portions of elongating neurons involved in the rearrangement of the cytoskeleton. It is observed that the function of growth cones is sensitive to the cytoplasmic gradient of cAMP. Therefore, by controlling the cytoplasmic gradient of cAMP, turning of growth cones can be controlled. In this cascade process, netrin-1 acts as first signalling messenger.[25 (ii)] A recent study by Harz *et al*. showed that controlled release of caged cAMP in the cytoplasm using light resulted in spatio-temporal effects on turning of growth cones in chick sensory neurons.[25 (i)]

Scott *et al*. used two caged cGMP derivatives (NPE-caged cGMP **20** and water soluble cGMP **21**, Figure 5) to regulate the inward current in cultured dorsal root ganglion (DRG) neurons in rat.[26] The study showed that, in about 12.5% of DRG neurons, rapid activating inward currents were aroused due to the activity of cGMP gated channels. In contrast, 52% of DRG neurons showed delayed Ca^{2+} dependent inward current through induction of cADP-ribose and mobilization of calcium from intracellular stores, due to intracellular release of cGMP. Both caged derivatives exhibited delayed inward currents but rapid activating inward current was elicited only by NPE-caged cGMP. Therefore this work suggested that cGMP is involved in distinct mechanisms to activate inward currents in DRG neurons.

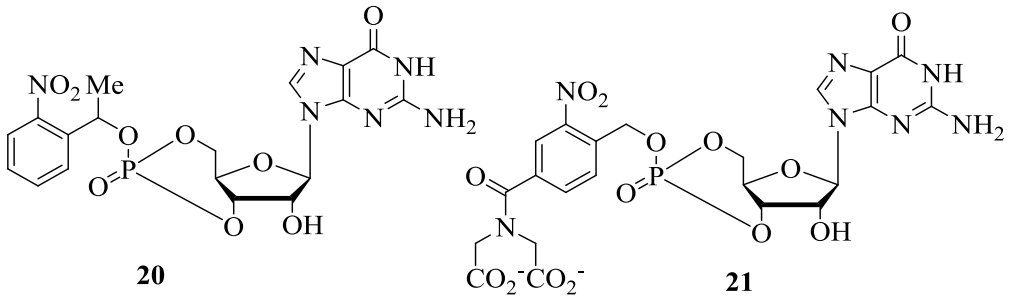

Figure 5. Structures of NPE-caged cGMP **20** and the structure of water soluble-caged cGMP **21**.

Cyclic nucleotide monophosphate (cNMP) was caged by coumarin-based photolabile protecting groups and water-soluble derivatives of nitrobenzyl-derived caging groups **22** (Figure 6) by Hagen's group.[21, 27] The advantage of these groups is that they allow for fast and efficient deprotection and release of cNMPs upon exposure to light. Since the coumarin that is released upon deprotection is fluorescent, it helps in detection of percentage of deprotection by fluorescence monitoring.

Nucleotide cofactors, such as nucleotide adenine diphosphate (NADP), were also caged to regulate the activity of the enzyme NAD glycohydrolase transglycosidase.[28, 29] A study performed by Salerno *et al.*[28, 29] showed that sterically hindered groups on caged NADP play a crucial role in directing the enzymatic transglycosidation of substrate NADP.

Caged guanosine triphosphate (cGTP) **23** and caged cytidine-5'-diphosphate (cCDP) **24** were synthesised (Figure 6).[30] cGTP was used to investigate the mechanism of Ras GTPase. Ras is a guanine nucleotide binding protein that plays a central role in the transduction of growth signals from plasma membrane. It acts as a switch cycling between an active GTP-bound and an inactive GDP-bound form. In the GTP-bound form, Ras interacts with its effector Raf.[30] Binding of the effector Raf activates a kinase cascade process, which transduces the external signal to the

nucleus via a series of phosphorylation reactions. The effector binding is terminated by hydrolysis of protein-bound GTP to GDP. Therefore, the Ras GTPase cascade reaction is controlled by regulating the interaction of Ras with GTP by employing caged guanosine triphosphate. The unphotolysed cGTP showed no interaction with Ras protein. However upon irradiation, cleavage of photosensitive group releases the active GTP which then interacts with Ras protein to initiate the cascade reaction.[30]

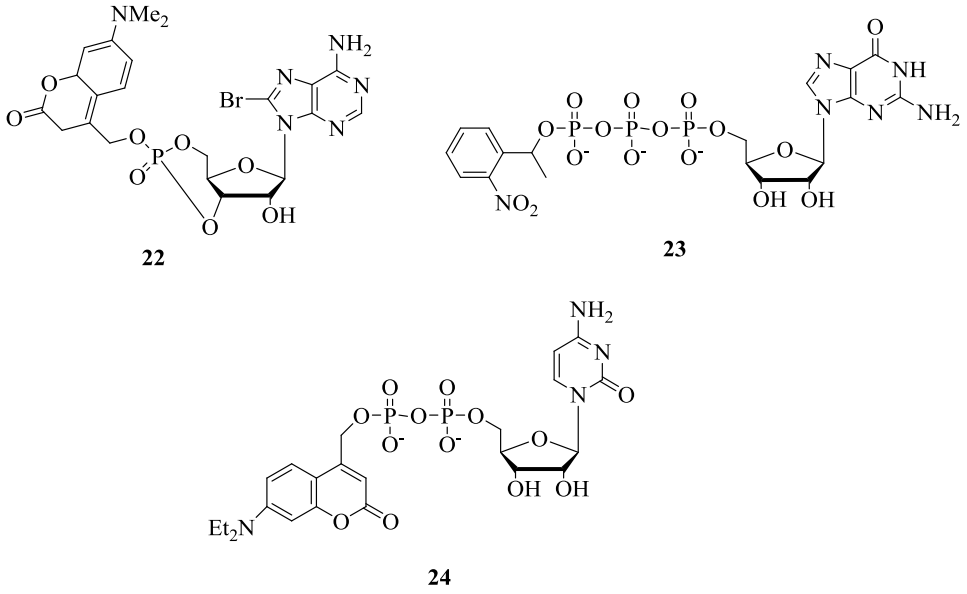

Figure 6. Structures of caged cNMP-**22**,[21, 27] cGTP **23**,[30] and cCDP **24**.[31]

1.3.1.2 Regulation of ribonuclease activities by caged molecules

Ribonuclease A (RNase A) is an enzyme involved in hydrolytic cleavage of RNA.[32, 33] However, another enzyme from the protease family called subtilisin cleaves a peptide bond of RNase A to give RNase S.[32, 33] The latter ribonuclease comprises two fragments, which are tightly associated together: S-peptide (1-20 amino acids) and S-protein (21-124 amino acids).[32, 33] RNase S possesses similar enzymatic activity to that of RNase A.

Hamachi *et al*. [33] developed caged ribonucleases by replacing the key amino acids in the α-helix region of RNase S with corresponding amino acids with a photolabile *o*-nitrobenzyl moiety (caged lysine **25**, glutamic acid **26**, aspartate **27**, and glutamine **28**, Figure 7a).[33] By incorporating photolabile groups at specific locations on RNase S, the RNase S activity was suppressed before irradiation. From the study it was observed that positions Q11 and D14 (Figure 7) were found to be suitable positions for effective caging and suppressing the RNase S activity. However the RNase S activity was restored after irradiation.[32, 33]

a)

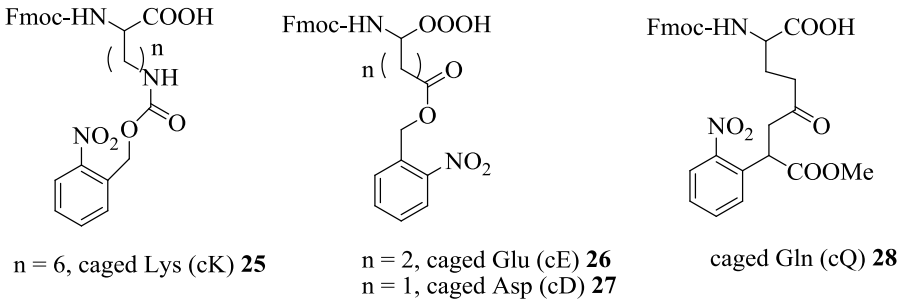

n = 6, caged Lys (cK) **25**

n = 2, caged Glu (cE) **26**
n = 1, caged Asp (cD) **27**

caged Gln (cQ) **28**

b)

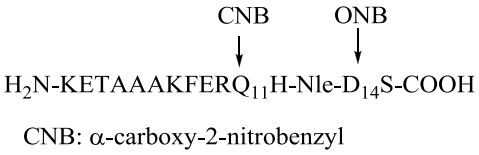

CNB: α-carboxy-2-nitrobenzyl

Figure 7. a) Structures of caged- lysine, glumatic acid, aspartate and glutamine. b) Sequence of caged peptide with amino acids bearing caging groups.[33]

Recently, Wu *et al.*[34] reported synthesis of three 20-mer caged circular antisense oligonucleotides (R20, R20B2 and R20B4) with a photocleavable linker [1-(*o*-nitrophenyl)-2-dimethoxytrityloxy]ethoxy-*N*,*N*-diisopropylamino-2-cyanoethoxyphosphine **29** and an amide linker between the 10-mer oligodeoxynucleotides (Figure 8). Photo-regulation of RNA-binding affinity and ribonuclease H activity were studied with these caged circular antisense oligonucleotides. *In vitro* studies showed that, upon light irradiation, the rate of RNA cleavage is greatly enhanced by up to ~ 43-, 25- and 15- fold for R20, R20B2 and R20B4, respectively. The presence of linker in R20, and 2- or 4- nt (nucleotides) gaps in R20B2 and in R20B4 affected their binding efficiency to the target RNA. The authors[34] also synthesized three more caged circular oligonucleotides (PS1, PS2 and PS3) with 2'-OMe modifications to target green fluorescent protein (GFP) expression. Photo-modulation of target RNA hybridization and regulation of GFP gene expression in cells were successfully achieved with PS1, PS2 and PS3 upon light activation. The caged circular antisense oligonucleotides employed in the study showed promising photo-modulation of gene expression through both ribonucleases H and non-enzyme involved antisense strategies.

a)

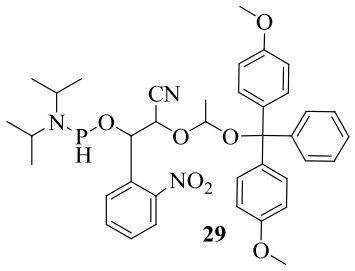

[1-(*o*-nitrophenyl)-2-dimethoxytrityloxyl] ethoxy-*N*.*N*-diisopropyl amino-2-cyanoethoxyphosphine

b)

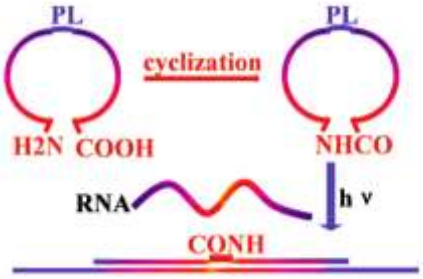

c)

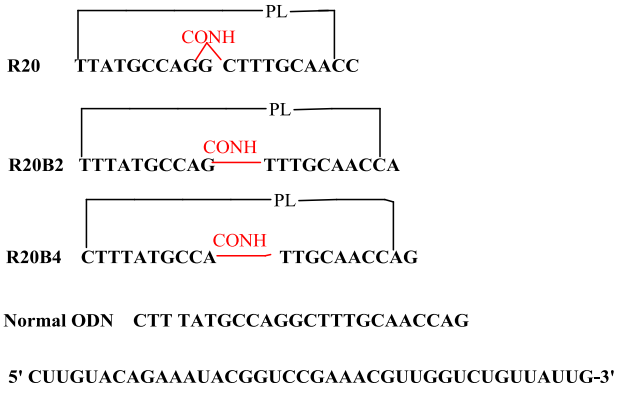

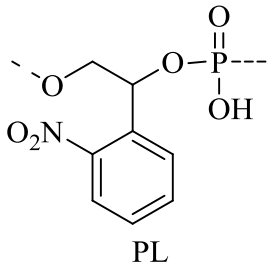

d) PS1-COOH: 5′-HOOCCH$_2$CH$_2$CONH-(CH$_2$)$_6$-**CUUGCUCACC**-*PL*-**GCUCCUCGCC**-(CH$_2$)$_6$ -NH$_2$-3′.; PS2-COOH: 5′-HOOCCH$_2$CH$_2$CONH-(CH$_2$)$_6$-**UUGCUCACCA**-*PL*-**AGCUC CUCGC**-(CH$_2$)$_6$-NH$_2$-3′.; PS3-COOH: 5′-HOOCCH$_2$CH$_2$CONH-(CH$_2$)$_6$-**UGCUCACCAU**-*PL*-A**GCUCCUCG**-(CH$_2$)$_6$-NH$_2$-3′

Figure 8. a) Structure of photo-cleavable linker [1-(*o*-nitrophenyl)-2-dimethoxytrityloxy]ethoxy-*N, N*-diisopropylamino-2-cyanoethoxyphosphine, b) Photoregulation of RNA digestion using caged circular asODNs and c) Sequences of caged circular as ODNs and complementary target RNA. R20B2 and R20B4 have 2- and 4-nucleotide gap in the middle when they bind their target RNA, and d) Sequences of photolabile circular antisense oligonucleotides (PS1, PS2, and PS3).

1.3.1.3 Photoregulation of nucleic acid functions using caged molecules

Caged nucleic acids provide a novel approach to modulate and regulate the functions of nucleic acids as well as control of gene expression by incorporating photo-labile groups, which are readily removed upon irradiation with light.

Recently, Deiters and co-workers developed two caged antibiotics using doxycycline **30** and toyocamycin **31** to regulate gene expressions.[35] Caged doxycycline **30** was used to regulate GFP expression under the control of the Tet-ON (Tetracycline-Controlled Transcriptional Activation) system using light irradiation (Figure 9).[35] The Tet-ON is a conditional gene control system commonly employed in transcription studies in eukaryotic cells. Transcription is reversibly turned on or off in the presence of the antibiotic tetracycline or its derivatives (doxycycline). Toyocamycin **31** is a natural antibiotic that effectively inhibits ribozyme functions *in vivo* at micromolar concentrations and thus activates gene expression. The study showed that the caged toyocamycin **31** was completely inactive and thus did not induce gene expression, however, upon exposure to light, the decaged toyocamycin induces spatially restricted activation of gene expression of GFP in a monolayer of human embryonic kidney cells.[35] In the study, the caged molecules are attached through covalent bonding to the silencing agent, such as antisense oligonucleotides or siRNA (Figure 10a).[35] In this approach caging molecules are installed on the nucleotide bases or on the phosphate backbone, thereby preventing the hybridization of silencing oligonucleotides with target mRNA. In another approach, the caging groups are incorporated on the complementary hybridising strands in order to prevent the inhibitory action of the antisense agent (Figure 10b).[35] In both cases, the unphotolysed antisense oligonucleotides did not show any

antisense activity; however, upon illumination, the liberated antisense oligonucleotides bind to the target mRNA, thus affecting the gene expression of GFP.

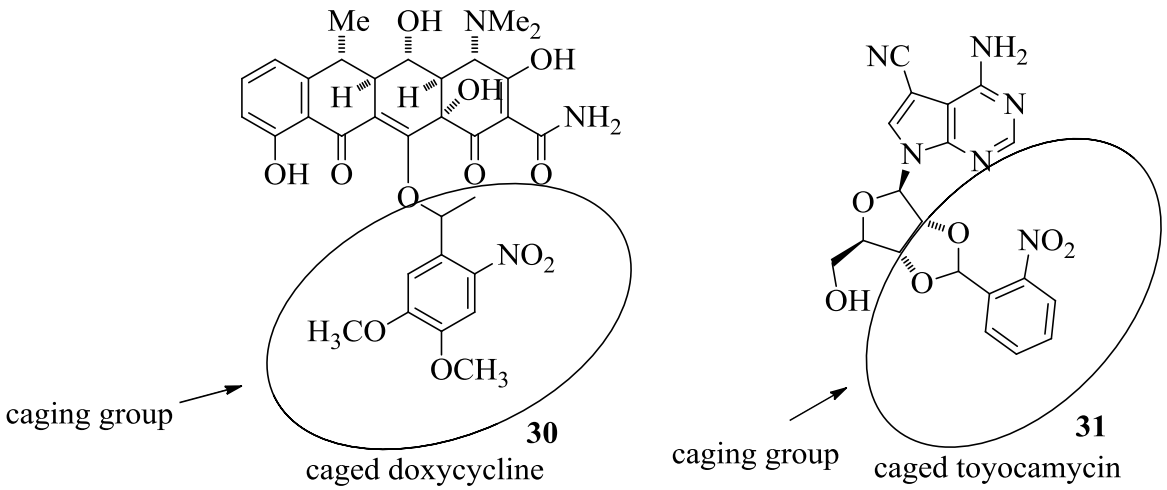

Figure 9. Light-responsive small molecule regulators of gene expression.

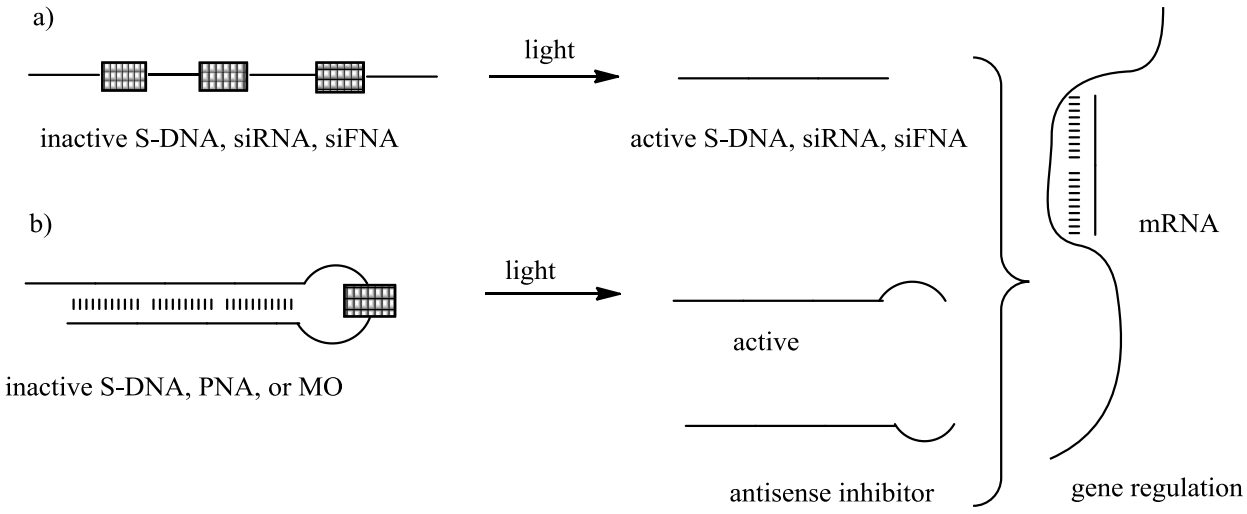

Figure 10. Two different approaches of photoregulation of gene downregulation via antisense agents/ RNA interference (S-RNA: small RNA, siRNA: small interfering RNA, PNA: peptide nucleic acid, MO: morpholino oligonucleotides, siFNA: small interfering fluoro RNA.

Haselton *et al.*[36] developed caged plasmid DNAs which encode for luciferase or GFP. The plasmid DNAs were caged with the Nv-group 1-(4,5-dimethoxy-2-nitrophenyl)diazoethane **32 (**Figure 11). The caged plasmid DNAs were then introduced into HeLa cells or rat skin cells. In both cell lines, the caged plasmid DNA blocked the transcription of GFP. The transcription of GFP was restored after irradiating the cells with light (355 nm).

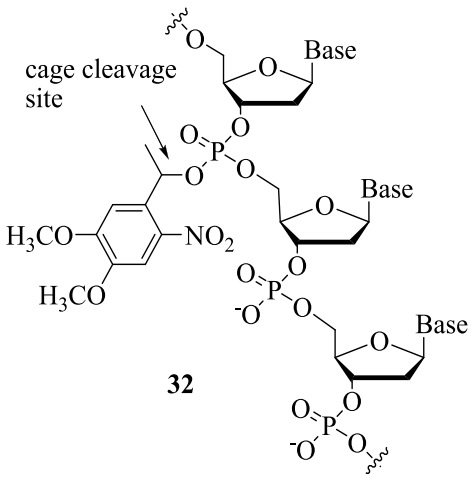

Figure 11. The structure of DMNPE caging group on the phosphate backbone of DNA.

A similar strategy was employed by Okamoto *et al.*[37] in developing Bhc-caged (6-bromo-7-hydroxycoumarin-4-ylmethyl) GFP-mRNA (Scheme 4). The mRNA was caged with a Bhc-caging group (as in **33)**, which upon irradiation with light, released uncaged mRNA. The Bhc-caged mRNA was injected into zebrafish embryos (one-cell stage). The study showed that the Bhc-caged mRNAs effectively inhibit the translation of GFP. Upon irradiation with light, the photo-labile group is cleaved, releasing the mRNA **34**, thus partially restoring the translational activity of mRNA.

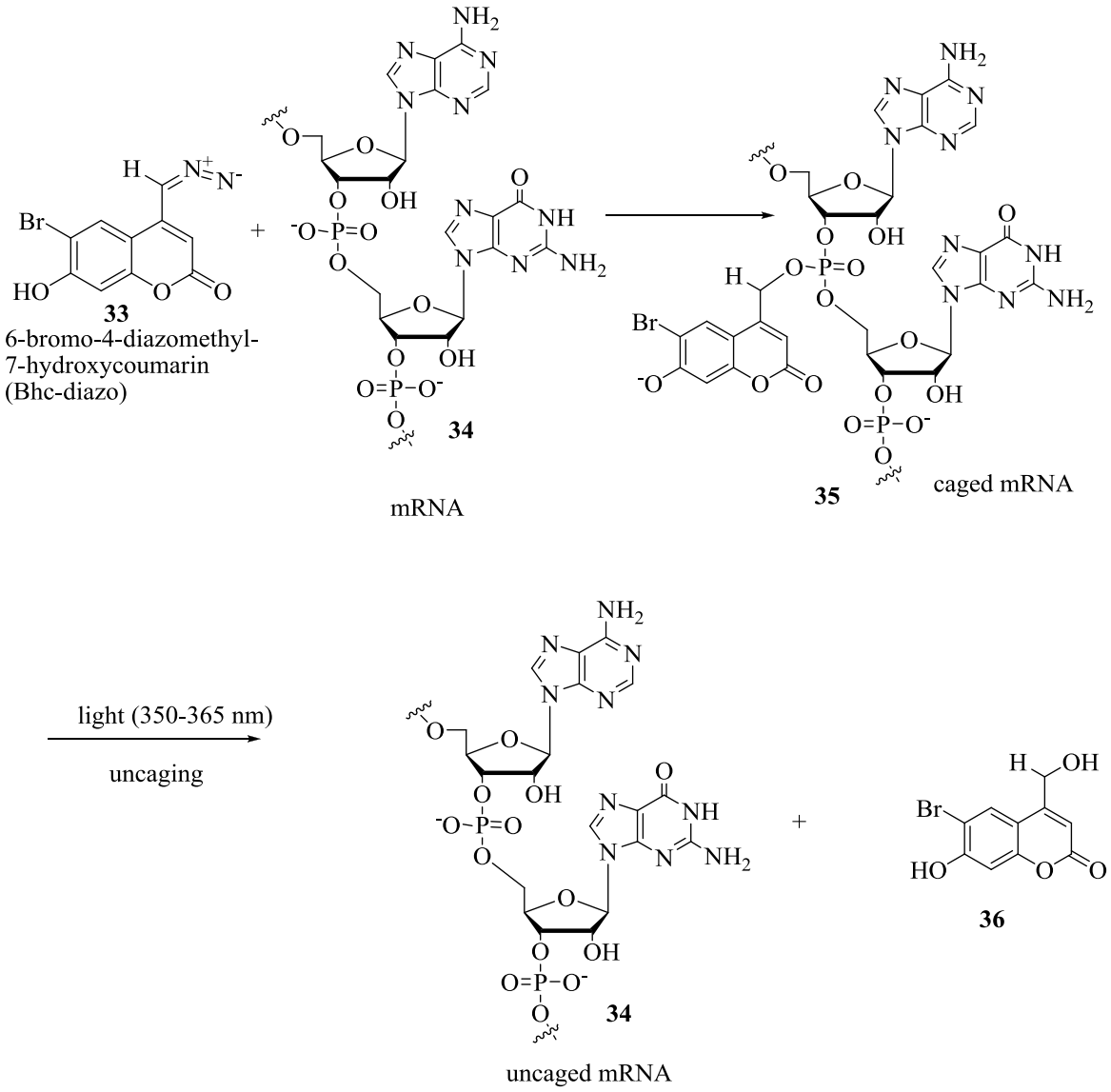

Scheme 4. Caging of RNA with Bhc-diazo and reactivation of the caged RNA by photolysis.[37]

In 2005, Friedman *et al.*[38] developed caged small interfering RNA (siRNA). siRNA are short double stranded RNA molecules that can downregulate gene expression through the RNA silencing pathway.[38] In this regulatory pathway, siRNAs are first recognised by the RNA-induced silencing complex (RISC), where one of siRNA strands, the guide strand, hybridises with the complementary sequence of mRNA, leading to degradation of mRNA.

Caged siRNA strands would inhibit the interaction of siRNAs with the RISC complex or mRNA, abolishing RNAi activities. In the study by Friedman *et al.*,[38] approximately 1.4 caging groups (4,5-dimethoxy-2-nitrophenylethyl, DMNPE) per duplex were introduced into siRNA molecules. Silencing of GFP expression in HeLa cell lines was used as a model system. Caged siRNAs **39** were not completely inactive prior to irradiation, but were fully activated upon irradiation with light. The incomplete inactivation of caged siRNA was due to a lower number of caging groups (DMNPE) per duplex. siRNAs with an increasing number of caging groups per duplex were completely inactive prior to light illumination; however, these siRNAs could not be fully activated upon exposure to light. The reason for the incomplete activation of siRNAs was insufficient irradiation time to cleave all caged siRNAs into fully active siRNAs. (Scheme 5).[38]

a)

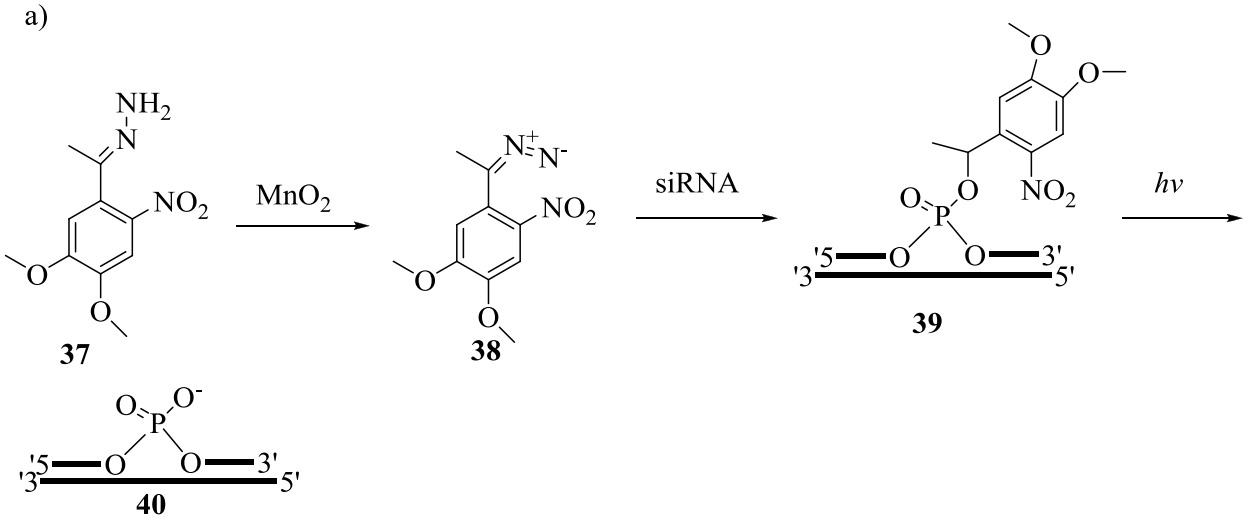

b)

Target	5' GCAGCACGACUUCUUCAAGdTdT 3' 3' dTdTCGUCGUGCUGAAGAAGUUC 5'
Control	5' GUGGGAGCGCGUGAUGAACdTdT 3' 3'dTdTCACCCUCGCGCACUACUUG 5'

Scheme 5. a) Reaction of siRNA with photo-labile caging group, and b) sequences of target and control siRNA used in the study.[38]

Heckel *et al.*[39] introduced caged-deoxyguanosine, dG^c **41**, and caged-thymidine, dT^c **42** (Figure 12) into siRNA duplexes at specific site. It was reported that nucleobase modification of siRNA at positions close to mRNA cleavage sites (10^{th} and 11^{th} nucleotides) can suppress RNAi activity. The caged siRNAs designed in this fashion were found to be completely inactive prior to exposure to light (expression of GFP was unaltered); however, after brief exposure (366 nm, 40 min) to light, RNAi activity was restored, leading to downregulation of GFP expression.[39]

a)

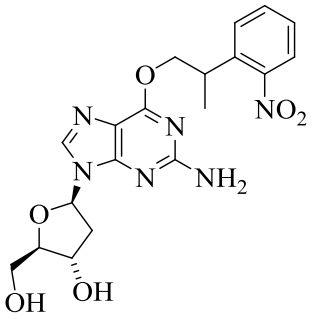

dG^{c}, **41**

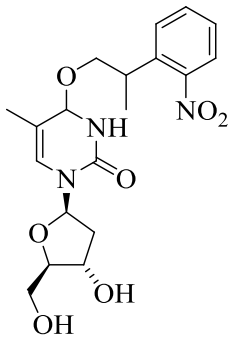

dT^{c}, **42**

b)

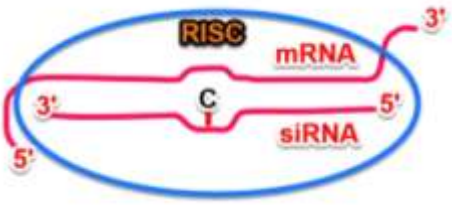

366 nm

activation of RNA interference

Figure 12.a) Structures of cG^{c}, and cT^{c}. b) The photolabile caging group masking the Watson-Crick interactions between the nucleobases, thus creates a temporary bulge region in the siRNA: mRNA duplex of the RISC. Upon irradiation, the photolabile group is completely removed, restoring the Watson-Crick base pairing.[39]

MacMillan *et al.*[40] used RNA as a model system to control the function of hammerhead ribozymes with light. Hammerhead ribozymes are capable of cleaving RNA via attack of one of the 2′-OH groups in the substrate at the adjacent 3′-phosphodiester linkage to form a cyclic

phosphate species, leading to the cleavage of the substrate RNA strand.[40] Since the nucleophilic attack of 2′-OH in the substrate is the key step for the cleavage, blocking the nucleophilic attack of 2′-OH on the adjacent 3′-phosphate group would allow for the regulation of catalytic activity of the ribozyme. RNA with their 2′-OH protected with a photolabile *o*-nitrobenzyl group (as in **43**, Scheme 6)[40] showed resistance towards ribozyme prior to exposure to light. Upon exposure to light, release of *o*-nitrobenzyl exposes the 2′-OH group of the substrate **44**, which is then cleaved by the ribozyme to the same extent as unmodified substrate.

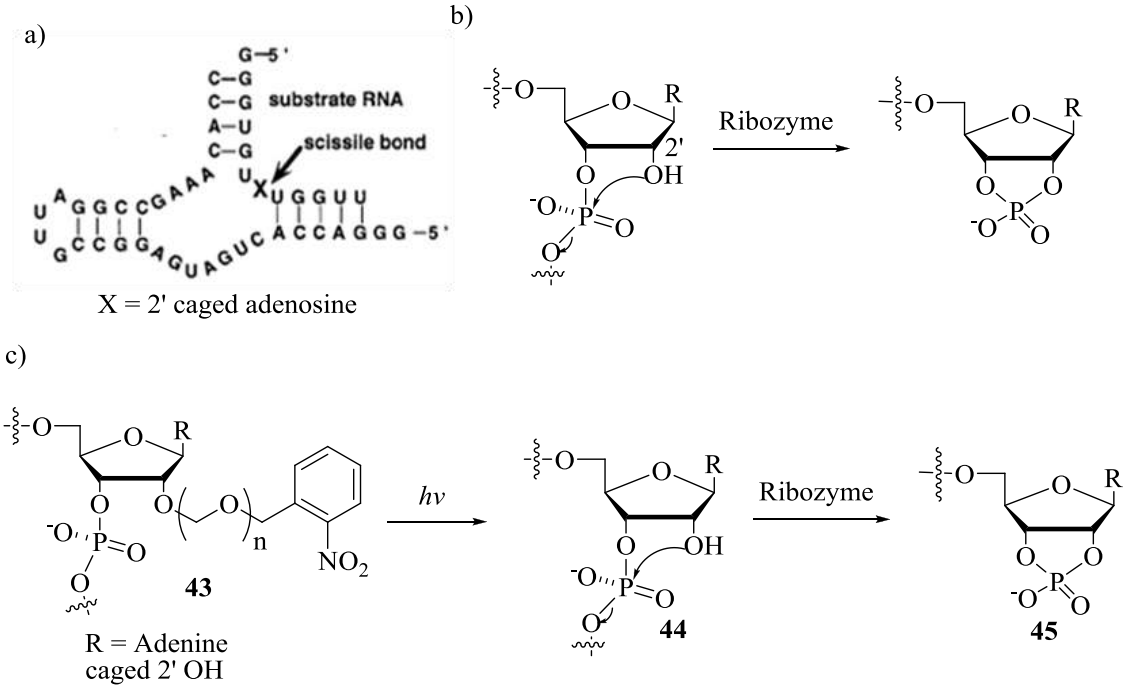

Scheme 6. a) Secondary structure of a hammerhead ribozyme with substrate, b) ribozyme catalysed intramolecular transesterification reaction, and c) photo-induced deprotection of 2'-caged hammerhead substrate leads to the hammerhead cleavage reaction.[40]

Modification of nucleobases by caging groups was first shown by Heckel and co-workers.[41, 42] In this work, thymidine was modified at the *O*4-position with a photolabile *o*-nitrophenyl-isopropyl (NPP) group (as in **46**, Figure 13), and then introduced into oligodeoxynucleotides.[41, 42] The caging group acts as a steric block, perturbing the hydrogen bonding capabilities of the base. The chemical modification introduced on thymidine was recognised as a mismatch by the T7 RNA polymerase, preventing the transcription of the duplex DNA by the T7 RNA polymerase. Upon exposure to light, the transcriptional activity of the T7 RNA polymerase was restored to the same extent as that of the unmodified DNA. Similarly, the modified guanosine **47** (caged with NPP) and the modified cytidine **48** (caged with *o*-nitrophenylethyl group, NPE) were synthesized.[41, 42]

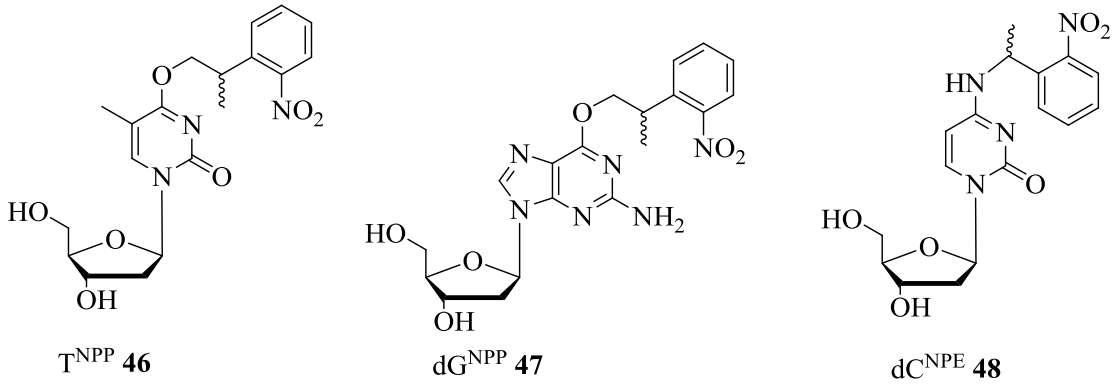

Figure 13. Structures of caged nucleobases used for light-responsive DNAs.[41,42]

Similar work with RNA bearing caged nucleobases was also demonstrated, using G^{NPE} **49**,[43] U^{NPE} **50**, A^{NPE} **51**, and C^{NPE} **52**[44] (Figure 14) to modulate the tertiary folding kinetics of RNA thereby regulating catalytic and regulatory functions of RNA.

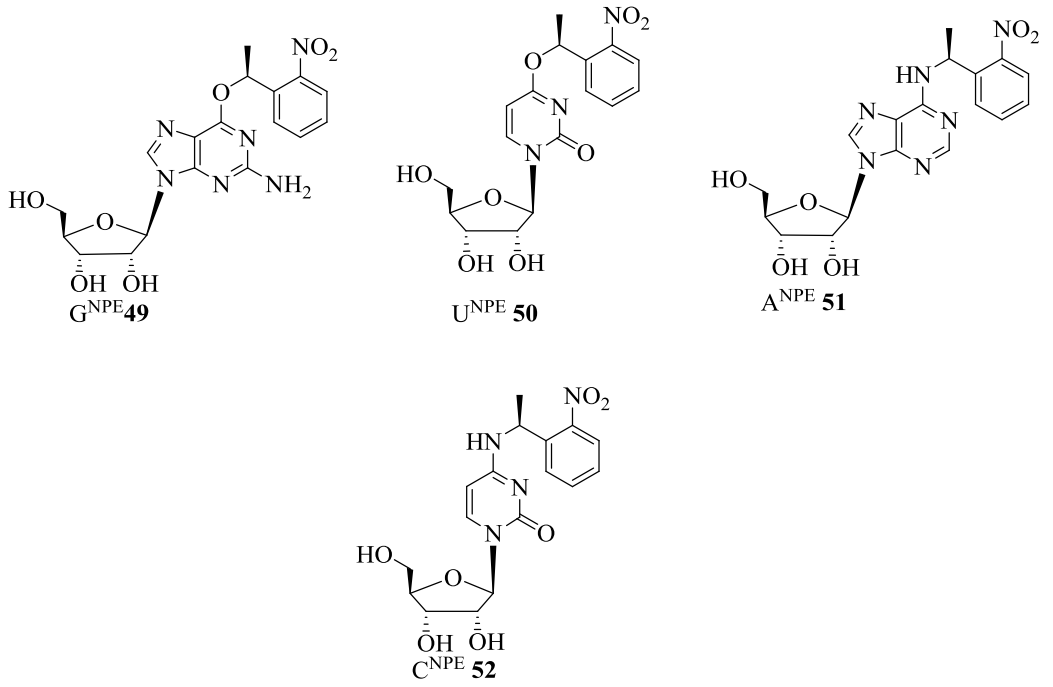

Figure 14. Structures of NPE-caged RNA nucleotides.[43, 44]

In work reported by Dmochowski *et al.*[45], oligonucleotides bearing caged FRET (Fluorescence or Förster Resonance Energy Transfer) pairs were synthesized. In this study adjacent cytidine residues were modified with fluorescein and caged Dabsyl (dimethylaminoazobenzenesulfonic acid), respectively (as in **53**, Scheme 7). Exposure of the oligonucleotide **54** to light led to cleavage of the caging group **55**, resulting in a 51-fold increase in fluorescence.

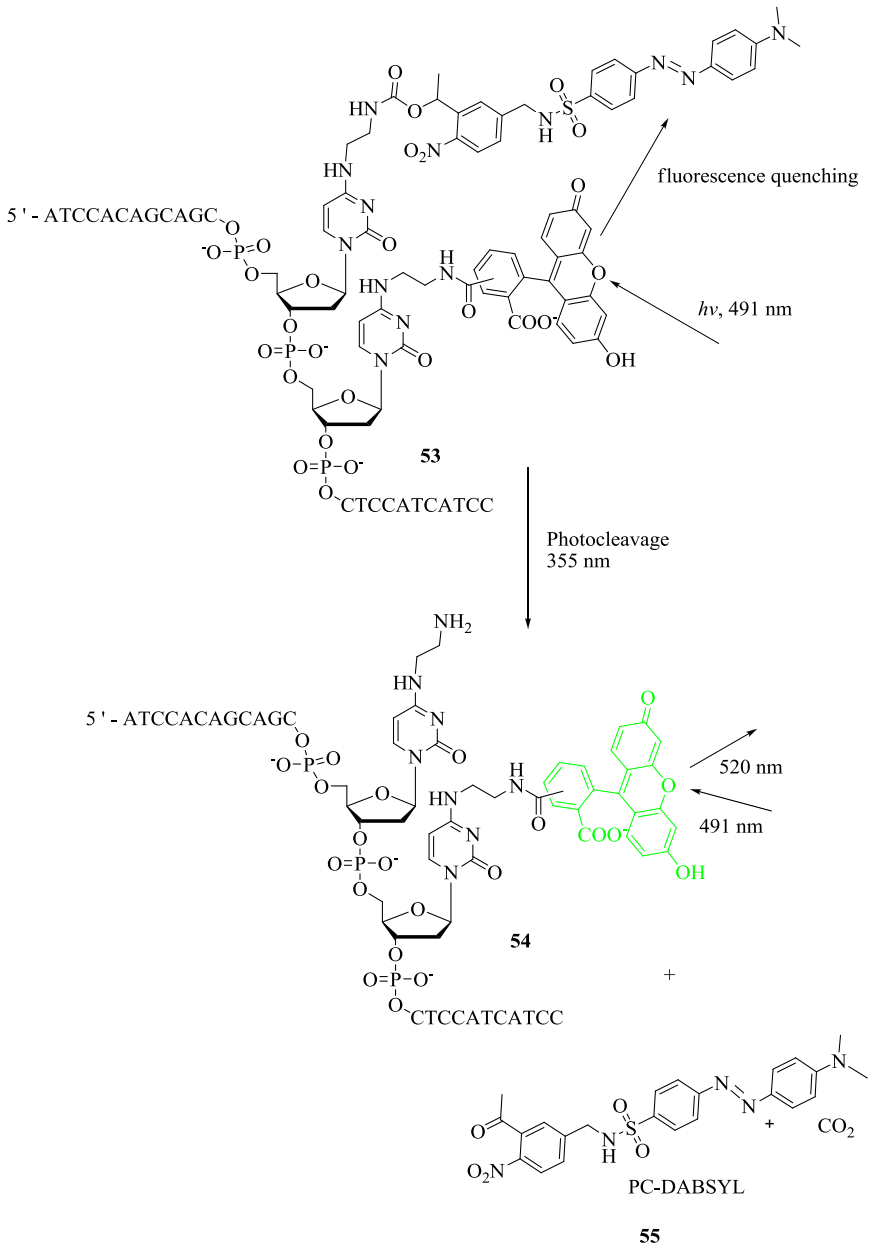

Scheme 7. Photolysis of oligonucleotides bearing caged FRET pair restoring fluorescence.[45]

Perrin *et al*.[46] synthesized caged adenosine residue **56** to regulate the activity of a DNAzyme using light. The C8-position of adenosine was modified with an alkylthioimidazole residue (Figure 15). This modification conferred fast and high-yielding cleavage either by homo- or heterolysis of the C-S thioether upon exposure to light without leaving any trace of the photolabile group on adenosine.[46]

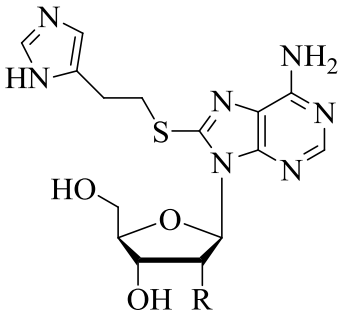

R = H, OH **56**

Figure 15. Structure of caged adenosine residue.

Molecular beacons are short single stranded oligonucleotides that hybridise with target nucleic acids in a sequence specific manner. Saito *et al*.[47] developed caged molecular beacons to regulate the hybridization of single-stranded DNA with its complementary sequences. In this approach, a molecular beacon or a single-stranded DNA which forms hairpin stem loop in the absence of complementary sequences is modified with a naphthalene quencher at the 5′-end and a photo-labile pHP (4-hydroxyphenacyl ester) group **57** to which biotin is linked at the 3′-end (Scheme 8). Upon irradiation with light, no cleavage was observed due to close proximity of quencher and photolabile group on the stem loop. The energy is transferred between the photolabile group and naphthalene quencher, thus no energy is retained to cleave the photo-labile group. In this system the photo-labile group and naphthalene quencher acts as a FRET pair.

In the presence of a complementary sequence, the stem loop is opened, and binds to the complementary sequence to form duplex DNA, which results in moving the quencher away from the *p*-hydroxyphenylacyl residue. This movement of quencher away from the *p*-hydroxyphenylacyl residue allows the cleavage of photolabile group upon the exposure to light, releasing the biotin residue **58**.

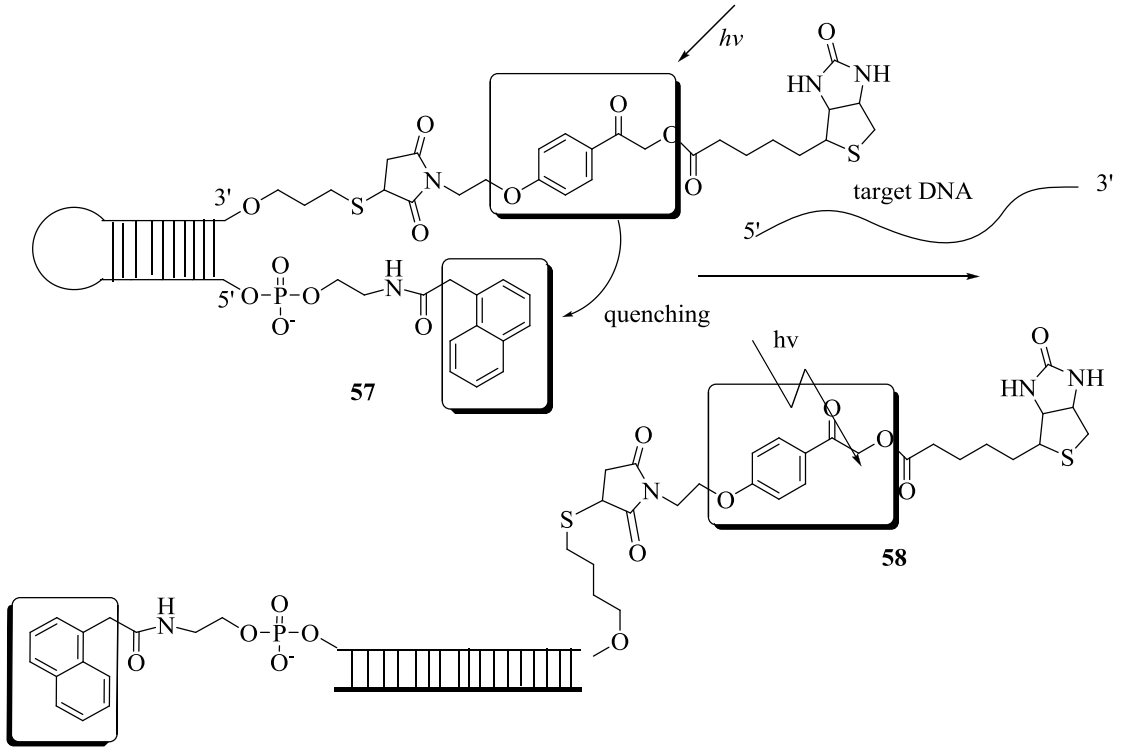

Scheme 8. Photoreaction of a molecular beacon carrying a single stranded DNA in the form of stem loop structure. In the absence of target DNA, the quencher blocks the photolysis of photo-liable linker. In the presence of the target DNA sequence, the stem loop structure unwinds, moving away from the quencher and photo-linker, thus inducing cleavage of the linker.[47]

1.3.1.4 Photoregulation of gene expression using caging molecules

Morpholino oligonucleotides (MOs) are synthetic DNA analogues in which the sugar phosphate backbone is replaced with morpholino moieties (Figure 16a).[48, 49] MOs have been found useful in inhibiting gene expression in a sequence dependent manner. Morpholino oligomers are widely employed in modulation and regulation of gene expression in zebrafish.[34, 49, 50] The zebrafish is ideally suited for this study for visualizing vertebrate ontogeny, because the embryos and the larvae of zebrafish are optically transparent and develop rapidly ex utero. Recently, Chen *et al*.[49] developed two caged morpholino oligomers, one with dimethoxynitrobenzyl **59** (DMNB) and another with bromohydroxyquinoline (BHQ) (Figure 16b), to regulate the expression of genes such as heart of glass (*heg*), floating head (*flh*) and endothelial-specific variant gene 2 (*etv 2*) in zebrafish.

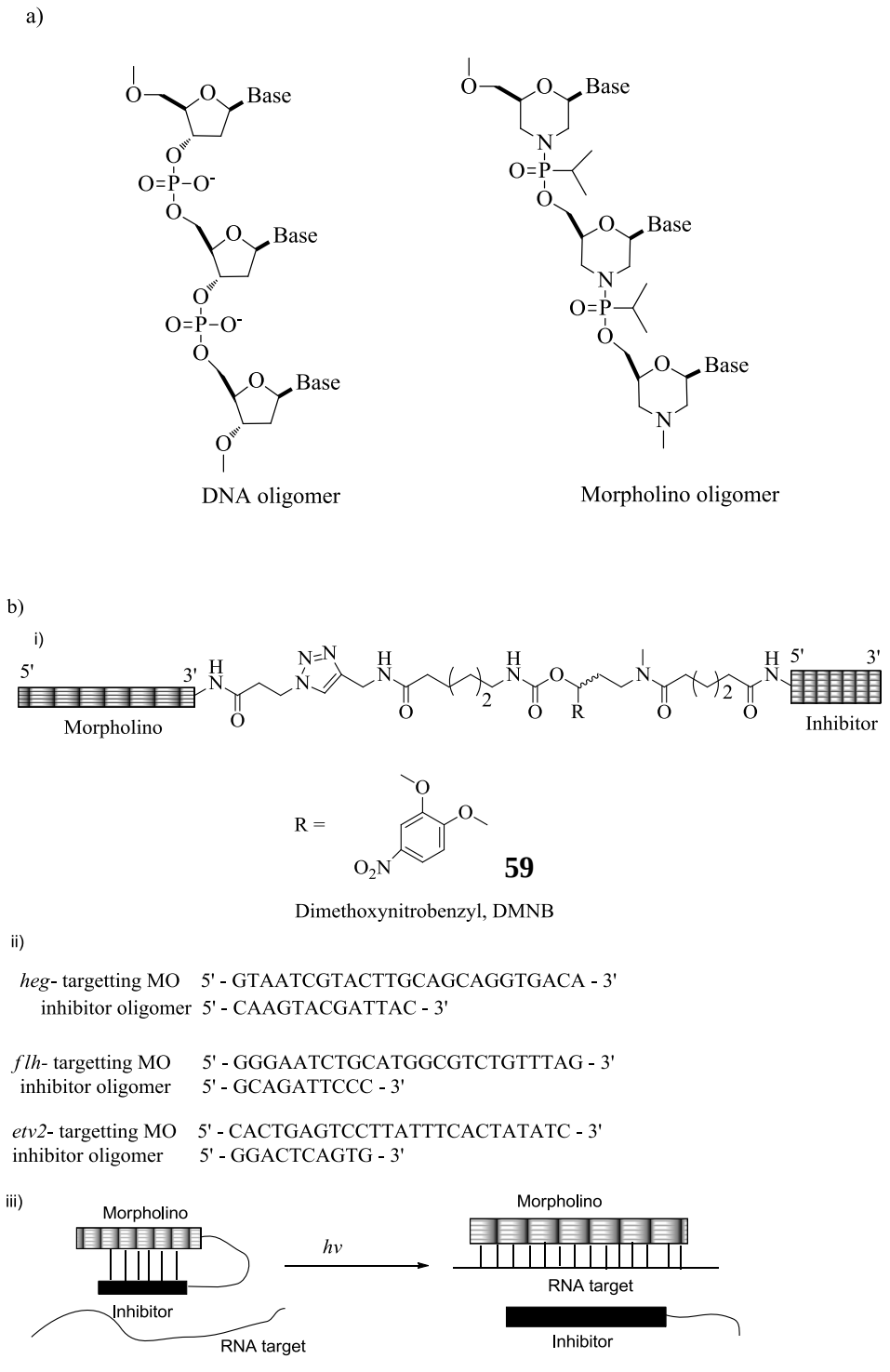

Figure 16. a) Structure of DNA and Morpholino oligomers. b) i) Structure of DMNB-caged morpholino oligomers, ii) Target and inhibitor sequences of *heg*, *flh*, and *etv2*, and iii) Schematic representation of the hairpin cMO strategy.[49]

The intramolecular duplex formed between the morpholino oligomers and the complementary inhibitor suppresses the binding of the targeting sequence (morpholino oligomers) with its complementary RNA. Upon exposure to light (360 nm), the dissociation of inhibitor allows the binding of morpholino oligomer to its complementary RNA, thereby preventing either splicing or translation of its RNA target (in this study,[49] translation of genes *heg, flh, and etv2*). In a similar study, Dieters *et al*.[51] reported the synthesis of morpholino oligomers caged with a photo-labile monomeric building block **60** (Figure 17), and demonstrated the application of the oligomer in the regulation of gene function in both cell culture and embryos using light. The caged morpholino oligomers were used to inhibit the expression of the EGFP (Enhanced Green Fluorescent Protein) in transfected cells, live zebrafish, and *Xenopus* frog embryos. The expression of EGFP was inhibited upon exposure to UV irradiation in both the transfected cells and in live embryos of zebrafish and Xenopus frog.

a)

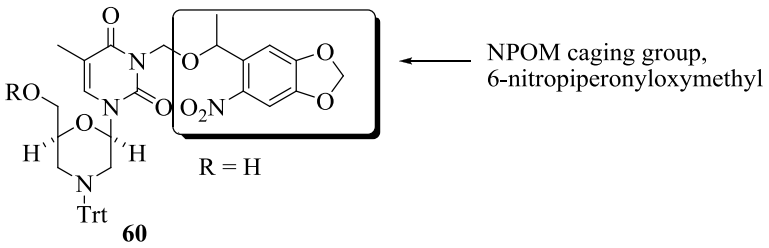

60

b)

Morpholino	Sequence
EGFP- MO^0	ACAGCTCCTCGCCCTTGCTCACCAT
EGFP-MO^4	ACAGCT* CCT* CGCCCT* TGCT* CACCAT

T* denotes caged monomer

Figure 17. a) Structure of NPOM caged morpholino oligomer, and b) morpholino sequences used in this study.[51]

Recently, Wu *et al.*[50] reported the synthesis of caged circular morpholino oligomers. Incorporation of multiple linear caging residues in nucleic acids sterically inhibited the interactions between the targeted sequence with its complementary sequence; however, incomplete uncaging upon exposure to light was observed. The incomplete uncaging of the nucleic acids could be overcome by employing a single caging residue; whereas, the relative thermostability of caged- and uncaged-oligonucleotides is difficult to balance, especially in *in vivo* studies.[50] To overcome these problems, Wu *et al.*[50] developed two caged circular morpholino oligomers (MO-cat2, MO-ntl), each consisting of a heterobifunctional photocleavable linker (PL) (Figure 18), to modulate the expression of the gene *β-catenin-2* and *ntl* in zebrafish embryos. The *β-catenin-2* gene is essential for the development of dorsal axial structures. Knockdown of this gene will cause pin head and truncated pattern defects in the embryos. The *ntl* gene is responsible for the formation of the nodal-independent tail somite. Knockout of this gene will result in embryos with missing notochord cells. Caged circular moiety cannot hybridise with complementary sequences in mRNA; however upon irradiation with light, loss of the caging group restores this ability, leading to annealing with mRNA (Figure 18). Upon injection of both caged MO-*cat2* and MO-*ntl* oligonucleotides into the embryos of zebrafish, gene expression of *cat2* and *ntl* was efficiently photoregulated.[50]

a)

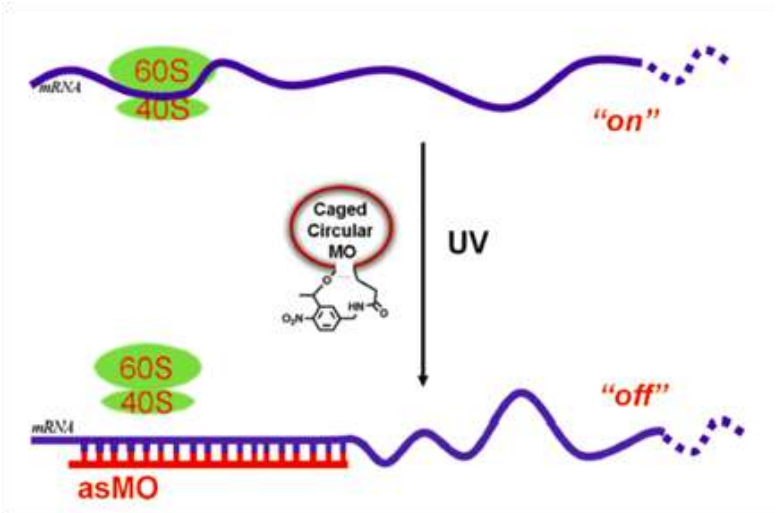

b)

MO-cat2 sequence, 5' - CCTTTAGCCTGAGCGACTTCCAAAC- 3'

Figure 18. a) Controlling the gene expression via photolysis of cMO oligomer and subsequent binding to target mRNA, b) Sequence of MO-cat2 used in this study.[50]

Even though the photo-regulation by caging molecules shows promising results and efficient photo-control of various bio-molecules, it lacks an important feature, *i.e.* reversibility, which has the advantage of controlling the functions of bio-molecules in a time dependent fashion. Also, by-products released from uncaging processes might not be tolerated by living systems. More importantly, reversibility renders control of a biomolecule's function in a multiple-cycle manner. In this fashion, no by-products are released in the photoswitching.

1.4 Reversible photoswitch molecules

Despite the advantages of caging technology in achieving clean photo-switch behaviour, formation of by-products in stoichiometric amounts during the irreversible reaction severely hampers its use as photo-switches. Reversible photoswitch molecules, such as azobenzene, spiropyrans, spirooxazines, fulgides, overcrowded alkenes and diarylethenes, can be employed as reversible photo-switches to regulate the functions and properties of biomacromolecules such as DNA, RNA, and proteins.[7] These reversible photoswitching molecules are classified into two categories based on the thermal stability of their photogenerated isomer:[52]

1. P-type (photochemically reversible type); these photoswitches do not convert back to the initial isomer at elevated temperature (e.g., fulgides and diarylethenes), and

2. T-type (thermally reversible type); the photogenerated isomer isomerises back to the initial isomer thermally (e.g., azobenzenes, stilbenes or spiropyranes).

1.4.1 Spiropyrans and spirooxazines

Spiropyrans are photochromic compounds discovered in 1952 by Fischer and Hirshberg.[53] Spiropyrans and spirooxazines undergo reversible photo-transformation between two forms upon exposure to light, exhibiting two different absorption spectra.[53] Upon photoisomerization, not only the optical properties but also the physico-chemical properties change, such as refractive index, dielectric constant, oxidation/reduction potentials, and geometrical structures.[54] This change in physico-chemical properties can be employed in various optical devices, such as erasable optical memory media and photo-optical switch components.

Scheme 9 shows a typical photo-reversible reaction of spiropyrans **61** and spirooxazines **63**.[53] In this photochromic reaction, the C-O bond undergoes reversible heterolytic cleavage upon UV irradiation (360-370 nm), resulting in the formation of a zwitterionic conjugated system known as the merocyanine form (**62**, **64**).[53] This photo-reversible property of spiropyrans has been employed in enzymes to confer reversible control on enzyme activity.[53]

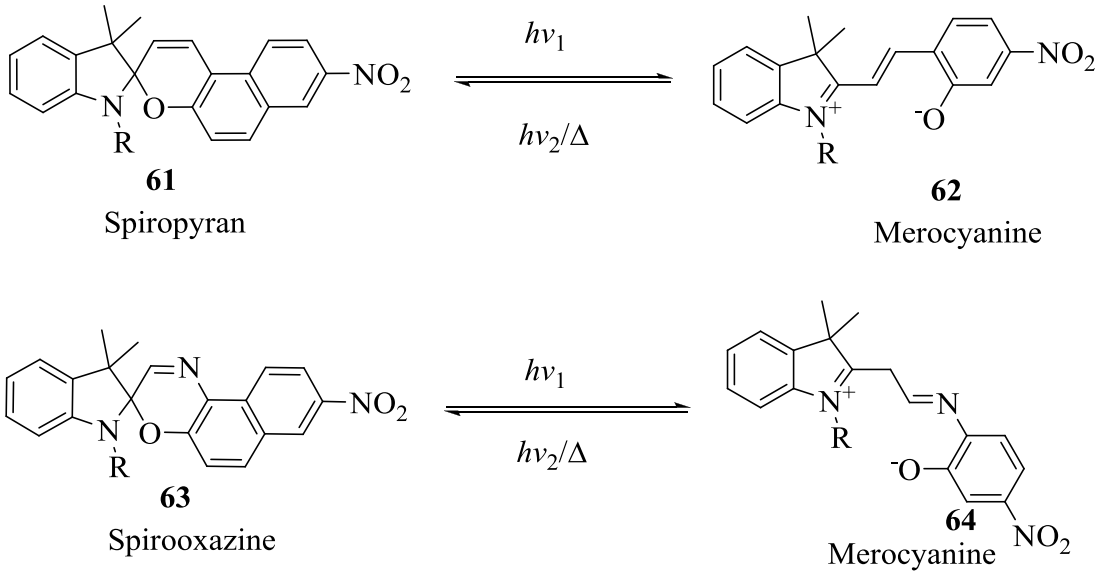

Scheme 9. Typical photo-isomerization of spiropyran and spirooxazine.[53]

As an example, Aizawa *et al.*[53] employed spiropyran to modulate enzyme activity. Binding of trypsin to its inhibitor was photoregulated by appending spiropyran to trypsin inhibitor, a small protein.[55] The photochromic property of spiropyrans has also been employed in the photoregulation of proteins. As the function of a protein is directly related to its three-dimensional structure, perturbation of the protein conformation will lead to changes in its activity.[53] In this regard; the photoisomerization of spiropyrans can be utilized to introduce conformational changes to proteins, leading to reversible modulation of protein function. [56]

Willner *et al*.[56] synthesized spiropyran-modified Concanavalin A (Con A), a protein that forms complexes with specific pyranoses, such as *α*-D-mannopyranoside, through a substitutent on the imide nitrogen of lysine residues. Binding of spiropyran-modified concanavalin A to the substrate, *α*-D-mannopyranoside **65**, was photoregulated. Photoisomerization of spiro-Con-A **66** to the zwitterionic Con-A **67** resulted in structural perturbation of the Con A, which further affected the binding ability of substrates to Con A (Scheme 10).[56]

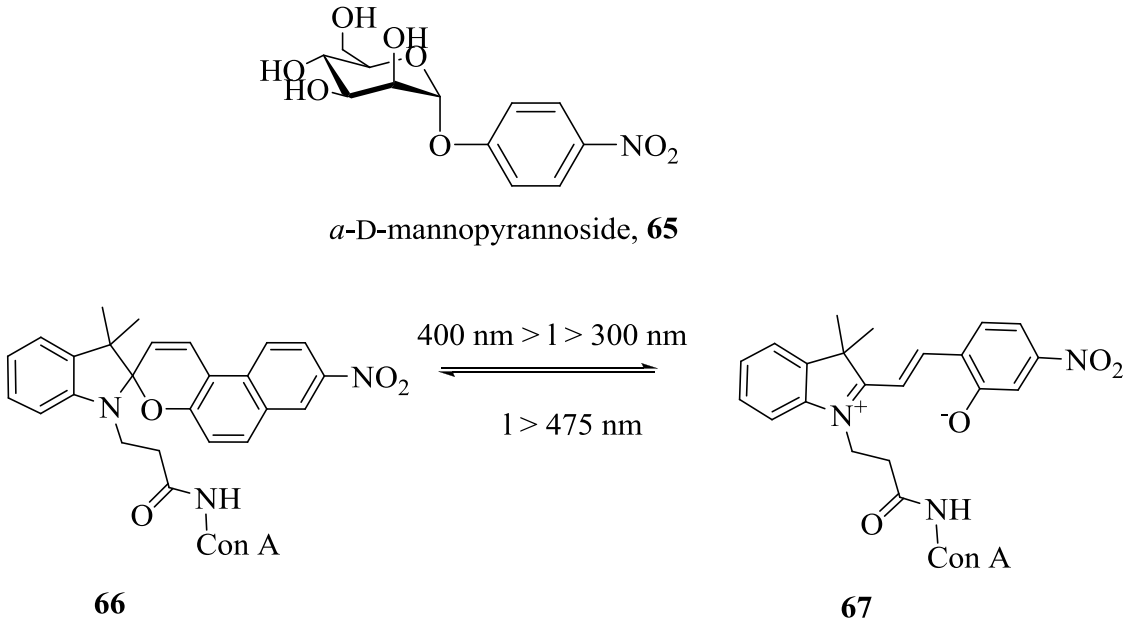

a-D-mannopyrannoside, **65**

66 **67**

Scheme 10. Structure of *α*-D-mannopyranoside and photo-isomerization of spiro-Con-A to zwitterionic Con-A.[56]

1.4.2 Fulgides

Fulgides were first synthesized by Stobbe in 1905.[57] Fulgide is the generic name given to derivatives of 1,3-butadiene-2,3-dicarboxylic acid (fulgenic acid **68**, Figure 19) and corresponding anhydride derivatives (fulgide **69**).[57]

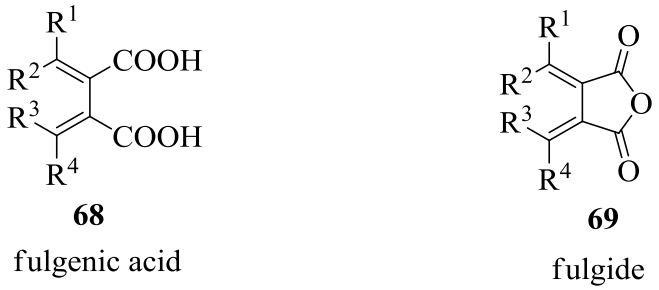

68
fulgenic acid

69
fulgide

Figure 19. Structures of fulgenic acid and fulgide.[57]

The photochromic fulgides contain at least one aromatic ring on the exo-methylene carbon atom, which forms a 1,3,5-hexatriene structure that can undergo a 6π-electrocyclization reaction (Scheme 11). Fulgides exists in two photochromic forms: one is an open colorless form (*E*-form), as the double bond connecting the aromatic ring and the succinic anhydride is usually *E*-form **70**, and the other is a photocyclized colored *C*-form **71** (Scheme 11).

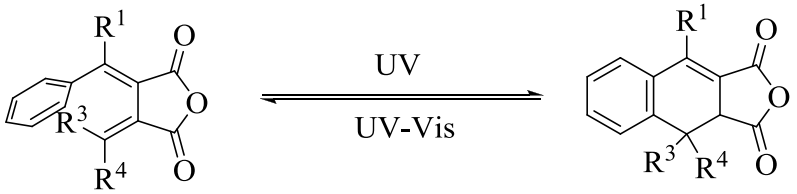

E-form
colorless
70

C-form
colored
71

Scheme 11. Typical photo-isomerization of fulgide from *E*- to *C*-form.[57]

Willner *et al*.[58] synthesized fulgimide-modified concanavalin A **72** (Figure 20) and *α*-chymotrypsin **73** analogues (Figure 20). Fulgimide is attached to the lysine residue of concanavalin A. The fulgimide-modified α-chymotrypsin consists of nine fulgimide moieties on each protein bound to lysine residues. The structural change of fulgimide induced upon photoirradiation affected the binding of 4-nitrophenyl-*α*-D-mannopyranoside **65** to Con A. The association constant of Con A **65** changed from $0.78\times 10^4\ M^{-1}$ for the *E*-form to $1.21\times 10^4\ M^{-1}$ for the *C*-form. Esterification of protein, Con A, on *N*-acetylphenylalanine in cyclohexane is photoregulated by fulgimide.[58]

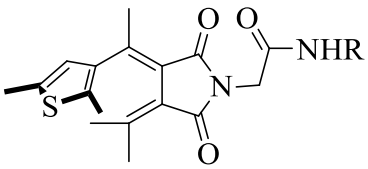

72 E: R = Concanavalin A
73 E: R = α- Chymotrypsin

Figure 20. Structures of *E*-form fulgide linked concanavalin A, and α-chymotrpsin.

1.4.3 Diarylethenes

Diarylethenes are thermally irreversible P-type photochromic compounds.[59] The most salient property of diarylethenes is their resistance towards fatigue. Diarylethenes can undergo reversible photoisomerization for more than 10^4 times without showing fatigue.[59] Thermal irreversibility and fatigue resistance of these compounds make them invaluable tool for optical devices such as memory device and photoswitches.[59]

Stilbene **74** is one of the examples of diarylethenes, which undergoes photoisomerization to produce dihydrophenanthrene **75**. The cyclised dihydrophenanthrene isomerizes back to stilbene in de-aerated solution in the dark. However in the presence of air, dihydrophenanthrene irreversibly converts to phenanthrene **76** in a reaction with oxygen thereby eliminating a molecule of hydrogen (Scheme 12).[59]

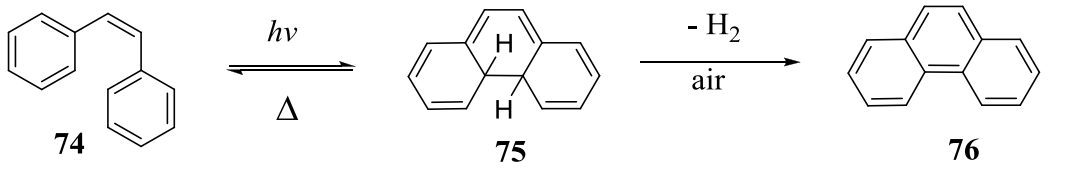

Scheme 12. The photo-isomerization of stilbene to dihydrophenanthrene and conversion of dihydro-phenanthrene to phenanthrene.

1.4.4. Overcrowded alkenes

Overcrowded alkenes are another class of photochromic compounds. Two subclasses of overcrowded alkenes are photochromic pseudoenantiomers and enantiomers.[60] The pseudoenantiomers consist of an unsymmetrical upper part (tetrahydrophenanthrene or 2,3-dihydronaptho(thio)pyran) connected via a double bond to a symmetric lower part (xanthenes, thioxanthene, and fluorene).[60] The molecule adopts a helical shape to avoid steric interactions around the central olefinic bond. The photoisomerization of pseudoenantiomers and enantiomers is shown in Scheme 13.[60] Scheme 13b shows a stereospecific photochemical isomerisation process that reverses the helicity of the enantiomer thioxanthene alkene using circularly polarized light.

a)

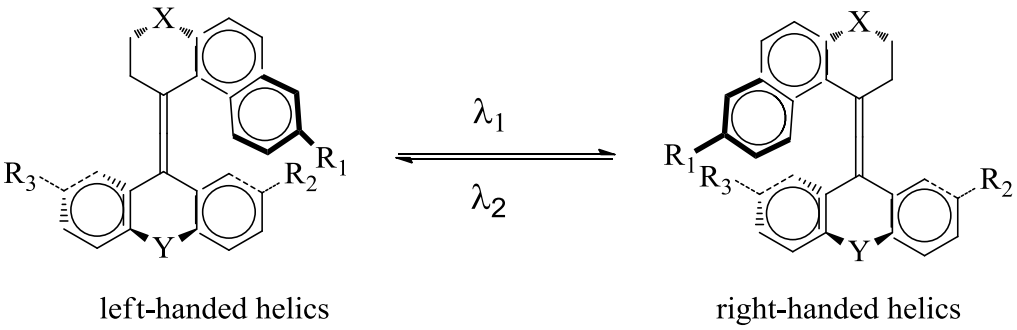

left-handed helics right-handed helics

R_1 = H, Me, NMe_2; R_2 = OMe, NO_2, R_3 = NO_2, H; X = CH_2; Y = S

b)

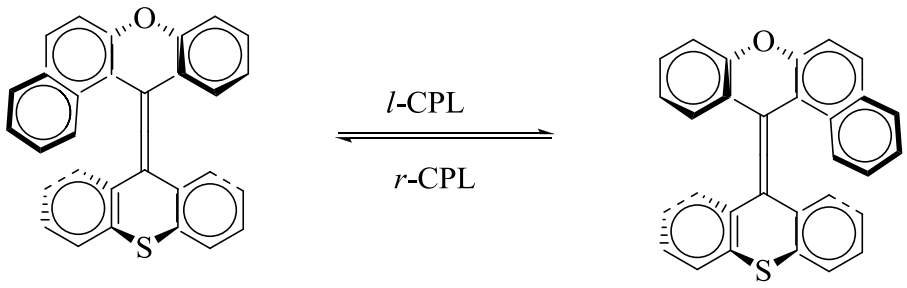

trans-isomer cis-isomer

Scheme 13. a) Photo-isomerization of dissymmetric alkenes; b) photoisomerization of thioxanthene alkenes with *l*-or *r*-CPL (circularly polarized light).[60]

CHAPTER 2- Photoisomerization and synthesis of azobenzenes

2.1 Azobenzene

One of the most widely used organic chromophores as an optical switch is azobenzene. Azobenzene, a T-type photochromic system, displays a reversible photoisomerization process between its *trans*- and *cis*-isomers. The two forms of azobenzene possess different stabilities and absorption spectra.[52] In the T-type system, photoisomerization causes rearrangement of the electronic and nuclear structures of the molecule without any bond breaking. The *trans*-isomer (*E*, **77**) of azobenzene is stable at room temperature, which isomerizes to *cis*-form (*Z*, **78**, less stable) upon exposure to light of a suitable wavelength. The *cis*-form isomerizes back to *trans*-form readily in the dark (Scheme 14).[52, 61]

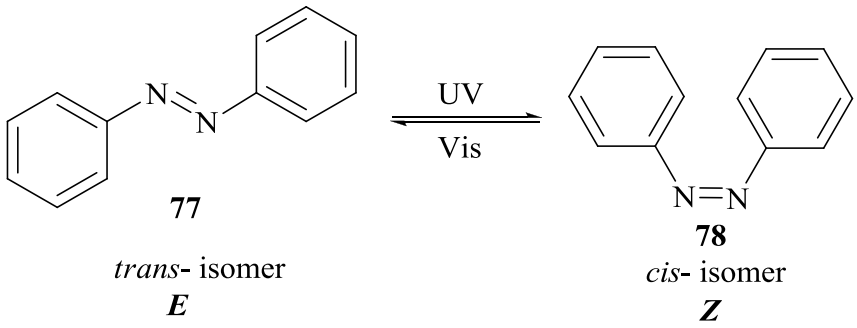

Scheme 14. *E-Z* isomerization of azobenzene.

The photoisomerization of azobenzene from *trans*- to *cis*-form can occur within femtoseconds with a strong light source, but the rate at which the *cis*-form isomerizes back to the *trans*-form mainly depends on the chemical structure of the system.[52]

Aromatic azo-compounds exhibit a conjugated π system that can be readily tuned through appropriate structural modification to adjust chemical and photochemical properties. They have thus found wide applications as dyes, pigments, food additives, radical initiators, therapeutic agents, as well as functional materials.[61]

Appropriate structural modification on the azobenzene core results in slow thermal back isomerisation of the azo-derivative, which results in a photoactive material valuable for information storage (memory) purposes. For azobenzene based photochromic systems to be used in real-time information transmitting systems, as well as in optical oscillators, back isomerisation to the *trans*-form (thermally stable form) from the *cis*-form should occur as fast as possible.[52]

2.1.1 Photo-isomerization of azobenzene

The first azo-dye was discovered by Martius in 1863.[62] In the following years, a wide variety of azo-dyes were synthesized and investigated to obtain a dye of desired color and shade which could be prepared reproducibly and cheaply.[63] The existence of the *cis*-form of azobenzene was first demonstrated by Hartley in 1937 using a solvent extraction method.[64]

Azobenzene has been shown to undergo photo- and thermo-isomerization from the *trans*-(*E*) to *cis*-form (*Z*). The *E*- and *Z*-forms oscillate back and forth when excited by light of a selected wavelength or by heat (Scheme 14). This reversible photoswitching property can be exploited as a useful photoswitch where a signal can be induced by light and harnessed.[61, 65, 66] One such application is incorporation of azobenzene into biomolecules, such as proteins and nucleic acids, to trigger conformational changes of the biomolecules that impact their functions.[61, 67-70]

Figure 21 shows the absorption spectra of azobenzene. The *E*-azobenzene isomer displays a strong absorption band at 318 nm and another weak absorption band at 432 nm. The *Z*-azobenzene isomer exhibits a strong absorption band at 260 nm and another weak absorption band at 440 nm.[61] The absorption spectra of the two isomers of azobenzene are distinct but overlapping. The absorption band of the *trans*-isomer shows a weak n-π^* band at 432 nm and a strong π-π^* band at 318 nm. In contrast, the *cis*-isomer of azobenzene shows a strong n-π^* band at 440 nm and a weak n-π^* band at 260 nm.[61]

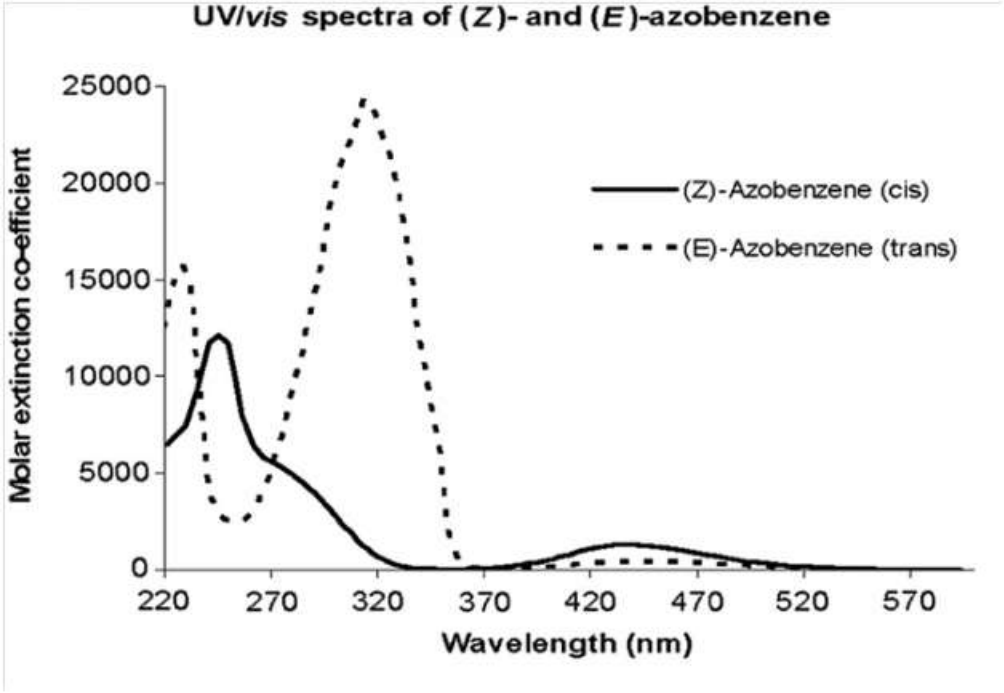

Figure 21. UV/Vis absorption spectra of azobenzene **77** and **78** (solid line: *Z*-isomer; dash line: *E*-isomer).[61] (Reprinted with permission from Zimmerman, G.; L. Y.; Paik, U. J. *J. Am. Chem. Soc*. **1958**, *80*, 3528-3531).

2.1.2 Structural features of azobenzene

The interesting application of azobenzenes lies in its facile and reversible photoisomerization about the azo bond, converting between the *trans*- and *cis*-geometric isomers. The photoisomerization is completely reversible and free from side reactions. Among the two isomers of azobenzene, the *trans*-isomer was found to be more stable at room temperature than the *cis*-isomer by 10-12 kcal mol^{-1} and the energy barrier to the photo-excited state (barrier to isomerization) is on the order of 46-48 kcal mol^{-1}. As a result of this stability the *trans*-isomer is dominant (> 99.99%) in the dark at equilibrium.[71, 72, 73 (i)]

The *trans*-isomer **77** of azobenzene is nearly planar with nearly zero dipole moment.[73 (ii), 74] A quantitative yield of *cis*-isomer **78** is obtained upon exposure of *trans*-isomer to light at 340 nm.[61, 75] The *cis*-isomer of azobenzene possesses a dipole moment of about a 3 debye.[73 (ii)] The distance between the two carbon atoms in the 4- and 4'-positions are 9.0 and 5.5 Å for the *trans*- and *cis*- isomers, respectively (Scheme 15). The *cis*-isomer is isomerized back to the *trans*-form either by placing the solution in dark or by irradiation at 450 nm. The photoisomerization of azobenzene occurs with moderate quantum yields, where $\phi_{Z\text{-}E}$ = 53 % and $\phi_{E\text{-}Z}$ = 24 %,[75] and with minimal photo-bleaching. During the photoisomerization process the distance between the carbons at the *para*-positions of the phenyl rings is changed by ~3.5 Å,[73 (ii)] and this change is exploited for applying azobenzene as photoswitch.

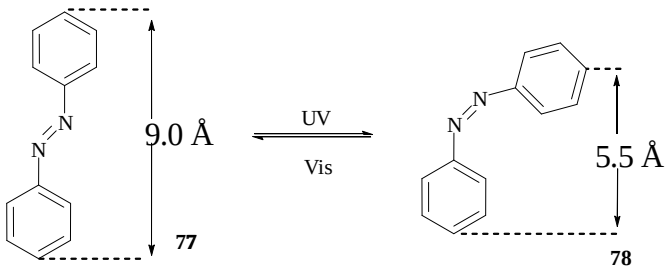

Scheme 15. Structural changes during the photoisomerization of azobenzene.[73 (ii)]

2.1.3 Mechanism of photoisomerization of azobenzene

The mechanism of photoisomerization of azobenzene is still controversial and under debate.[76] However, recent work on the influence of solvent on the photoisomerization of azobenzene suggests that photoisomerization in azobenzenes can occur through rotation about the -N=N- bond or by an inversion process involving a rehybridization mechanism about one of the nitrogen atoms (Figure 22).[76] Upon irradiation, the *cis*- isomer thus formed via inversion or rotation mechanism, adopts a bent conformation with its phenyl rings twisted ~ 55^{o} out of the plane from the azo group.[61]

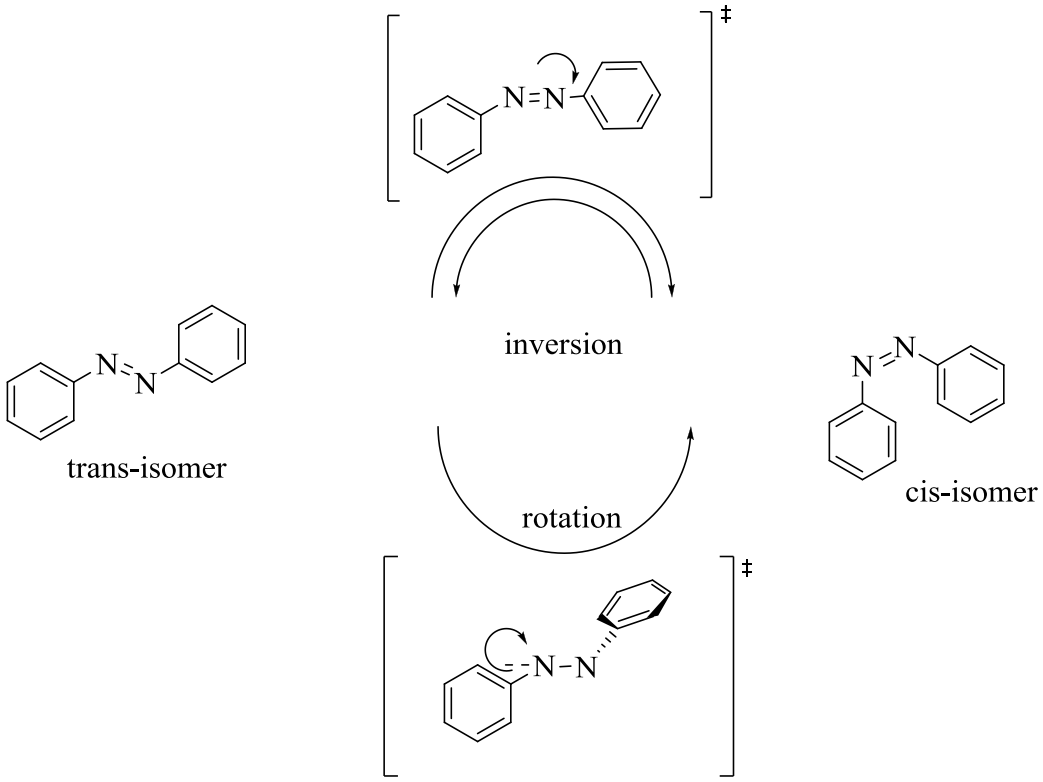

Figure 22. Photoisomerization pathway from *trans*-to *cis*- azobenzene and *vice versa*.[76]

Changes in structural and physical properties of azobenzenes upon photoisomerization are exploited as a valuable tool for the regulation of various functions of nucleic acids.

2.2 Synthetic methods for the preparation of azobenzene derivatives

2.2.1 Oxidation of primary aromatic amines

Symmetrical azobenzene derivatives have been prepared through the oxidation of primary aromatic amines with oxidizers such as manganese dioxide, potassium permanganate and silver/ iodine. Using this approach, azobenzene analogues **81** and **82** were synthesized in 69 and 61% yields, respectively, by the oxidation of aniline derivatives **79** and **80** using manganese dioxide in hexane under reflux (Scheme 16).[77]

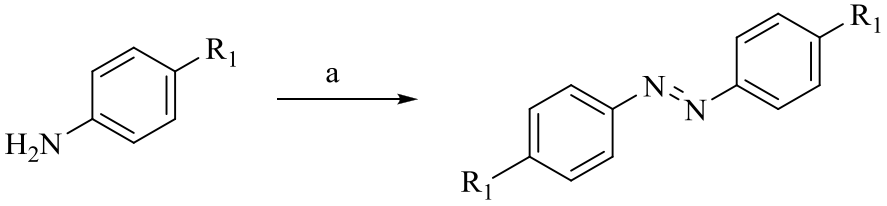

79 R_1 = H
80 R_1 = Cl

81 R_1 = H
82 R_1 = Cl

Scheme 16. *Reagents and conditions*: a) MnO_2, molecular sieves, hexane, reflux.

Gilbert *et al.* recently reported the synthesis of azobenzene analogues by treating 4-chloroaniline **80** with MnO_2 in toluene under reflux (Scheme 17).[78] This approach, however, only afforded azobenzene **82** in low yield **(**49%). Oxidation of *para*- or *meta*-halogen substituted aniline derivatives **80, 83-85** resulted in the formation of the corresponding azobenzene analogues **82, 86-88** in 89, 88, and 79% yields..

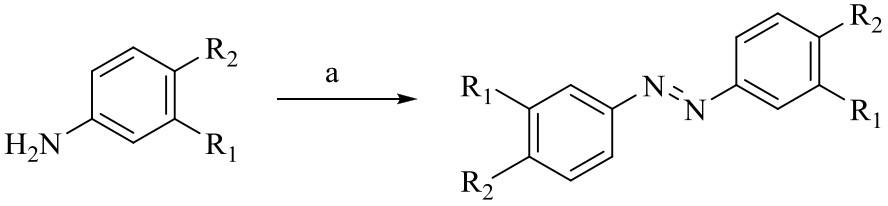

80 R_1 = H, R_2 = Cl
83 R_1 = , R_2 = Cl
84 R_1 = Cl, R_2 = H
85 R_1 = H, R_2 = F

82 R_1 = H, R_2 = Cl
86 R_1 = , R_2 = Cl
87 R_1 = Cl, R_2 = H
88 R_1 = H, R_2 = F

Scheme 17. *Reagents and conditions*: a) MnO_2, toluene, 110 ^{o}C

Noureldin *et al*. reported the synthesis of azobenzene derivatives **84**, **91**, and **92** from aniline derivatives **83**, **89**, and **90** using supported potassium permanganate in 77-78% yield, respectively (Scheme 18).[79]

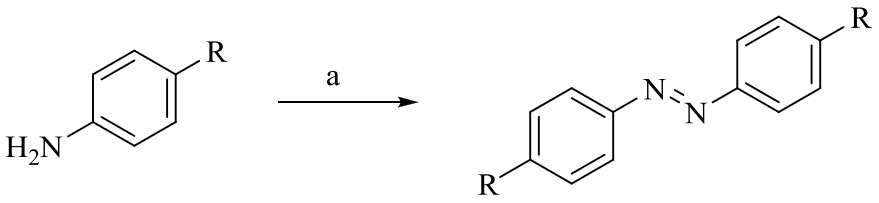

79 R = H
89 R = *sec*-Bu
90 R = I

81 R = H
91 R = *sec*-Bu
92 R = I

Scheme 18. *Reagents and conditions*: a) $KMnO_4$, $CuSO_4 \cdot 5H_2O$, CH_2Cl_2.

Sodium perborate has also been used in the oxidation of aromatic amines. Abelt *et al*. reported the oxidation of aniline derivative **93** with sodium perborate tetrahydrate in the presence of boric acid in acetic acid to give the corresponding azobenzene analogue **94** in 64% yield (Scheme 19).[80]

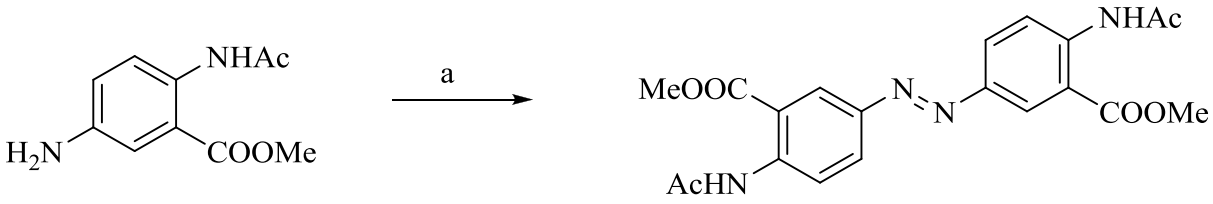

93 **94**

Scheme 19. *Reagents and conditions*: a) $NaBO_3 \cdot 4H_2O$, $B(OH)_3$, AcOH.

2.3.2 Reduction of aromatic nitro compounds

Azobenzene derivatives have been synthesized by the reduction of nitro compounds under various conditions, such as using zinc metal under basic conditions, via catalytic transfer hydrogenation, treatment with NEt_3/Pb and reduction using glucose in a basic medium.[81] Recently, Hecht *et al.* reported the synthesis of azobenzene derivative **95** in 63% yield by bromination of methyl-3-nitrobenzoate **96**, followed by reduction with zinc metal under basic medium (Scheme 20).[82]

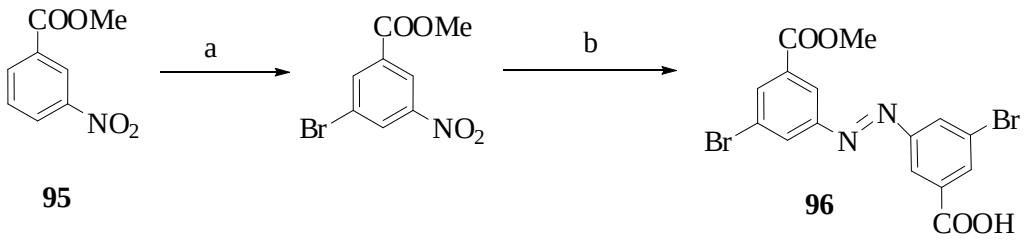

95 **96**

Scheme 20. *Reagents and conditions*: a) Diacetoxyiodobenzene (DIB), H_2SO_4; b) Zn, NaOH, *aq*. EtOH.[82]

2.3.3 Coupling of primary arylamines with nitroso compounds (Mills reaction)

Symmetrical azobenzene derivatives can be synthesized by treating aromatic nitroso compounds with primary arylamines via the Mills reaction.[83] In this manner azobenzene analogue **99** was obtained in quantitative yield by treating nitroso compound **97** and **98** in acetic acid at 60 °C (Scheme 21).[84]

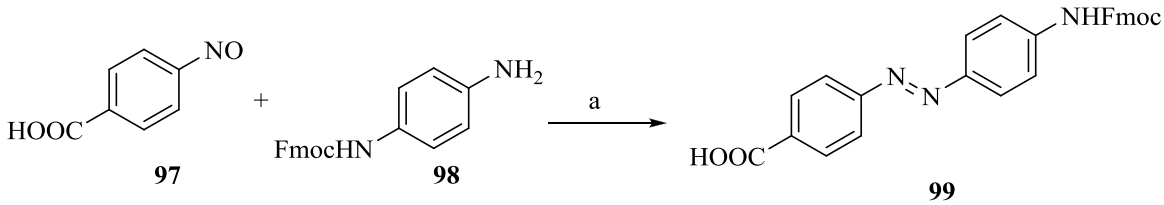

97 **98** **99**

Scheme 21. *Reagents and conditions*: a) AcOH.

2.3.4 Diazo-coupling via diazonium salts

One of the most common approaches towards the synthesis of symmetrical azobenzene derivatives is to couple diazonium salts with a nucleophilic aromatic compound in an acidic or basic medium.[85] Yang *et al*. reported the synthesis of azobenzene derivative **100** by treating phenol **101** and diazonium compound **102** in sodium acetate (Scheme 22).[86a, 86b]

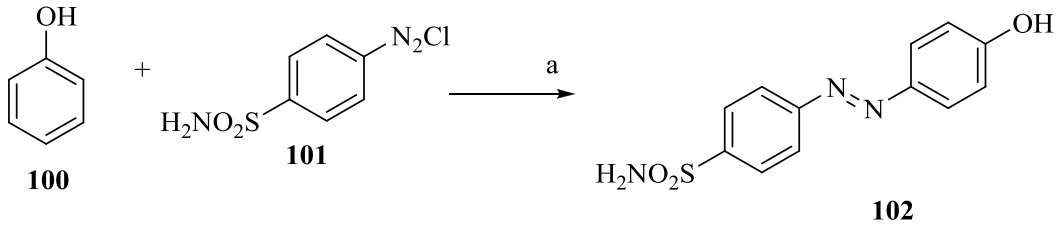

100 **101** **102**

Scheme 22. *Reagents and conditions*: a) AcONa.[86]

2.3.5 Oxidation of hydrazo derivatives

Azobenzene derivatives have also been prepared through the oxidation process of hydrazo compounds with H_2O_2, MnO_2, sodium hydroxide, and ferric chloride.[83] As an example, oxidation of hydrazobenzenes **103-105** were effected with pyridinium tribromide and *t*-BuOCl to give the corresponding azobenzene **106-108** in 70% yields. However, selenium containing hydrazobenzene **108** was not oxidised with *t*-BuOCl (Scheme 23).[87]

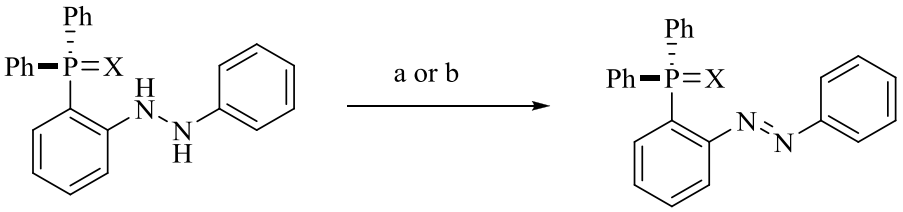

103 X = O
104 X = S
105 X = Se

106 X = O
107 X = S
108 X = Se

Scheme 23. *Reagents and conditions*: a) $pyH^+ Br_3^-$, $CHCl_3$; b) *t*-BuOCl, toluene.

2.3.6 Reduction of azoxy derivatives

Various metals have been employed to deoxygenate azoxybenzene derivatives. Yus *et al*. reported the reduction of azoxy compounds **109** and **110** using $NiCl_2$/Li/DTBB (4,4'-di-*tert*-butylbiphenyl) as reducing agents to obtain corresponding azobenzene derivatives **111** and **112** in 83 and 79 % yields, respectively (Scheme 24).[88]

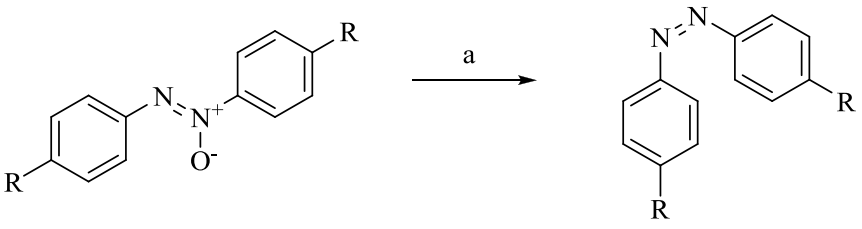

109 R = H
110 R = OMe

111 R = H
112 R = OMe

Scheme 24. *Reagents and conditions*: a) $NiCl_2 2H_2O$, Li, DTBB, THF.

CHAPTER-3 Application of azobenzene as a photoswitch

3.1 Photocontrol of functions of nucleic acids

The photocontrol of nucleic acid functions is achieved with mainly two approaches: 1) using a photo-switchable molecule that can interact with oligonucleotides and 2) tethering a photoswitch molecule to the oligonucleotide covalently.

Recently, Baigl *et al*.[89] reported the synthesis of photosensitive cationic surfactants AzoCx **113** (Figure 23) with varying hydrophobic tail lengths. These surfactants were used as photosensitive nucleic acid binders (pNABs) to photo-control the conformation of DNA. The study showed that addition of the *trans*-isomers of various AzoCx compounds resulted in more compact DNA compared to their *cis*-isomers. Increase in hydrophobicity of AzoCx resulted in enhanced ability to compact DNA, however this increase in hydrophobicity greatly limited the potential for reversible photo-control of conformation of DNA.

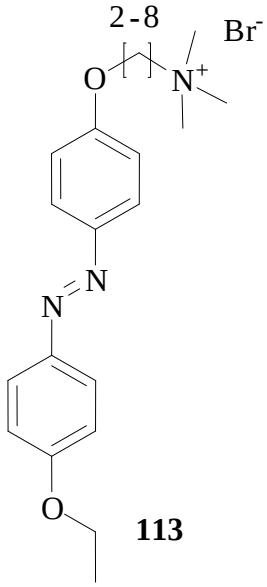

113

Figure 23. Chemical structure of AzoCx.

In a similar study reported by Baigl *et al*.[90] pNABs were used for sequence-independent, reversible photo-control of transcription and gene expression. As a pNAB, azobenzene trimethylammonium bromide surfactant (AzoTAB) was used. AzoTAB is a cationic surfactant with an polar tail which undergoes *trans* to *cis* isomerization at 364 nm. This study showed photoregulation of binding affinity of AzoTAB with nucleic acids. Binding of AzoTAB to nucleic acids resulted in structural changes, and thus affected processes such as transcription and translation. It was demonstrated that *in vitro* production of RNA, expression of GFP, and EGFP expression were successfully inhibited in the dark and restored back to normal upon exposure to light at 365 nm in the presence of AzoTAB. Changes in the conformation of DNA due to binding of AzoTAB upon exposure to light led to structural changes in the DNA recognition sites for proteins binding, thereby regulating the gene activity in an efficient, reversible and sequence-independent manner (Scheme 25).[90] Addition of AzoTAB resulted in formation of compact DNA. This structural change in DNA led to the inhibition of transcription. However, upon exposure to UV light, the AzoTAB isomerizes to the *cis*-form. Due to the bent conformation of the *cis*- isomer, the AzoTAB cannot stack properly between the nucleobases in the DNA thus resulting in the loss of compactness in the DNA. This conformational change in DNA thus favours transcription.[90]

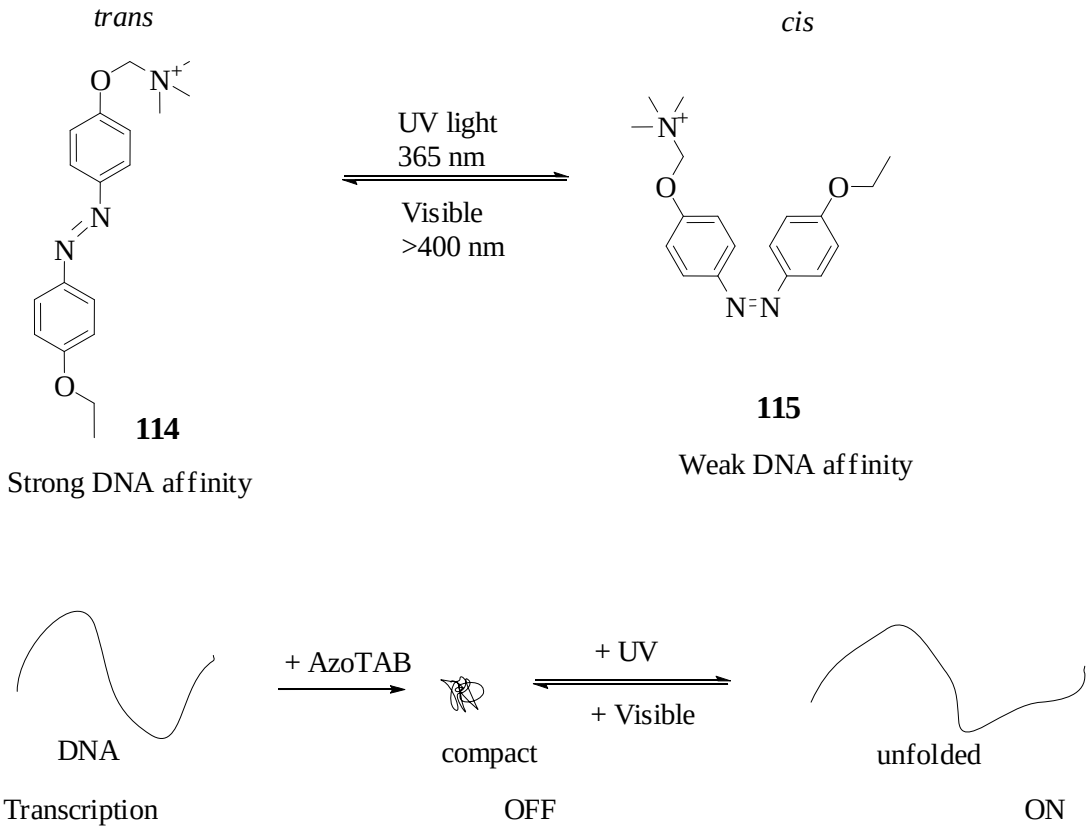

Scheme 25. The conformation and transcription activity of genomic DNA is controlled by UV irradiation in the presence of the photosensitive condensing agent AzoTAB.[90]

RNA aptamers are short oligonucleotides of RNA with high specific binding affinity to a target molecule. Nakatani *et al*.[91] synthesized a short peptide sequence incorporating azobenzene (Lys-Arg-azobenzene-Arg, KRAzR **116**, Figure 24) to photoregulate the binding of RNA aptamers to the modified peptide sequence.

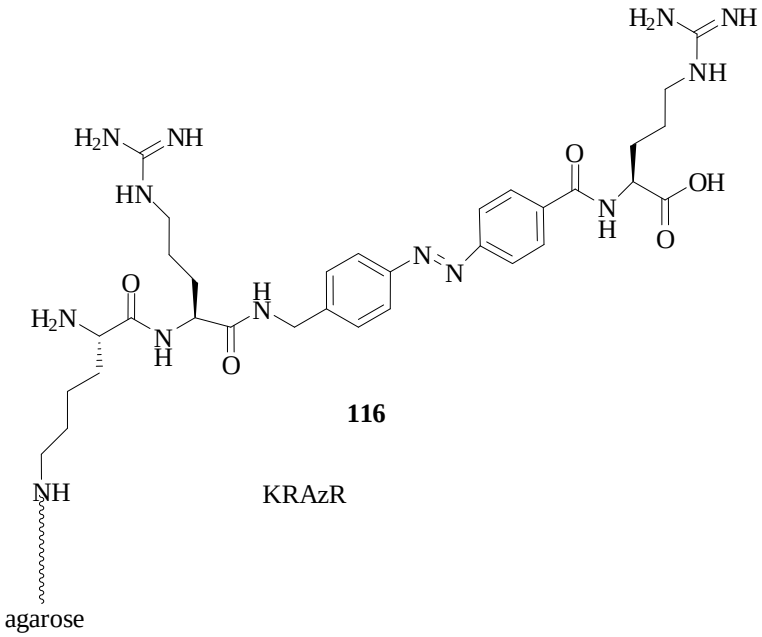

Figure 24. Chemical structure of photoresponsive peptide KRAzR. KRAzR was immobilised to *N*-hydroxysuccinimide (NHS)-activated agarose through the ε-amino group of the lysine residue.[91]

Upon photoirradiation at 360 nm of KRAzR-immobilized on a gold surface, the binding of RNA aptamers to the surface was decreased significantly; however, this binding was restored upon exposure to light at 430 nm. When the azobenzene exists in *trans*-isomer form, but not in the *cis*-form, the RNA aptamer's binding to the surface was induced. From this study a plausible secondary structure of aptamers specific to the *trans*-photoresponsive peptide was identified.[91]

3.1.1 Photoregulation of DNA hybridization by azobenzene

DNA hybridization is a natural process where two complementary strands join together to form duplex DNA. Nucleic acid hybridization is responsible for genomic rearrangements via both homologous and site-specific recombination. Nucleic acid hybridization is a fundamental tool in molecular biology to detect specific DNA sequences. It is also an integral part of processes such

as polymerase chain reaction (PCR). Therefore regulation of nucleic acid hybridization in a spatio-temporal fashion will provide more insight into the hybridization process and gene expression. One way to achieve spatio-temporal control is by using light.

Nakatani *et al*.[92] reported an approach to photo-control duplex formation of two natural, unmodified ssDNA sequences containing a G-G mismatch. In their study, azobenzene was modified with a naphthyridine carbamate dimer. The naphthyridine carbamate dimer selectively binds to the 5'-CGG-3'/5'-CGG-3' sequence, which involves a G-G mismatch flanked by two C-G base pairs. The study showed that the *cis*-form of the azobenzene derivative favoured the hybridization of DNA strands despite of the G-G mismatch. It was noted that hybridization of these sequences containing the mismatch did not occur spontaneously in the absence of naphthyridine carbamate dimer (Figure 25).[92, 93]

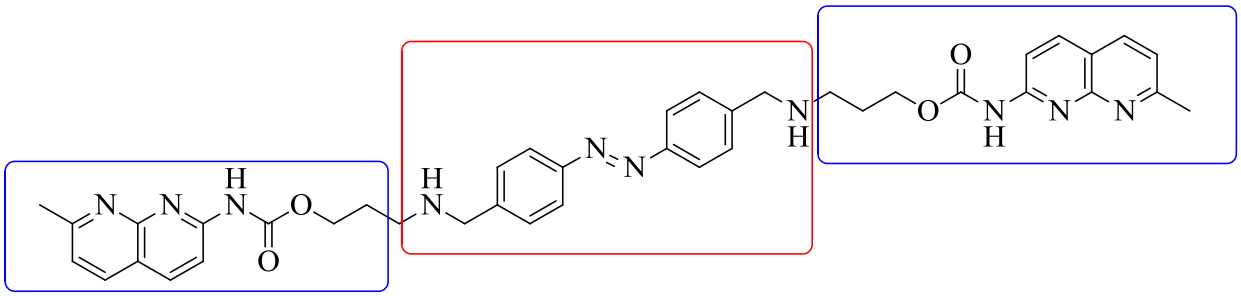

Azobenzene nathathyridine carbamate dimer

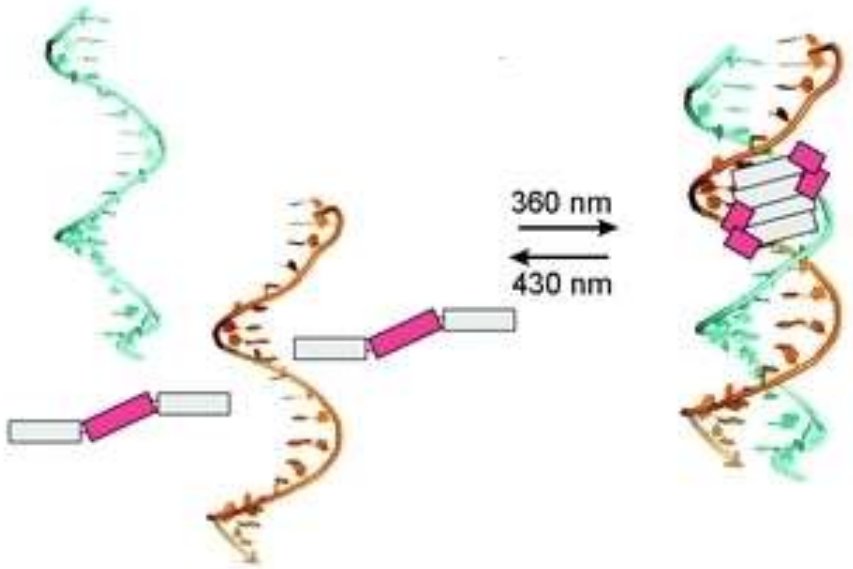

Figure 25. Photocontrol of duplex formation by modified azobenzene napthathyridine carbamate dimer.[92, 93]

In 2007 Komiyama *et al.*[94] reported the synthesis of azobenzene tethered to DNA, for the photoregulation of duplex formation through *trans*-*cis* isomerization of azobenzene. In this approach, the azobenzene monomer was synthesized for the incorporation in DNA. Thus, 4-(phenylazo) benzoic acid **117** was first linked to D-threoninol **118**. The resulting D-threoninol linked azobenzene was then used to prepare azobenzene phosphoramidite monomer **121** (Scheme 26).[94] D-Threoninol, instead of L-threoninol was employed because L-threoninol was found to lower the stability of the duplex significantly, even in the *trans*-form.

Azobenzene monomer **121** was installed at any selected position using phosphoramidite chemistry-based solid phase synthesis.

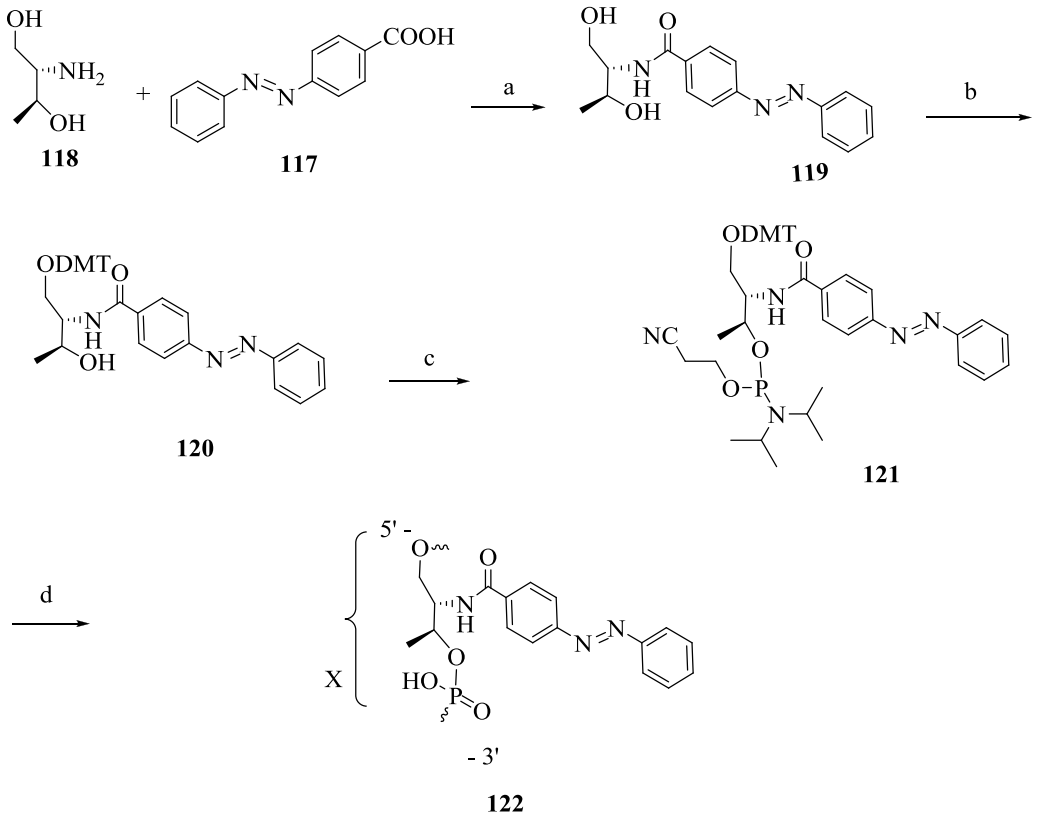

Scheme 26. *Reagents and conditions:* a) DCC, 1-hydroxybenzotriazole, DMF, b) DMT-Cl, 4-DMAP, pyridine, CH_2Cl_2, c) 2-cyanoethyl *N',N',N',N'*-tetraisopropylphosphoramidite, 1*H*-tetrazole, MeCN, d) Incorporation of azobenzene phosphoramidite monomer **121** into oligonucleotides using solid-phase synthesis.[94]

Asanuma *et al*. reported the synthesis of 20-mer oligonucleotides and photo-regulation of DNA hybridization through incorporation of nine azobenzene residues. The azobenzene residues are

intercalated between the adjacent base pairs. Owing to the planar conformation of azobenzene in its *trans*-form, duplex formation is stabilised via base stacking interactions.[94, 95] Conversely, the non-planar conformation of *cis*-form of azobenzene results in destabilization of the duplex owing to steric hindrance, thus favouring dissociation of duplex (Figure 26a).[94] To achieve efficient photoregulation of duplex formation, incorporation of multiple azobenzene units (**X**) was recommended (Figure 26b).

The percentage of hybridization was quantified using a FRET pair consisting of fluorescein (FAM) attached to the 3'-end of the unmodified oligomer and a fluorescent quencher (Dabsyl) attached to the 5'-end of the modified oligomer. When the solution containing the azobenzene-modified strand and its complementary sequence is irradiated with visible light, azobenzene adopts the *trans*-form. Owing to the planar structure of *trans*-azobenzene, the modified and complementary strands are annealed together and thus the fluorescence from the FAM is quenched by the Dabsyl.[94] However, the fluorescence is regenerated when the solution containing the azobenzene-modified strand and its complementary sequence was irradiated with UV light, due to isomerisation of azobenzene from the *trans*- to the *cis*-form.

a)

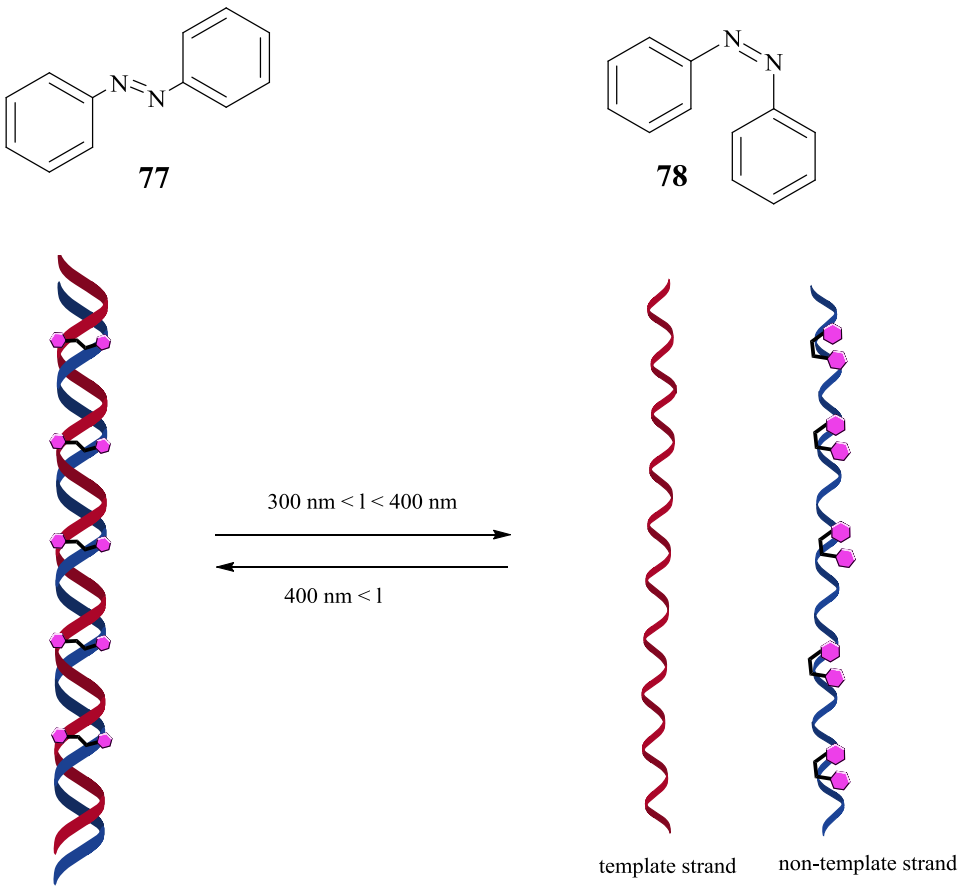

b)

Figure 26. a) The photoregulation of DNA hybridization through incorporating azobenzene residues into oligonucleotides (X: azobenzene units); b) Sequence of FRET pair used in the incorporation of multiple azobenzene moieties.[94]

In addition, photoisomerisation of azobenzene also affected the melting temperature of DNA duplexes. The incorporation of azobenzene units in the oligomer distorted the duplex due to the asymmetry of the strands; however the melting temperature was not significantly affected because the distortion effect is countered by the increased stacking interactions.

When the sample containing the azobenzene-modified strand and its complementary sequence was exposed to UV light at 37 ^{o}C, partial isomerization of azobenzene to its *cis*- form (50%) was observed. At temperatures (e.g. 37 ^{o}C) lower than the melting temperature of the *trans*-form (57.6 ^{o}C), the photoisomerization from the *trans*- to *cis*- form is hindered, due to formation of relatively stable duplex. However, when the solution containing the azobenzene-modified strand and its complementary sequence was exposed to UV light at 60 ^{o}C, about 70 % conversion from *trans* to *cis* was observed, which resulted in approximately 85% dissociation of duplex.[94]

3.1.2 Photoregulation of transcription by T7-RNA polymerase

T7-RNA polymerase is an enzyme responsible for the synthesis of mRNA from duplex DNA via transcription. Tethering azobenzene units to the promoter region of T7-RNA polymerase allows reversible photo-regulation of the transcription process. The promoter region of T7-RNA polymerase consists of two functional regions: the RNAP recognition region (from -11 and -4 site, also known as the loop binding region, Figure 27b), and the unwinding region (from -4, and -1 site, Figure 27b).[96]

Asanuma *et al.* introduced azobenzenes into the specific T7 promoter regions, thereby efficiently photoregulating the transcriptional activity of T7-RNA polymerase (Figure 27a).[94, 96] For effective photo-regulation of transcription, two azobenzene units are incorporated between the -3 and -4 sites (unwinding region loop) and between the -9 and -10 sites (loop-binding region) in the non-template strand of the T7 promoter region, keeping the template strand intact (Figure 27b). The experiment was performed below the melting temperature of the *trans*-form isomer, thus the duplex remains intact throughout the photoreaction. However during the photoisomerization from *trans*- to *cis*-form, the local environment around the duplex is distorted, thus affecting the binding mode of the T7-RNA polymerase with the T7-promoter region.[94, 96]

Upon exposure to visible light, the *trans*-form suppresses the transcriptional activity of the T7-RNA polymerase by affecting its binding to the T7-promoter region. The transcriptional activity was restored upon irradiation with UV light (Figure 27c). After the UV irradiation the transcriptional activity was found to be 7-8 times as fast as after visible-light irradiation. (Figure 27c).[94, 96]

a)

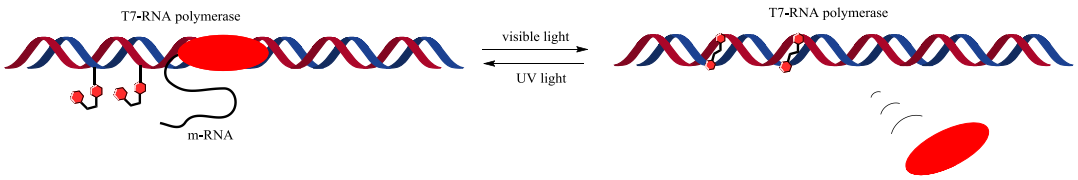

b)

T7 promoter region

-17 -11 -7 -4 -1

Non-template 5' - **ATAATACGA**X**CTCACT**X**ATA**GGGAGGAAGATAGAGCA - 3'

template 3' - **TATTATGCT GAGTGA TAT**CCCTCCTTCTATCTCGT - 5'

c)

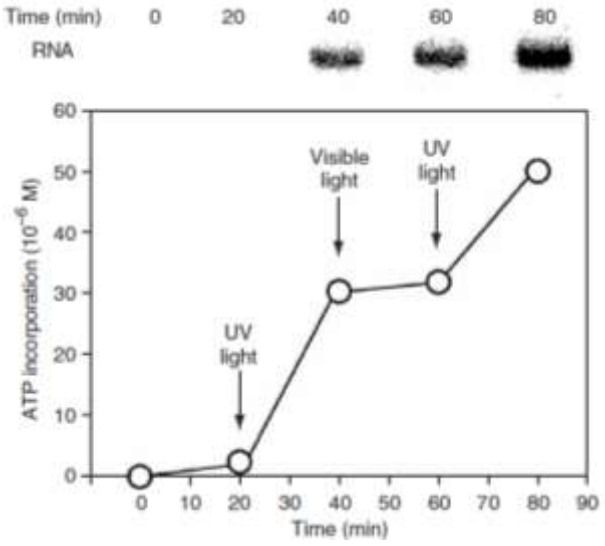

Figure 27. a) Photoregulation of transcription by T7-RNA polymerase using azobenzene tethered DNA, b) Sequence design of the photoresponsive T7 promoter and c) Photoswitching of transcription by T7-RNA polymerase (X : azobenzene units).[94]

Although azobenzene has been employed as a photoswitch for the reversible photoregulation of nucleic acids, the overlapping of absorption spectra of two isomers (Figure 21) has hampered its photoisomerization efficiency. To use azobenzene as a photoswitch, one has to switch azobenzene back and forth in the $S_1(n\pi^*)$ and $S_2(\pi\pi^*)$ bands. The latter band is located in the UV-region, which readily causes damages to biomolecules such as DNA and RNA.[61, 75] However it is possible to derivatize azobenzene to achieve reversible photoswitching without UV- light.[61] In addition, azobenzene has relatively low quantum yields for direct photoisomerization (*trans*-*cis*, and *cis*- *trans*).[97]

3.2 Cyclic or Bridged Azobenzene

3.2.1 Photoisomerization of cyclic azobenzene

Among the many azobenzene analogues known in the literature, the cyclic ("bridged") azobenzene (cAB), 5,6-dihydrodibenzo[c,g][1,2] diazocine compound is of particular interest.[75(i)] In cyclic azobenzene, the two phenyl rings are confined with an ethylenic bridge. Conversely from azobenzene, in which the *trans*-form is more stable, the *cis*-isomer (*Z*, **123**) of cyclic azobenzene is more stable compared to *trans*-isomer (*E*, **124**). Cyclic azobenzene has been known for more than 100 years but attracted little attention until very recently, when its potential as a molecular photoswitch was discovered by Siewersten *et al*.[75(ii)]

The photochromic properties of cAB is much more favourable for photoswitching compared to plain azobenzene (AB).[61,75] The *trans*-isomer of cAB is switched with blue light (370-400 nm) to the *cis*-isomer with an efficiency >90%, and switched back to *cis*-isomer in ~100 % efficiency with green light (480-550nm) (Scheme 27).[61, 75]

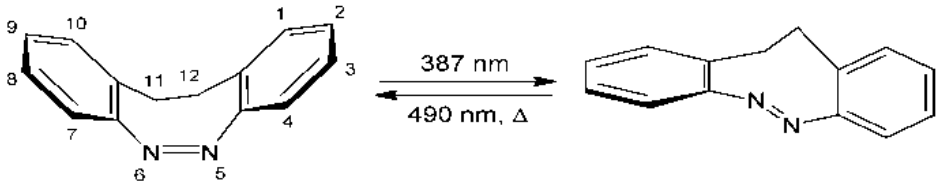

cis-isomer, **123** *trans*-isomer, **124**

Scheme 27. Photoisomerization of cyclic azobenzene.[61]

A UV spectroscopic study of unmodified cyclic azobenzene showed that the *trans*-isomer exhibits a characteristic absorption band with a peak at 404 nm due to its nπ* excitation band.[98] Upon irradiation with blue light at 385 nm, the absorption band at 404 nm almost disappears, and a more intense absorption band at 490 nm was observed (Figure 28). The photoisomerization quantum yields in the forward and backward directions are 72±4% and 50±10%, respectively.[98]

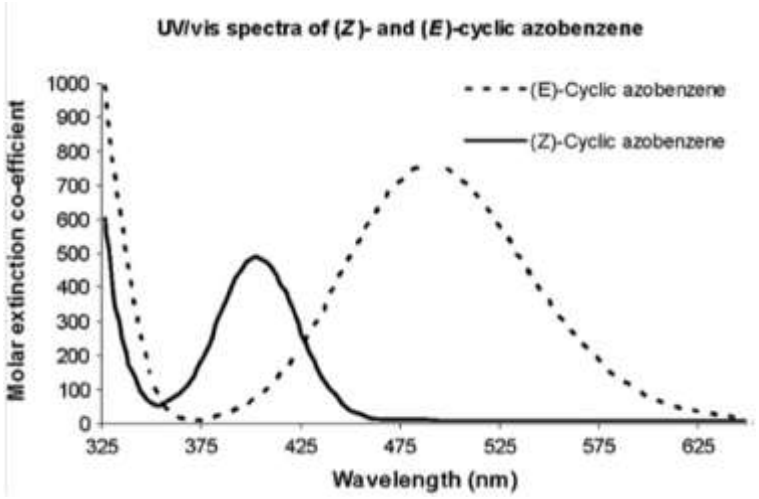

Figure 28. UV/Vis absorption spectra of cyclic azobenzene **123** and **124** (Solid line: (*trans* or *Z*)-isomer; dash line: (*cis* or *E*)-isomer.[61] (Reprinted with permission from Siewertsen, R.; Neumann, H.; Buchheim-Stehn, B.; Herges, R.; Näther, C.; Renth, F.; Temps, F. *J. Am. Chem. Soc.* **2009**, *131*, 15594-15595).

Efficient photoswitching of cAB in *trans*-*cis* and *cis*-*trans* directions can be accomplished with visible light, contrary to the photo-switching of linear azobenzene that requires irradiation with light in the UV region for the *trans*-*cis* isomerization.

The highly efficient photoswitching with a photoconversion yield greater than 90% and distinctive absorption bands for *trans*- and *cis*- isomers make this molecule a very attractive and invaluable tool for designing shape switchable molecules.[99]

Because of these characteristic properties, a considerable amount of interest has been invested towards understanding this new photoswitch, particularly from theoretical point of view.[100, 101] Like linear azobenzene, the clean photoisomerization property of cyclic azobenzene can also be exploited to regulate the nucleic acid functions such as transcription, hybridization, and gene expression using light.

3.4 Proteins

Proteins are made up of amino acids covalently linked by polypeptide bonds. Proteins are synthesized *in vivo* in a process called translation. Proteins play diverse roles, such as forming cytoskeleton structures, catalyzing metabolic reactions, signal transduction, and transporting molecules from one location to another location in multicellular organisms.[102]

Protein structures are characterized at four levels: primary, secondary, tertiary and quaternary. The primary structure of proteins is formed by linear chains of amino acid residues along the polypeptide chain.[103 (i)] Every protein is defined by a unique sequence of amino acid residues and all subsequent levels of organization (secondary, tertiary and quaternary) rely on the primary structure. Polypeptide chains are organised into secondary structures via hydrogen bonding patterns between the backbone peptide bonds.[103 (i)] The most common types of secondary structure are the right-handed α-helix, parallel and antiparallel β-pleated sheets (Figure 29).

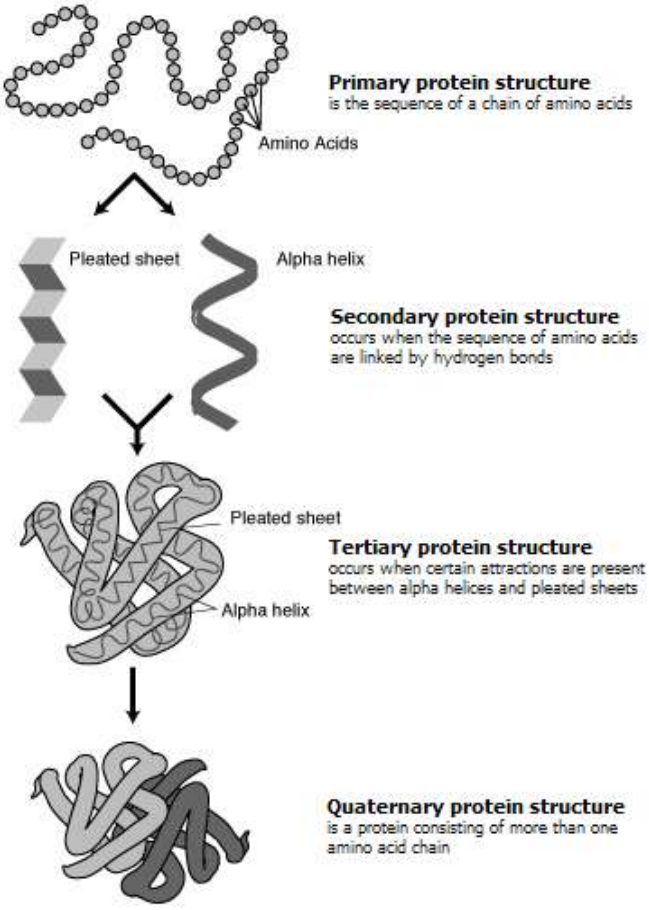

Figure 29. Graphical representation of primary, secondary (*β*-sheet and α-helix), tertiary, and quaternary structure of protein ("Courtesy: National Human Genome Research Institute").

Tertiary structure of a protein is the three-dimensional structure formed by the packing of protein secondary structures into compact units.[103 (ii)] Three-dimensional structures in proteins are maintained by ionic bonds, hydrogen bonds, -S-S- bridges, van der Waals forces and hydrophobic interactions.[103 (i) (ii)] The first protein whose tertiary structure was determined is myoglobin, an oxygen-binding protein consisting of 153 amino acid residues.[103(i)] Its structure was deduced from X-ray studies by Kendrew, Perutz *et al*. This study provided not only the first three-dimensional representation of a globular protein but also insight into the important bonding

modes in tertiary structures.[103(ii)] Quaternary structure is formed by bringing multiple protein subunits into a complex. Subunits are held together by noncovalent forces; as a result, oligomeric proteins can undergo rapid conformational changes that affect biological activity.

The secondary structure of proteins creates unique binding pockets for other biomolecules such as DNA and other ligands such as lipids, carbohydrates, flavins, heme group, phosphate group, and metal ions. Interaction of proteins with these ligands constructs many aspects of biological activity. Therefore, by controlling the conformation of proteins, the interaction between ligands and proteins is regulated, thereby affecting a particular function of the protein.

There is a need to understand more about protein-biomolecule interactions and the role of protein conformations in various diseases. Regulation of protein interaction with biomolecules would provide more insight into protein functions and their biological roles. Often the conformational changes produced in large and complex proteins are small, which makes it more difficult to interpret and predict the outcome. Incorporation of light-sensitive molecules into proteins would provide a means to regulate protein structures. In addition, reversible control of protein structures and functions via photoinduced isomerisation can be achieved by employing reversible photoswtiches such as azobenzene.

3.4.1 Incorporation of cyclic azobenzene analogues into proteins

Recently, Woolley *at al*. reported photocontrol of peptide conformations with a bi-functional bridged azobenzene derivative.[104] In this study, a thiol-reactive cross linker **132** was synthesized from bromonitrobenzyl **125** via *p*-acetamido substitution. The thio-reactive cross linker was then introduced into biomolecules such as peptides and proteins (Scheme 28).[104]

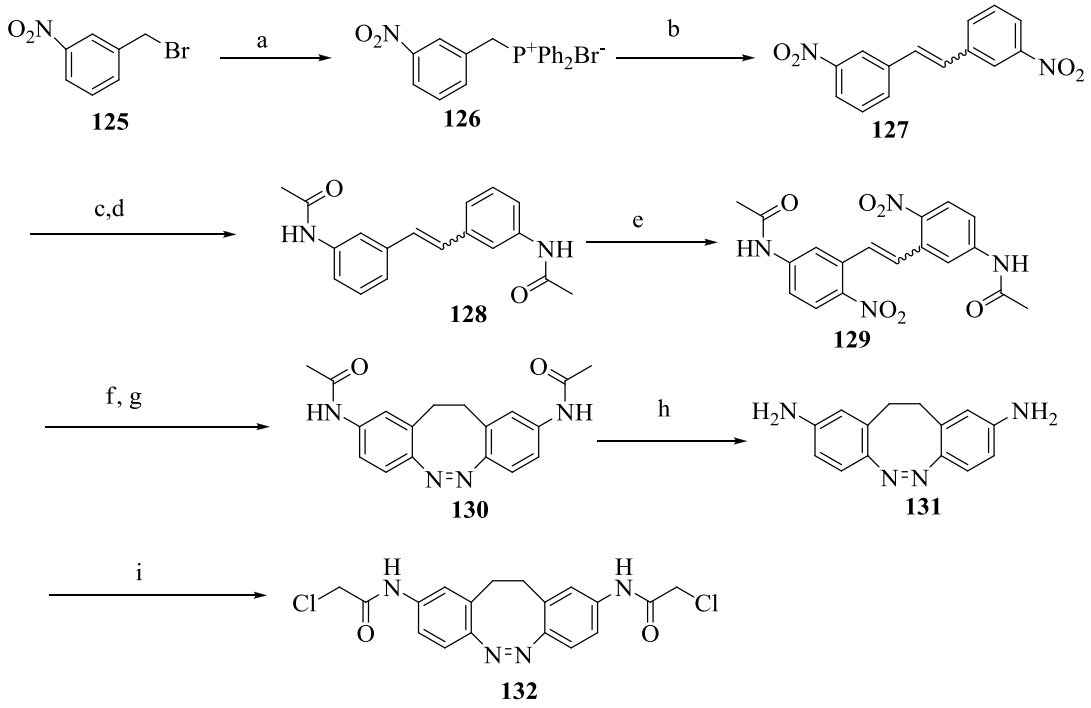

Scheme 28. *Reagents and conditions:* a) PPh_3, toluene, reflux, 96%; b) *t*-BuOK, 3-nitrobenzaldehyde THF, 0 ^oC RT, 57%; c) H_2, Pd/C, MeOH, 90%; d) Ac_2O, Py, THF, 78%; e) KNO_3, $AcOH/H_2SO_4$ (conc.), 0 ^oC, RT, 31%; f) $Ba(OH)_2 \cdot 8H_2O$, Zn, EtOH, reflux; g) HgO, EtOH, reflux (overall yield for two steps 8%); h) KOH, MeOH, reflux, 70%; i) chloroacetic anhydride, Py, diethyl ether, 50%. Py = pyridine.[104]

The characteristic photoisomerization of bridged azobenzene was used to control the conformation of peptide FK-11, which is known to form a helical conformation in aqueous solution. In this peptide, cystine residues were cross-linked intramolecularly with a thiol-reactive azobenzene-based photoswitch. Upon exposure to violet light (407 nm), the peptide cross-linked with the thiol-reactive species, isomerizes from the *cis*-form to the *trans*-form, resulting in an increase in helix content.Irradiation with green light (518 nm) resulted in a decrease in helix content due to isomerization of the *trans*- to the *cis*-form (Figure 30).[104]

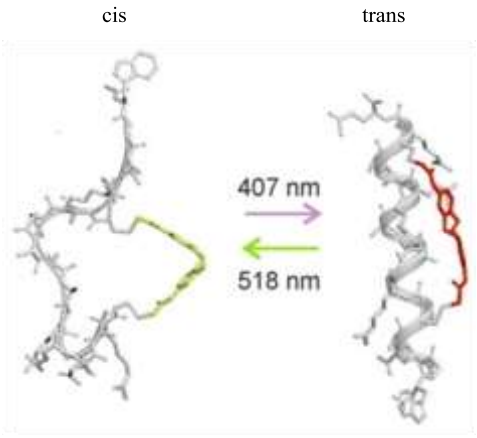

Figure 30. Models showing FK-11 (AcWGEACAREAAAREAACRQ-NH_2) crosslinked with **132** in the *cis* (left) and *trans* (right) conformations.[104]

One of the major problems with this system in an *in vivo* experiment is the instability of the azobenzene inside the cellular environment and its sensitivity to enzymes, such as glutathione, which can readily reduce azobenzene.[104] In the study performed by Woolley *et al*., the *cis*-isomer was found to be completely stable to overnight incubation with 10 m*M* reduced glutathione, In the contrary the *trans*-isomer exhibited some photo bleaching in the presence of reduced glutathione in a concentration dependent manner.[104]

3.5 Polymers

3.5.1 Incorporation of azobenzene analogues into polymers

By attaching a photoresponsive moiety to the polymer, the chemical structure of the polymer surface can be modified.[105] In the past several decades, progress has been made from the synthetic, functional design and application of photo-controllable polymers. Among several approaches, azobenzene-containing polymers have gained significant interest.

The characteristic photoisomerization of azobenzene has been used to modulate the chemical structure of polymers, which in turn regulates the surface morphology of the polymer.[105, 107-108]

Several experiments have been carried out to investigate the mass migration phenomenon which occurs at the surface of polymer-films containing azobenzene when irradiated with light. Eisenbach *et al.* reported for the first time the reversible photoinduced expansion and contraction in an azobenzene containing elastomer.[109]

Very recently, Ikeda *et al.*[110] reported the bending motion of liquid crystals containing azobenzene elastomer (Figure 31). In this study, thick liquid crystalline elastomer (LCE) was employed to avoid the penetration of UV light to the back of the film. The molecules in the elastomer were aligned anisotropically by rubbing. Upon irradiation with light, photoisomerization occurs only near the surface of the film on the side of incident light. The photoisomerization resulted in shrinkage or expansion of the surface of the film that results in the bending motion of the elastomer (Figure 31).[110]

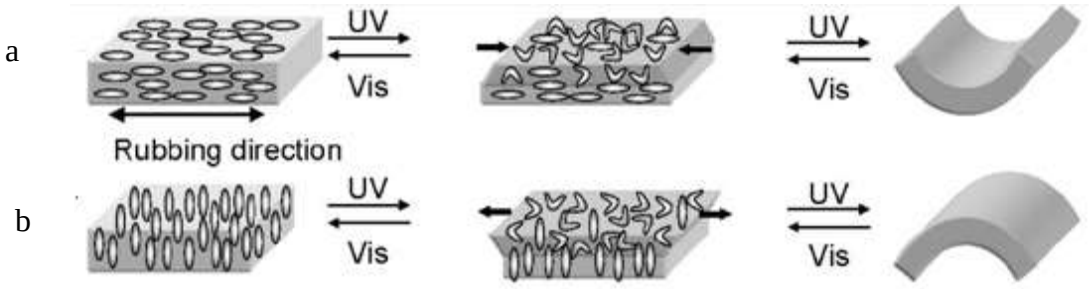

Figure 31. Schematic figure of phototriggered film bending a) homogeneously and (b) homeotropically aligned thick film, respectively.

As shown in Figure 31a,[110] the deformation of homogeneously aligned LCEs can be induced by actinic light, bringing about photomechanical and photomobile properties of LCEs. Upon irradiation, photomodulation of LCEs occurs only in the surface region because of the large molar extinction coefficient of photochromic LCs. Light cannot penetrate through a thick film (thickness > 10μm), and induces the volume change only in the film surface. When the alignment of LC molecules is parallel to the surface, volume contraction is observed just along the pre-aligned direction, contributing to the anisotropic bending behaviour towards a light source.

In contrary, volume expansion is brought about when the LC molecules are aligned perpendicularly to the surface, resulting in different bending behavior away from the light source (Figure 31b).[110] Furthermore, the photomechanical behavior is reversible if azobenzene molecules are used as photoresponsive mesogens. By this way light energy can be directly transferred into mechanical energy, which attracts much attention in LC research.

Hu *et al.*[111] recently reported azobenzene functionalized hydroxypropyl methylcellulose (AZO-HPMC **133**, Figure 32) polymers and their α-cyclodextrin (*α*-CD) complexes. Incorporation of the azobenzene chromophore into the polymer is confirmed by FT-IR, ^{1}H NMR, and FT-Raman

spectroscopies. The study showed that the interaction of α-CD with the side groups of azobenzene on AZO-HPMC improved the water solubility of AZO-HPMC polymer. The interaction of *α*-CD with side groups of azobenzene is employed to control the rheological properties of the AZO-HPMC polymer.

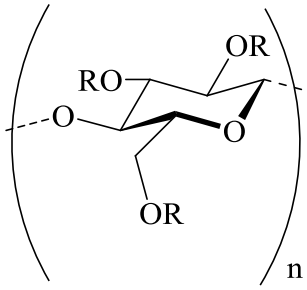

133

R = H, CH_3, or $CH_2CH(OH)CH_3$

Figure 32. Chemical structure of hydropropyl methylcellulose.[111]

The AZO-HPMC polymers with varying azobenzene content were prepared by mixing HPMC-OH **134** and 4-phenylazobenzoyl chloride **135** (Scheme 29).

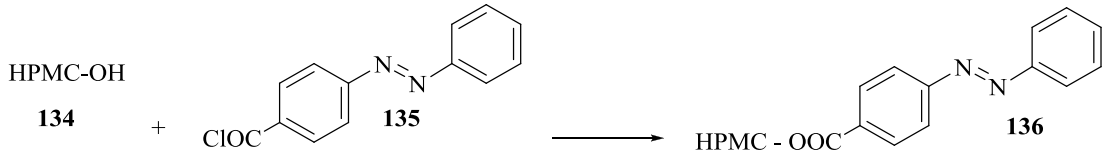

Scheme 29. Synthesis of AZO-HPMC polymers.[111]

In the absence of *α*-CD, the photoisomerization of azobenzene from the *trans*-form to the *cis*-form resulted in an increase in gelation temperature (Figure 33).

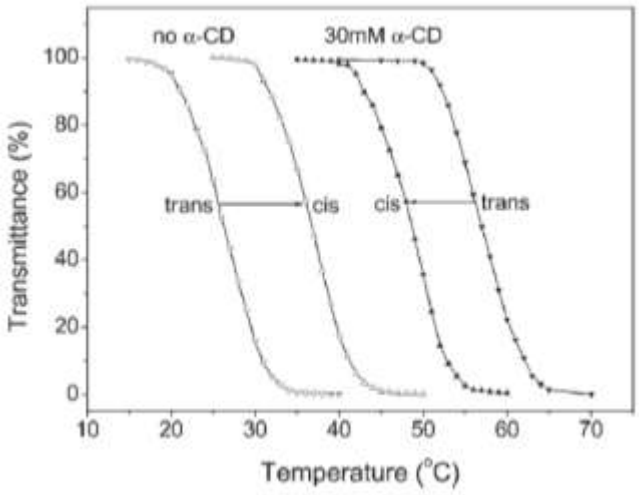

Figure 33. Sol-gel transition of AZO-HPMC polymer in presence and absence of α-CD.

The increase in gelation temperature was due to the higher polarity of the *cis*-form compared to that of the *trans*-form.[111]

In the presence of *α*-CD, however, opposite results were observed, that is, photoisomerization from *trans*- to *cis*-azobenzene resulted in a decrease in gelation temperature. Upon photoirradiation, the *cis*-azobenzene is excluded from the *α*-CD cone, leading to an increase in the hydrophobic character of AZO-HPMC/*α*-CD complex and thus a decrease in the gelation temperature (Figure 34).[111]

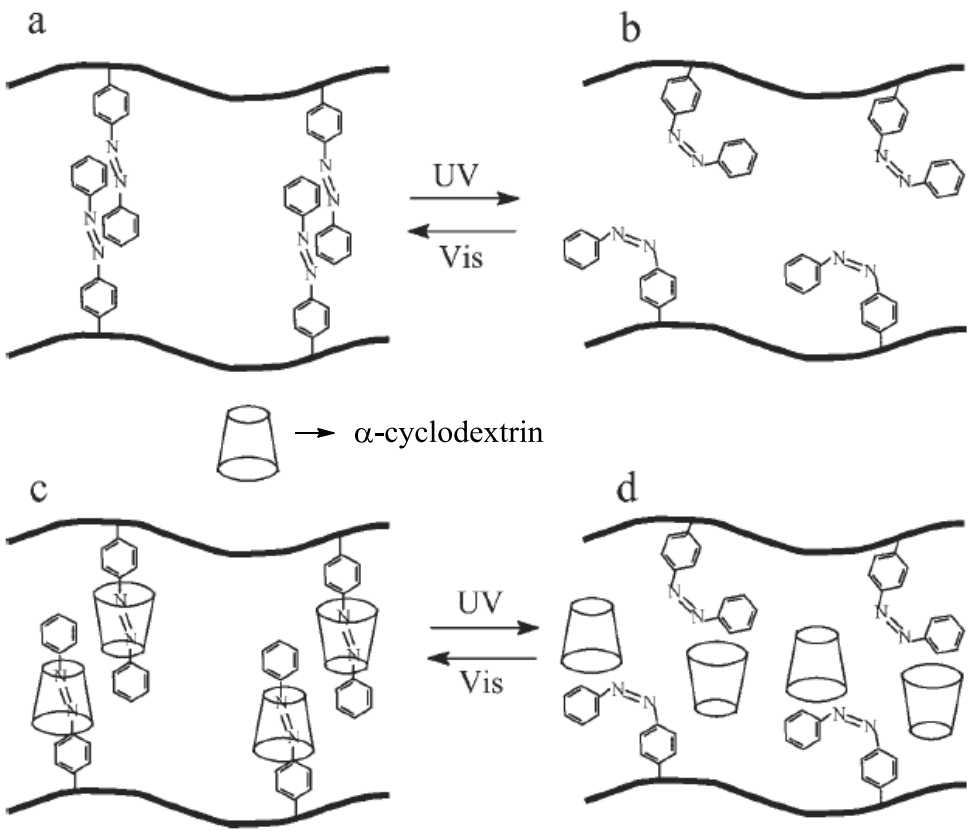

Figure 34. Schematic representation of interaction between *α*-CD and AZO-HPMC polymer in aqueous solution.

3.6 Objectives of the thesis

The objectives of the thesis work are to synthesize suitably derivatized cyclic azobenzene analogues for the incorporation into oligonucleotides, peptides, and polymers. It is anticipated that these covalently linked cyclic azobenzene residues will allow for spatiotemporal control of the structures, properties, and functions of these macromolecules. Emphasis is placed on the incorporation of cyclic azobenzene into oligonucleotides.

3.6.1 Synthesis of cyclic azobenzene analogues for the incorporation into oligonucleotides

In recent years, a significant amount of work has been invested to understand the new photoswitch cyclic azobenzene, particularly from the theoretical point of view.[61] The objective of this project was to improve the yield for the preparation cyclic azobenzene from 2,2'dinitrodibenzyl (4% yield from current synthetic strategy).[75(i), 100] Synthesis of cyclic azobenzene analogues would allow for further incorporation of this cyclic azobenzene into biomolecules. The goal was to synthesize by solid phase DNA synthesis, 20-mer and 35-mer oligonucleotides using a carboxyl cyclic azobenzene analogue. The aim was to synthesize sequences similar to those employed by Asanuma *at al*.[94] in order to compare and contrast the effect of photoisomerization of azobenzene and cyclic azobenzene on DNA hybridization, DNA melting temperature, and T7-RNA polymerase transcription activity.

3.6.2 Synthesis of cyclic azobenzene analogues for the incorporation into peptides

The overall yield for the synthetic strategy developed by Woolley *at al*. for the synthesis of bi-functional cyclic azobenzene derivative was less than 10%.[104] The objective of this project was to improve the overall yield for the preparation of bi-functional cyclic azobenzene in fewer synthetic steps as compared to the synthetic scheme developed by Woolley *at al*., which has 9 synthetic steps. The dicarboxyl cyclic azobenzene analogue will then be incorporated into a short peptide using solid phase peptide synthesis. Following the incorporation, the modified short peptide sequence will then be used to study the effect of photoisomerization on the conformation of modified short peptide.

3.6.3 Incorporation of cyclic azobenzene analogues into polymers

The objective of this project was to incorporate a carboxyl cyclic azobenzene analogue into a polymer (poly(2-hydroxyethyl)methacrylate) to study the effect of cyclic azobenzene photoisomerization on the polymer structure and properties. The percentage incorporation of cyclic azobenzene will be determined by UV/Vis spectroscopy. The goal was to prepare thin films of polymer containing cyclic azobenzene by spin-coating equipment. These thin films will be then used to study the effect of photoisomerization on the surface morphology of the polymer upon irradiation with light of desired wavelength. The structural changes on the surface of thin films of polymers will be studied using scanning electron microscopy.

CHAPTER 4- Results and Discussion

4.1 Synthesis of cyclic azobenzene analogues

Although a number of approaches were reported for the synthesis of azobenzene from arylnitro-compounds with high efficiency,[112, 113] treatment of 2,2'-dinitrodibenzyl **137** under these conditions has invariably failed to give the cyclic azobenzene **140** in sufficient yields.

Cyclic azoxybenzene **140** can also be synthesized from the *N*-nitrosohydroxylamine ammonium salt of 2,2'-dinitrodibenzyl as previously documented (Scheme 30).[114] This literature procedure was not used in the present study as it necessitates an extra step from a commercially available compound.

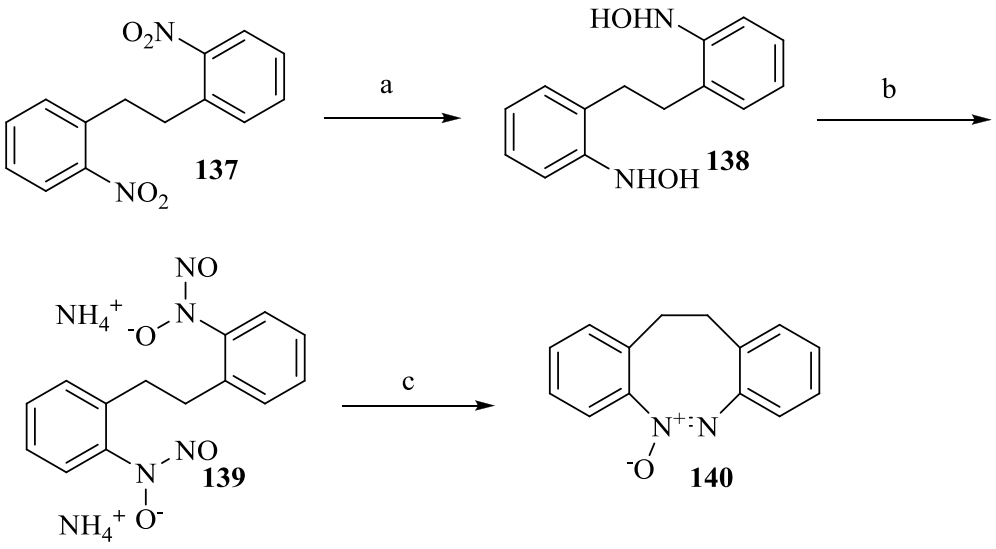

Scheme 30. *Reagents and conditions:* a) 5% Rh-C, $NH_2NH_2.H_2O$, THF, 30 ^oC; b) *n*-BuO-NO, NH_3, Et_2O, 0-10 ^oC; c) Δ or *hv*, EtOH.

When 2,2'-dinitrodibenzyl **137** was treated with zinc powder under neutral pH, cyclic hydrazine 4-(5,6,11,12-tetrahydro-dibenzo[c,g] [1,2]diazocine) **141** (Scheme 31) was formed in moderate yields (up to 70%), however, this transformation was found to be highly dependent on the surface properties and/or impurity of zinc powder, as use of newer batches of zinc powder only gave **141** in very low yields (<5%).

Treatment of 2,2'-dinitrodibenzyl **137** with lead metal at pH 9.5 in methanol gave cyclic azoxybenzene (11,12-dihydrodibenzo[c,g][1,2]diazocine-5-oxide) **140** in moderate yields (61%) (Scheme 31). However the above reaction was found to be dependent on the stirring speed as well as the surface properties and/or impurities in metal compound. For larger scale reactions (more than 2.00 g), the reaction time spans from 2 to 5 days or even longer. When zinc powder was used the reaction time was reduced to 12 h under similar condition (pH 9.5).

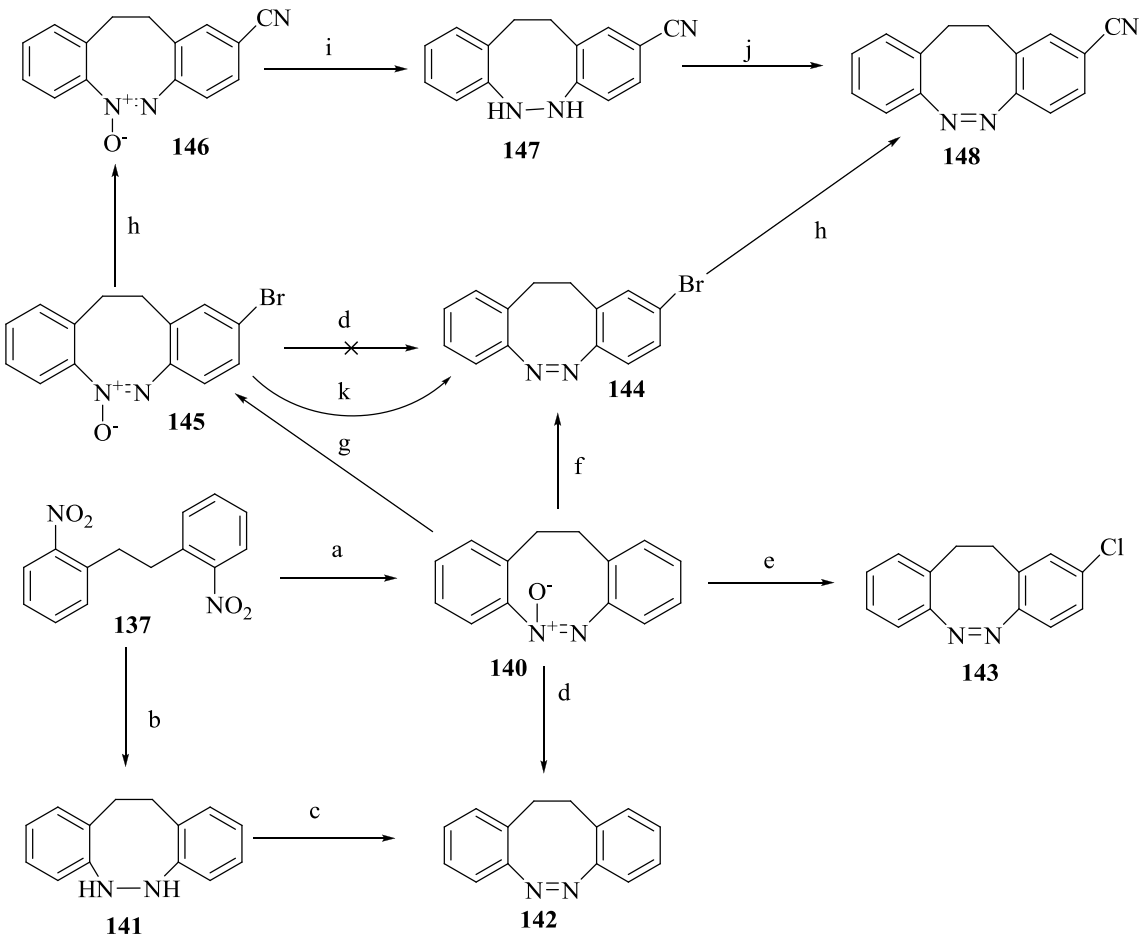

Scheme 31. *Reagents and conditions:* (a). Pb, pH 9.5, MeOH, 65%; (b). Zn, pH 7.0, EtOH, 71%; (c). $TiCl_3$, aq. HBr, H_2O_2, 78%; (d). Ph_3P, $MoCl_2O_2$ $(dmf)_2$, THF, 59%; (e). $AlCl_3$, CS_2, 8%; (f). $AlBr_3$, CS_2, 9%; (g). Br_2, CH_3COOH, 70%; (h). CuCN, DMF, 75%; (i). Al, NH_2NH_2, 64%; (j) $TiCl_3$, HBr, H_2O_2, MeOH; (k) PCl_3, dry benzene, 89%.

The azoxybenzene **140** was subsequently transformed into the corresponding bridged azobenzene **142** in 59% yield through catalytic deoxygenation using triphenylphosphine as oxygen acceptor in the presence of a molybdenum catalyst.[115, 116] Structure of the cyclic azobenzene **142** was confirmed by X-ray crystallography, where the ethylene bridge is disordered over two sets of sites with refined occupancies of 0.552 (14) and 0.448 (14) (Figure 35a).

The azoxybenzene **140** also undergoes concomitant deoxygenation and halogenation when treated with aluminium halide (chloride or bromide) in carbon disulfide[117] to give the corresponding chloro **143** or bromo **144** analogues in poor yields (8 and 9% for **143** and **144**, respectively).

It was found, however, that azoxybenzene **140** can be brominated with bromine[118] to give the corresponding bromoazoxybenzene **145** (2-bromo-11,12-dihydrodibenzo[c,g][1,2] diazocine- 6-oxide) in 70% yield. The identity of bromoazoxybenzene **145** was confirmed by its X-ray crystal structure (Figure 35b), where two independent molecules with slightly different conformations were found in the asymmetric unit.

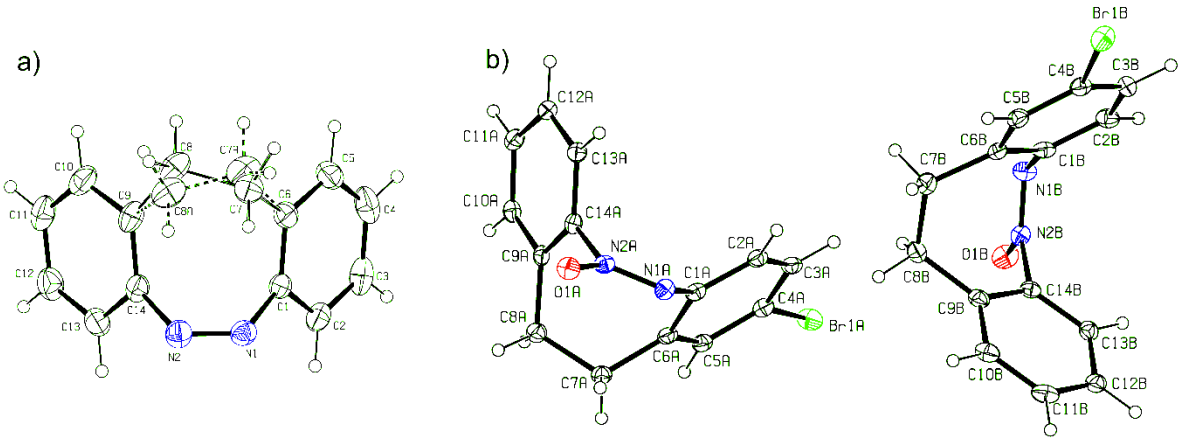

Figure 35. The molecular structure of (a) **142** (the dashed lines indicate the bonds of a minor component of disorder) and (b) **145** (two independent molecules with slightly different conformations were found in the asymmetric unit) with 30% probability displacement ellipsoids (prepared with PLATON).[119]

Interestingly, treatment of bromoazoxybenzene **145** with triphenylphosphine and the molybdenum catalyst failed to give cyclic bromoazobenzene **144**. However, it was found that

treatment of **145** with freshly distilled phosphorus trichloride (PCl_3) in dry benzene gave the corresponding bromoazobenzene **144** in 60% yield.[117] Cyanoazoxybenzene **146** was obtained in 69% yield by treating bromoazoxybenzene **145** with copper (I) cyanide.[120]

Treatment of the latter compound **146** with aluminium and hydrazine hydrate[121] gave a mixture of cyclic cyanoazobenzene **148** and the over-reduced hydrazine **147**, with the latter being a major product. The hydrazine **147** was further oxidised to the corresponding cyclic cyanoazobenzene **148** by treatment with titanium (III) chloride, hydrobromic acid and hydrogen peroxide.[122]

The cyclic cyanoazobenzene **148** was also synthesized by treating **144** with copper (I) cyanide in dry dimethylformamide to obtain **148** in 60% yield. Finally, cyclic cyanoazobenzene **148** was hydrolyzed under basic conditions to give the corresponding carboxylic acid **149** in 78% yield (Scheme 32).

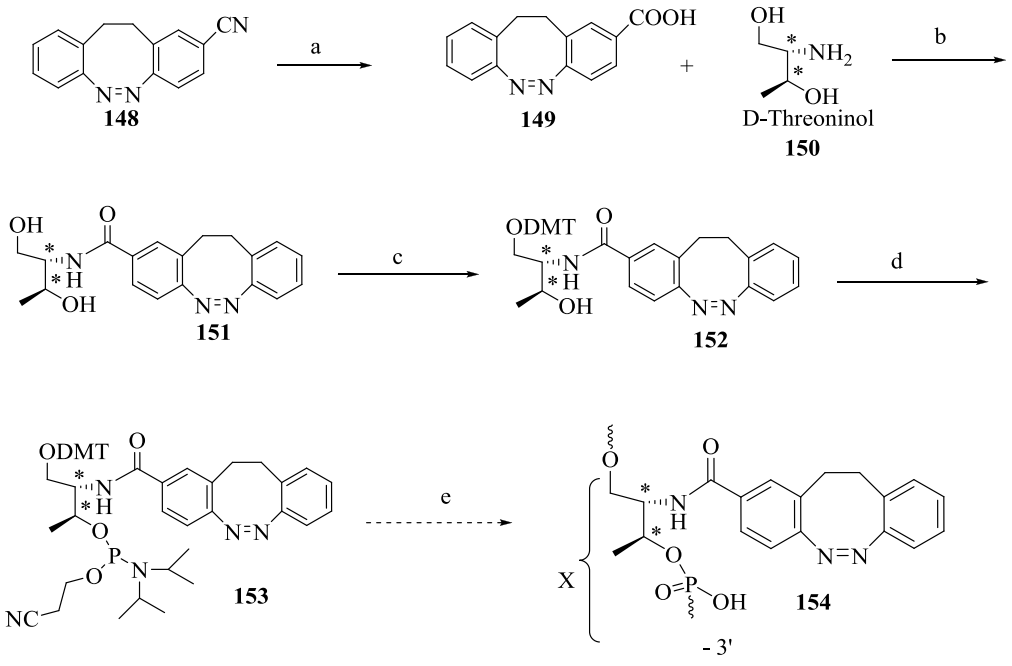

Scheme 32. *Reagents and conditions:* (a). KOH, EtOH, H_2O, reflux, 76%; (b). D-threoninol, DCC, *N*-hydroxysuccinimide, DMF, 93%; (c). DMT-Cl, pyridine, 86%; (d). (2-cyanoethyl)-*N*,*N*-phosphochloridite, *N*,*N*-diisopropyl ethylamine, THF, 67%; (e). Solid phase DNA synthesis.

The cyclic carboxylic analogue **149** was condensed with D-threoninol **150** (D-th) using dicyclohexylcarbodiimide as activator in the presence of *N*-hydroxysuccinimide to obtain D-threoninol-linked cyclic carboxylazobenzene **151** (D-th-cAB).

The corresponding DMT-protected D-th-cAB **152** was obtained in 86 % yield by treating carboxylazobenzene **151** with DMT-Cl in pyridine. Cyclic azobenzene phosphoramidite **153** was synthesized in 67% yield by treating DMT-protected D-th-cAB **152** with the phosphitylation agent (2-cyanoethyl) -*N*,*N*-diisopropylphosphochloridite in the presence of *N*.*N*-diisopropyl ethylamine (DIPEA, Hünigs base) in freshly distilled tetrahydrofuran (THF). As expected, this amidite consists of two diastereomer as indicated by ^{31}P NMR spectroscopy (Figure 36).

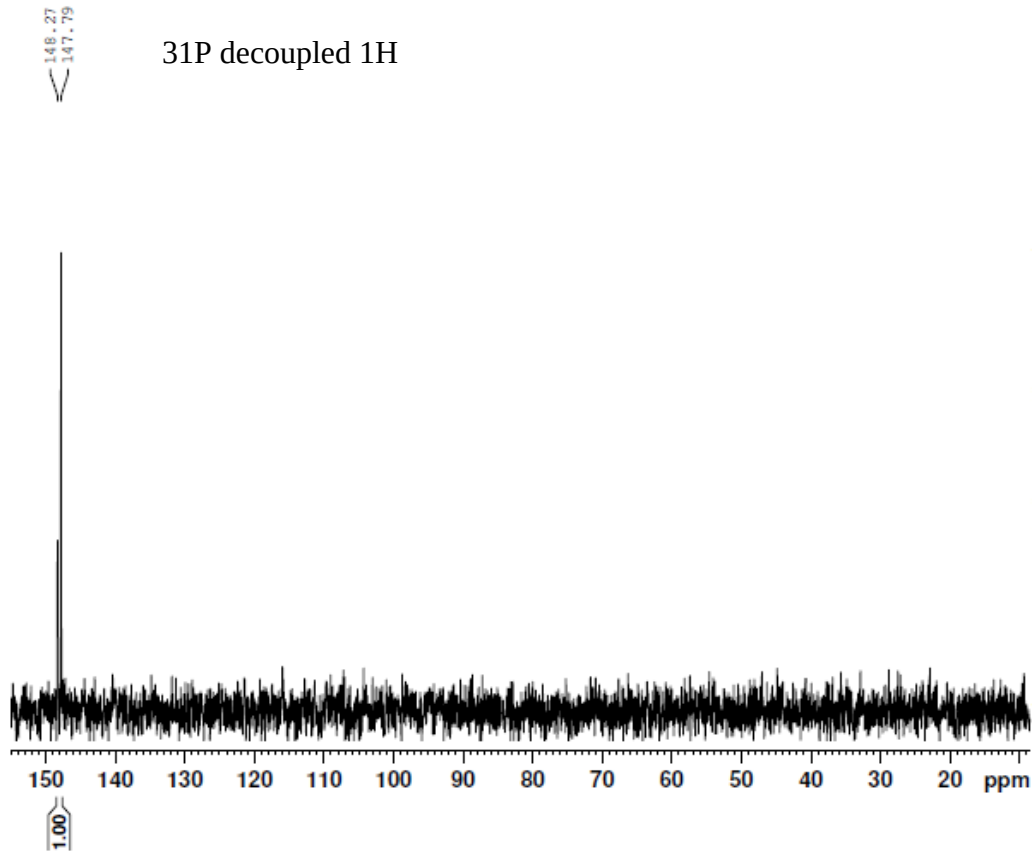

Figure 36. ^{31}P NMR of cyclic azobenzene amidite **153**.

4.2 Synthesis of the monomer for the incorporation of azobenzene into DNA

From the D-threoninol analogue **151**, a phosphoramidite monomer analogue was synthesized bearing an azobenzene group covalently through an amide bond, as depicted in Scheme 33. Use of D-threoninol was important, in particular for subsequent hybridization experiments, because L-threoninol significantly lowers the stability of DNA duplexes.[94] In order to incorporate the azobenzene moiety into an oligonucleotide, the D-threoninol functionality is used as a substitutent on the sugar group. The distance between two nucleobases in oligonucleotide **155** is five bond spaces, as shown in Figure 37. Use of D-threoninol as a linker **156** (Figure 37) exceeds the requirement of five bond spaces without destabilising the duplex.[94]

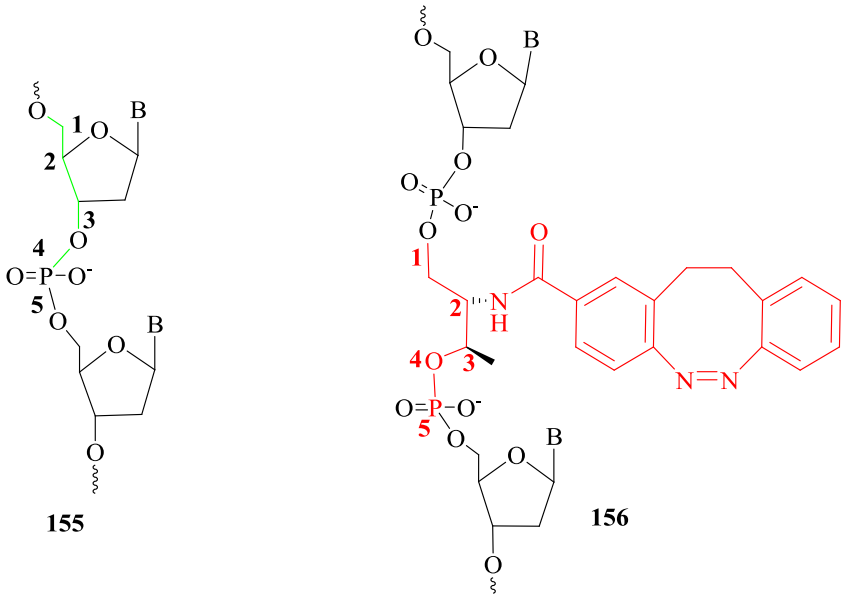

Figure 37. Structures of unmodified and modified oligonucleotides.

4.3 Synthesis of oligonucleotides using solid phase DNA synthesizer

Four steps are involved in the synthesis of DNA via the phosphoramidite method (Scheme 33) [123] detritylation, coupling, capping and oxidation.

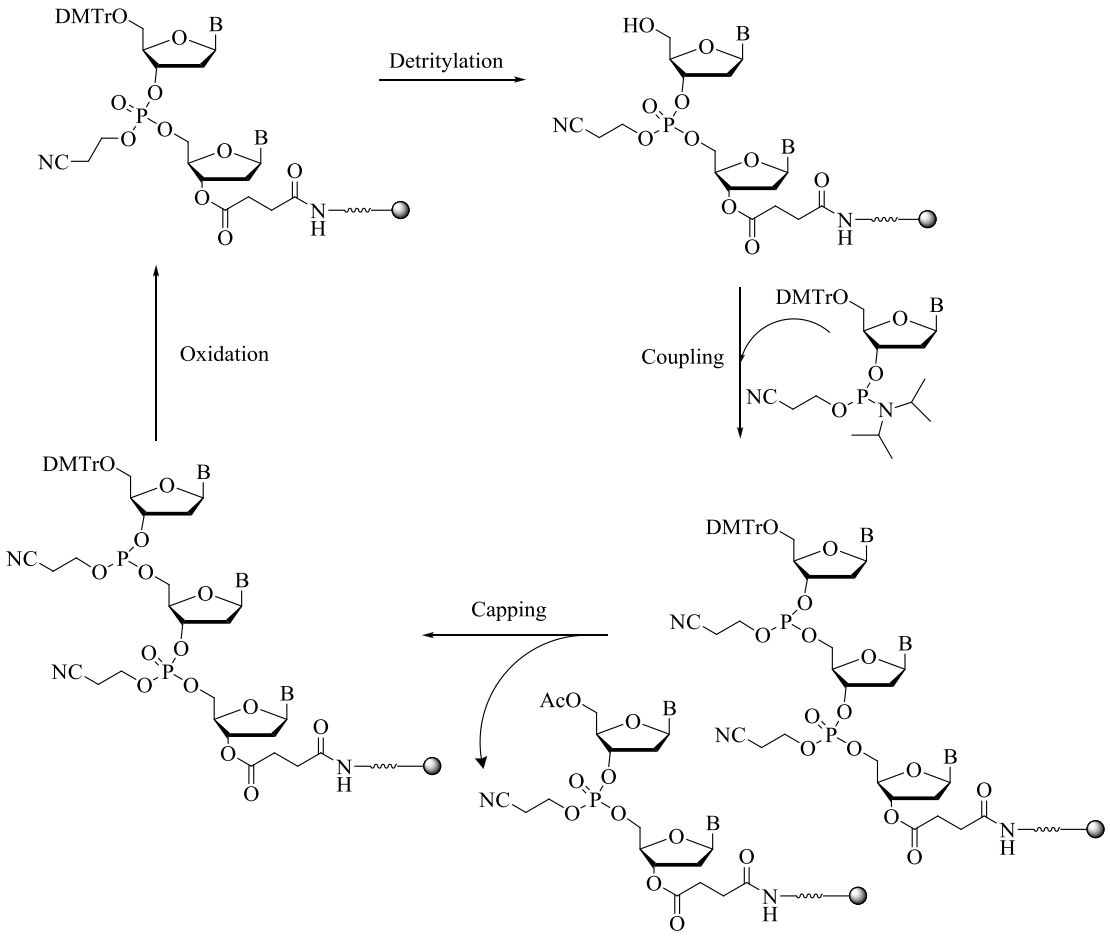

Scheme 33. Chemical steps for the solid phase synthesis oligonucleotides.

4.4 Photoisomerization study on cyclic azobenzene amide 151

When the amide **151** was subjected to LED irradiation at either 380 or 400 nm (the LED light source spans ± 5 nm), a clear colour change from yellow (the (*Z*) -isomer) to red (the (*E*) -isomer) was observed (Figure 38).[61]

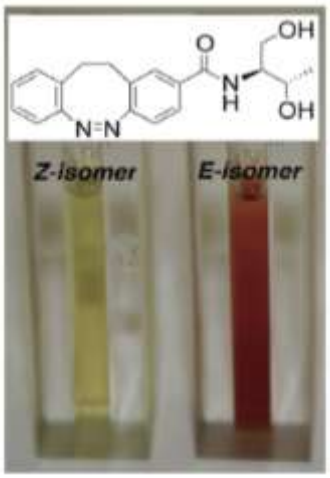

Figure 38. Change in the color of bridged azobenzene **151** during photoisomerization.

4.4.1 Study of extent of photoisomerization via HPLC

Extents of photoisomerization can be qualitatively determined by HPLC (Figure 39). Figure 39a shows the HPLC profile of the *trans*-isomer of unmodified cyclic azobenzene **142** before irradiation with light. As can be seen in Figure 39b, when the unmodified cyclic azobenzene **142** was subjected to irradiation with LED light at 380 ± 5 nm for 2 h, 90% of the (*trans*)-isomer was converted to the (*cis*)-isomer (Figure 39b). The extent of the isomerization of **142** is consistent with the yield reported in the literature.[75]

Under the same conditions, approximately 70% of (*cis*)-isomer of amide **151** was converted to the corresponding (*trans*)-isomer (Figure 39d), whereas Figure 39c shows the HPLC profile of *cis*-isomer of amide 112 before irradiation. The small peak at 13.54 min in Figure 39d shows the 30% of *cis*-isomer of amide **151** that did not isomerise into *trans*-isomer.

The reason behind 70% photoisomerization of amide **151** compared to 90% photoisomerization of **142** is still unclear but one possible reason could be, absorption of light due to presence of amide bond in cyclic azobenzene linked D-threoninol.

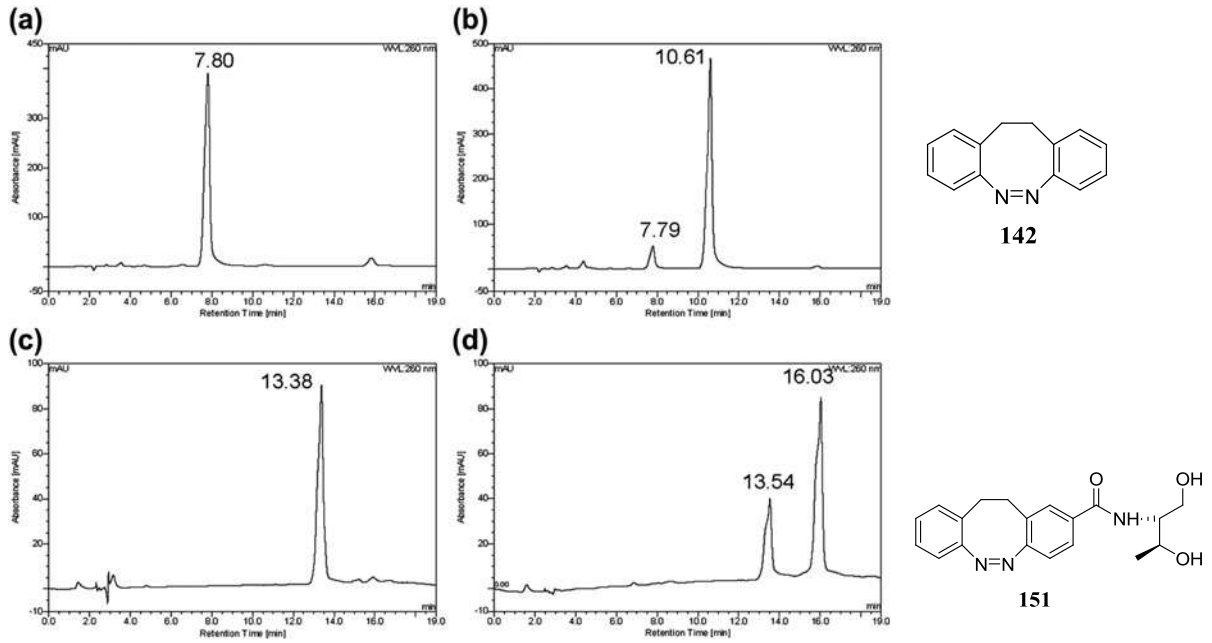

Figure 39. HPLC profiles of cyclic azobenzene **142** and **151**. (a). (*Z*)-**142**; (b). (*E*)-**151**; (c). (*Z*)-**151**; (d). (*E*)-**151**. (Profiles a and b: linear gradient of water-acetonitrile (55:45 to 15:85, v/v) over 15 min; profiles c and d: linear gradient of water-acetonitrile (90:10 to 55:45, v/v) over 15 min).[61]

4.4.2 Study of extent of photoisomerization using UV/visible spectrometer

Photoisomerization of **142** and **151** was studied by UV-visible spectrometer in methanol. The UV/vis spectra of (*Z*)-**151** and the isomerization product (with an approximate *Z*/*E* ratio of 30:70) are shown in Figure 40a. The small absorption signal (blue line in Figure 40a) at 400 nm shows the 30% of (*Z*)-**112** that did not isomerise to (*E*)-**151**.

Compared with the UV/vis spectra of (*Z*)-**142** and the corresponding isomerization product (with an approximate *Z*/*E* ratio of 10:90) (Figure 40b), the maximal absorption wavelengths for (*Z*)-**142** and (*Z*)-**151** are the same (at 400 nm), whereas that of (*E*)-**151** shifted from 483 nm for (*E*)-**142** to 487 nm. Similarly, the small peak at 400 nm (blue line in Figure 40b) shows the 10% of (*Z*)-**142** that did not isomerise to (*E*)-**142**.

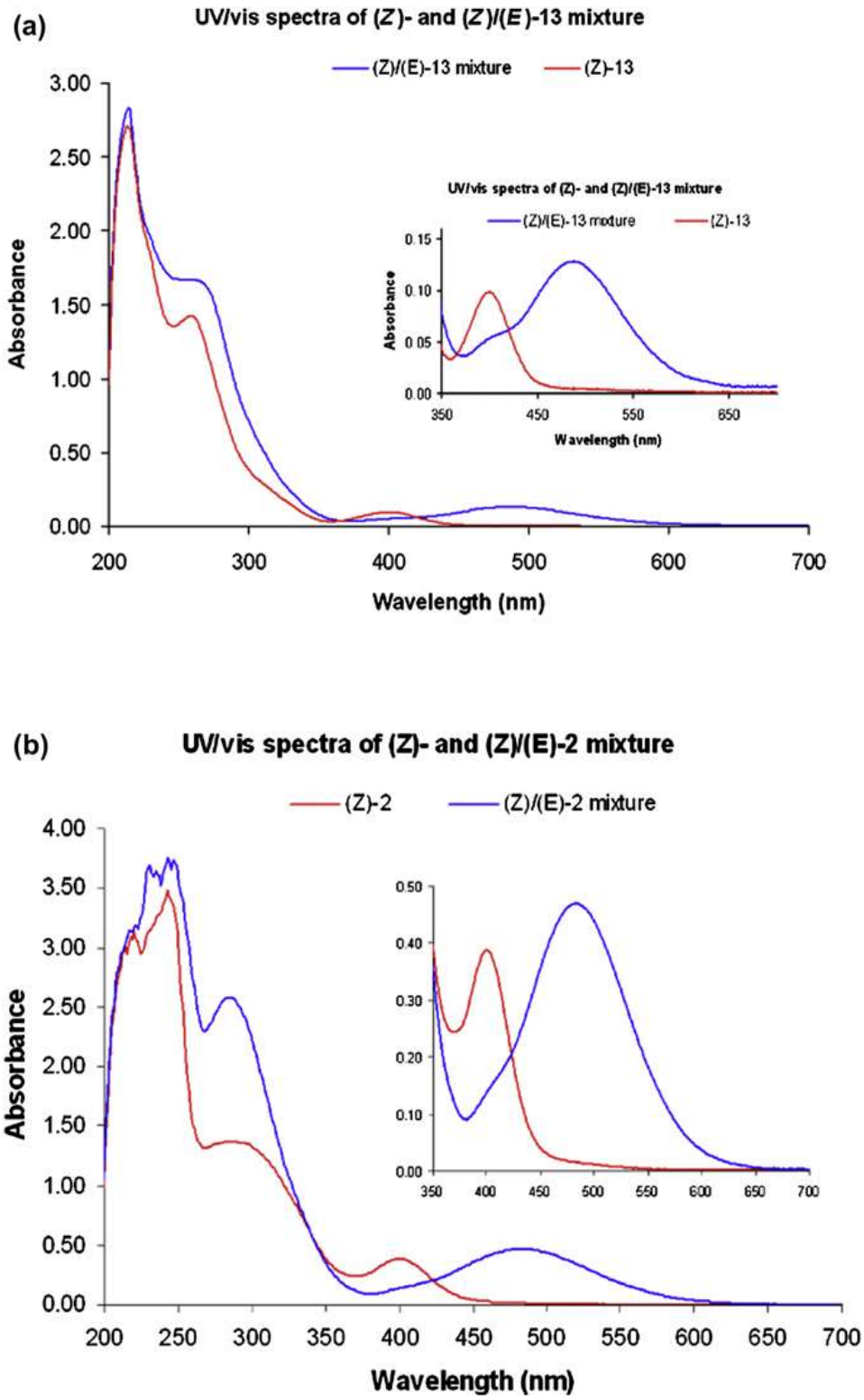

Figure 40. UV/vis spectra. (a). (*Z*)- and (*Z*)/(*E*)-**142** in methanol (0.60 m*M*); (b). (*Z*)- and (*Z*)/ (*E*)-**151** in methanol (1.1 m*M*).[61]

4.5 Time course study on photoisomerization of cyclic azobenzene 151

The time course of (*Z*)/(*E*)-**151** isomerization was followed by measuring the percentage transmission at 480 nm of the methanol solution exposed to 380 nm LED light over time. When the solution was irradiated with light at 380 nm using LED, the *cis*-isomer of **151** isomerizes to *trans*-isomer over time. During this process, the transmission at 480 nm decreases because of the increase in the percentage of *trans*-isomer compared to *cis*-isomer. Eventually, the transmission reaches a minimum (approaches steady transmission reading). In a similar fashion, the *trans*-isomer solution was illuminated at 480 nm and the transmission at 480 nm was measured again over time.

During this process, back isomerization of *trans*-isomer to *cis*-isomer occurs and the percentage of *trans*-isomer decreases, resulting in an increase in the transmission at 480 nm. As can be seen from Figure 41, under this condition, the (*Z*)/(*E*) isomerization reached the minimum steady state after approximately 40 min, whereas the (*E*)/(*Z*) isomerization was slower with a full recovery of transmission after approximately 2 h. The back isomerization of **151** from the *trans*- to the *cis*-isomer greatly depends on the chemical architecture of the system (*i.e.* appropriate modification of the substitution on azobenzene core helps to modulate the relaxation rate of azo-compounds). The slow back isomerization of *trans*- to *cis*-isomer could be due to presence of electron-withdrawing groups such as carbonyl and amide. It also depends on the mechanism through which it undergoes photoisomerization, *i.e.*, either rotation or inversion process.

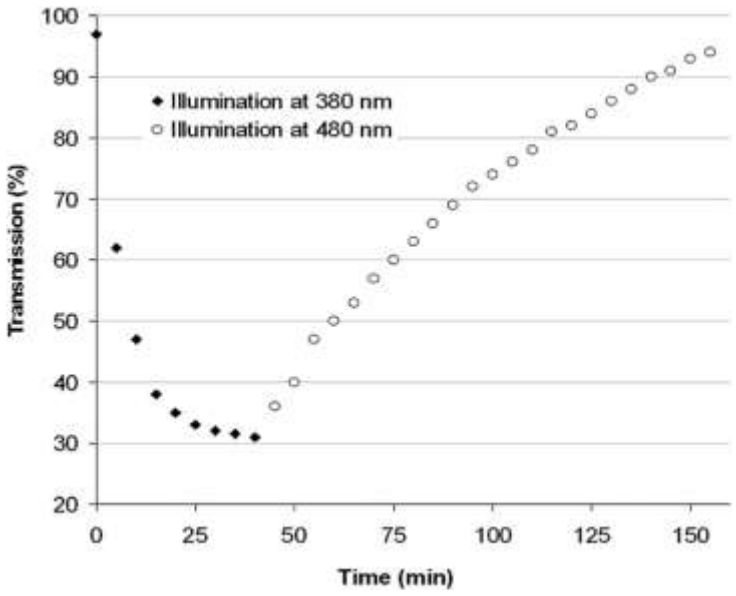

Figure 41. Isomerization time course of **151** in methanol (0.94 m*M*) as determined by the percent transmission at 480 nm. ♦ : (Z)/(E) isomerization illuminated at 380 nm; ○ : (E)/(Z) isomerization illuminated at 480 nm.[61] Light intensity- 32.3 mW/cm^2.

4.6 Conclusion

Bromo **144-**, chloro **143-**, cyano **148-**, carboxyl **149** and unsubstituted cyclic azobenzene **142** analogues were synthesised from 2,2'-dinitrodibenzyl **137**. Condensation of the carboxyl analogue with D-threoninol gave a building block that can be readily isomerised by illumination with light. The extent of photoisomerization was quantitatively determined by HPLC. Upon illumination with light at 400 nm, approximately 70% of *cis*- isomer of D-threoninol linked cyclic azobenzene was readily isomerised to the corresponding *trans*-isomer. The UV/vis study has also showed approximately 70% isomerisation of *cis*- isomer to corresponding *trans*-isomer, which correlates to the HPLC data. The time course study showed time dependent isomerisation of the *cis*- to the *trans*- isomer and *trans*- to *cis*- isomer. *Cis*- isomer was isomerised to *trans*- isomer in approximately 40 min, whereas the *trans*- to the *cis*- isomerisation was slower where full recovery was obtained after approximately 2h. Cyclic azobenzene phosphoramidite was

successfully prepared from DMT-protected D-threoninol linked cyclic azobenzene. Like unmodified azobenzene, modified cyclic azobenzene analogues such as carboxyl cyclic azobenzene, which showed 70% photo- isomerization efficiency, can be exploited as a useful photoswitch. Modified cyclic azobenzene systems are more likely to be tolerated in biological systems as irradiation wavelengths are shifted away from the UV region that readily cause damage to biomolecules. Future work includes incorporation of cyclic azobenzene into oligonucleotides using solid phase DNA synthesizer.

4.7 Synthesis of bi-functional cyclic azobenzene analogues for incorporation into proteins

Although considerable interest has been invested towards the synthesis and incorporation of azobenzene in proteins, synthesis of bi-functional cyclic/bridged azobenzene analogues for the incorporation into proteins is relatively new. What has been challenging with this system is poor availability of synthetic methods to prepare a bi-functional cyclic azobenzene derivative.

In this thesis, synthesis of a cyclic azobenzene biscarboxyl acid **162** was undertaken. Treatment of 4-(bromomethyl) benzonitrile **157** in dry tetrahydrofuran with manganese slurry, lithium metal and naphthalene yielded the corresponding homo-coupling product, dicyanodibenzyl **158** in 44 % yield (Scheme 34).

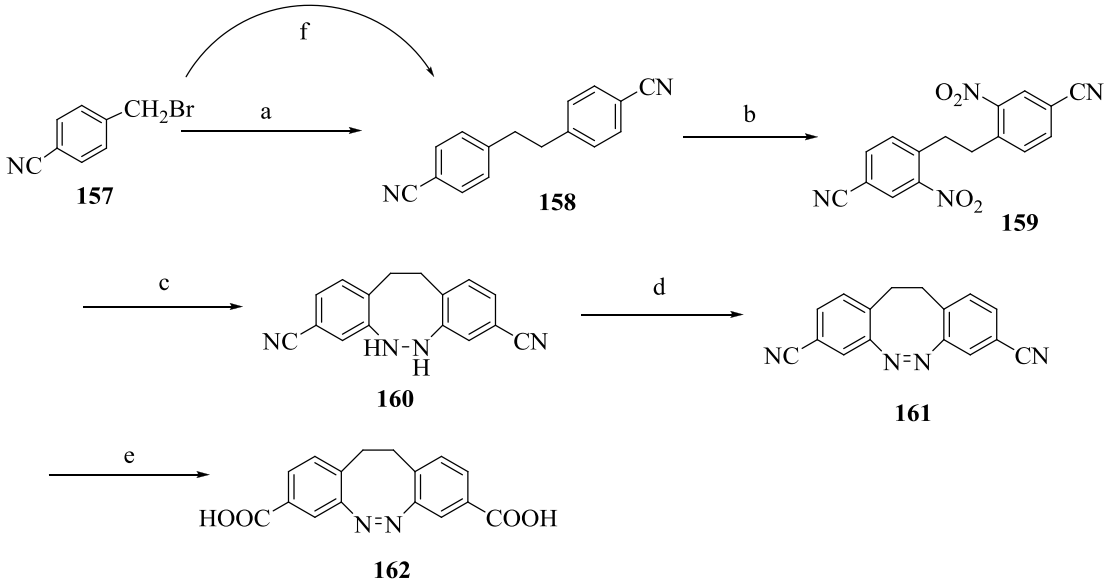

Scheme 34. Reagents and conditions: (a). $MnCl_2$, lithium metal, naphthalene, THF, 44%; (b). H_2SO_4, HNO_3, 72%; (c). Zinc metal, NEt_3, HCOOH, pH 7, EtOH, 74%; (d). $TiCl_3$, HBr, H_2O_2, MeOH, 90%; (e). a. KOH, EtOH, H_2O, reflux; b. *aq*. HCl, 73%; (f). Iron nanoparticles, CuBr, H_2O, 72%.

Upon nitration of **158** with nitric acid and sulphuric acid, the corresponding nitro product dicyanodinitrodibenzyl **159** was obtained in good yield (70%). The nitro product **159** was then reduced to hydrazine **160** with zinc metal in aqueous ethanol (pH 7) in good yield (75%). The cyclic hydrazine **160** was then oxidised with titanium chloride, hydrogen bromide and hydrogen peroxide in methanol to give cyclic diazine **161** in good yield (84%). Finally the cyclic diazine **161** was converted to the corresponding final product bi-functional carboxylic cyclic azobenzene **162** by base hydrolysis with KOH in good yield (70%).

The major problem with this synthetic scheme was the poor yield (44%) for the first step with manganese metal and lithium metal. Another approach to prepare homo-coupling adduct **158** is to use iron nanoparticles (Fe^0). Recently Taghipoor *et al.*[124] reported synthesis of 1,2 diarylethanes using iron nanoparticles in the presence of Cu(I).

Following this approach to synthesize a homo-coupling adduct for bifunctional cyclic azobenzene, iron nanoparticles were generated by treating ferric chloride with sodium borohydride in water solution containing sodium lauryl sulfate. Treatment of 3-nitro-4-(bromomethyl)benzonitrile **157** with iron nanoparticles (Fe^0) gave the corresponding homo-coupled product **158** in moderate yield (50%, Scheme 35).

This latter synthesis suffers from instability of the iron particles in the presence of oxygen. For small scale reactions (50-100 mg), handling of iron nanoparticles was straightforward, however with larger scale reactions (more than 100 mg), extreme caution must be taken during handling these nanoparticles, which could readily catch fire in air. In addition, over-reduction of **158** to the corresponding amine was also observed. Reaction of dicyanodinitrodibenzyl **159** with zinc metal to obtain the dicyanohydrazine cyclic azobenzene analogue often lacked reproducibility and resulted in over-reduction of the nitro group to the amine due to differences in zinc powder batches. When **159** was treated with an older batch of zinc powder under neutral pH, cyclic dicyanohydrazine was obtained; however with newer batches of zinc powder, cyclic dicyanohydrazine was obtained only twice in ten attempts. This transformation was found to be highly dependent on the surface properties and/or impurity of zinc powder.

The conventional way of incorporating azobenzene into peptides is shown in Scheme 35.

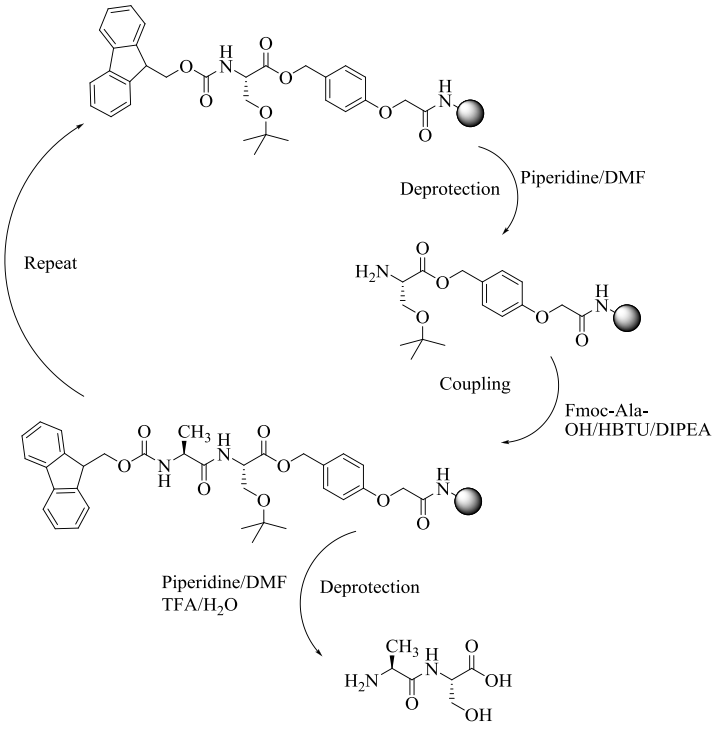

Scheme 35. Incorporation of azobenzene into peptides using Fmoc solid phase peptide synthesis.

4.7.1 Conclusion

Bi-functional carboxyl cyclic azobenzene was prepared from 4-(bromomethyl) benzonitrile. However synthesis of dicyanodibenzyl from 4-(bromomethyl) benzonitrile poses several problems, such as low yield, when 4-(bromomethyl) benzonitrile was treated with magnesium slurry, and fire hazard when 4-(bromomethyl) benzonitrile was treated with iron nanoparticles. The treatment of dicyanodinitrodibenzyl with zinc metal to obtain the dicyanohydrazine cyclic azobenzene adduct lacked reproducibility and often resulted in over-reduction of the nitro group to the amine group.

Biscarboxyl cyclic azobenzene was not obtained in sufficient quantities to continue with incorporation into peptides using a peptide synthesizer. Future work will include optimization of the current synthetic scheme to achieve reproducibility and overall good yield.

4.8 Synthesis and incorporation of cyclic azobenzene analogue into polymer

In order to explore the impact of cyclic azobenzene on polymer structure and properties, cyclic azobenzene carboxylic acid **149** was incorporated into a commercial polymer, poly (2-hydroxy-ethyl) methacrylate **163.** Poly (2-hydroxyethyl) methacrylate **163** was treated with cyclic azobenzene carboxylic acid **149** dissolved in dry chloroform, in the presence of 1-ethyl-3- (3-dimethylaminopropyl)carbodiimide) (EDC) and a catalytic amount of 4-dimethylaminopyridine DMAP (Scheme 36). The reaction was allowed to proceed at room temperature for 24 h and then extracted successively with water and chloroform. The chloroform layers were concentrated to dryness to obtain the desired product as yellow colored solid **164**.

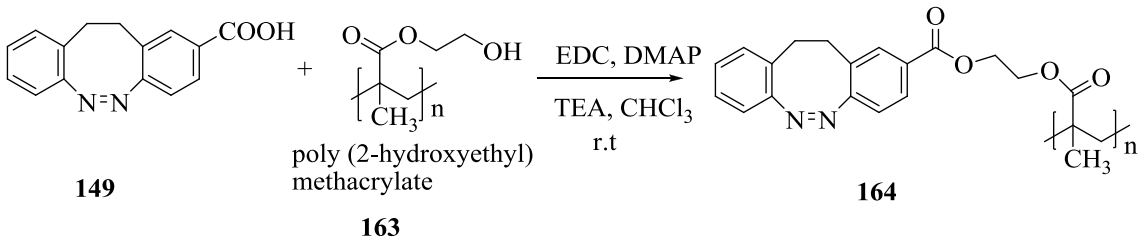

Scheme 36. Synthetic strategy for the incorporation cyclic azobenzene into polymer.

4.8.1 Determination of incorporation rate by UV/vis spectroscopy

In order to determine the percentage of incorporation of cyclic azobenzene into the polymer, a standard curve of UV absorbance of cyclic azobenzene **149** at various concentrations in chloroform at 400 nm was recorded (Figure 42).

In order to differentiate the UV absorbance of unreacted azobenzene residue with that of the polymer linked azobenzene, the obtained yellow solid was dissolved in dichloromethane (1 ml) and triturated with diethyl ether (10 ml). The unreacted cyclic azobenzene partially dissolves in diethyl ether. This trituration process is repeated until the diethyl ether layer showed no absorbance at 400 nm.

Percentage incorporation of cyclic azobenzene into the polymer was determined for two polymer samples; one sample was taken from the reaction mixture after 10 h and another sample after 24 h. From UV/vis data (Figure 43) it is observed that the sample collected after 24 h has a higher percentage (9%) of incorporation of cyclic azobenzene compared to the sample collected after 10 h percentage incorporation (6%).

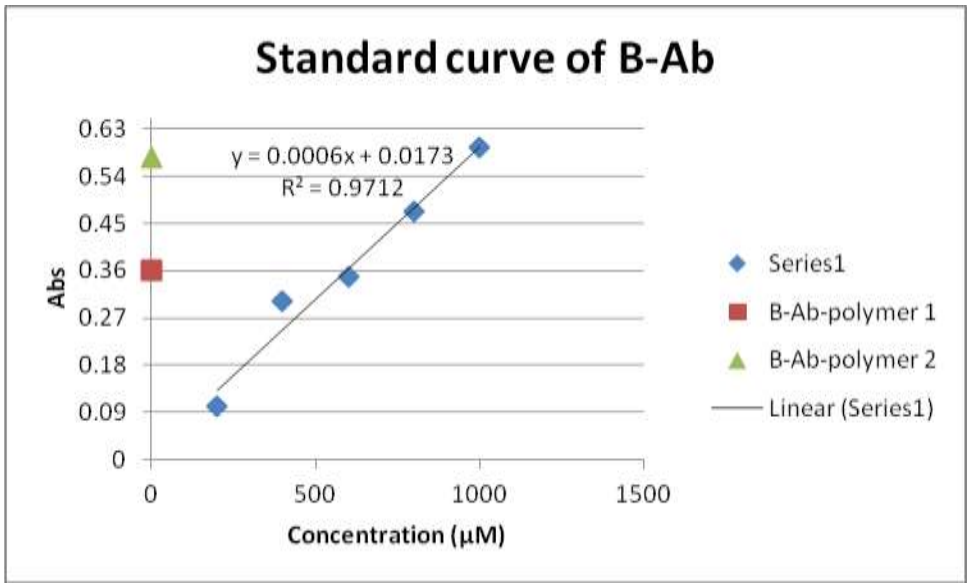

Figure 42. A standard curve of UV absorbance at 400 nm of cyclic azobenzene.

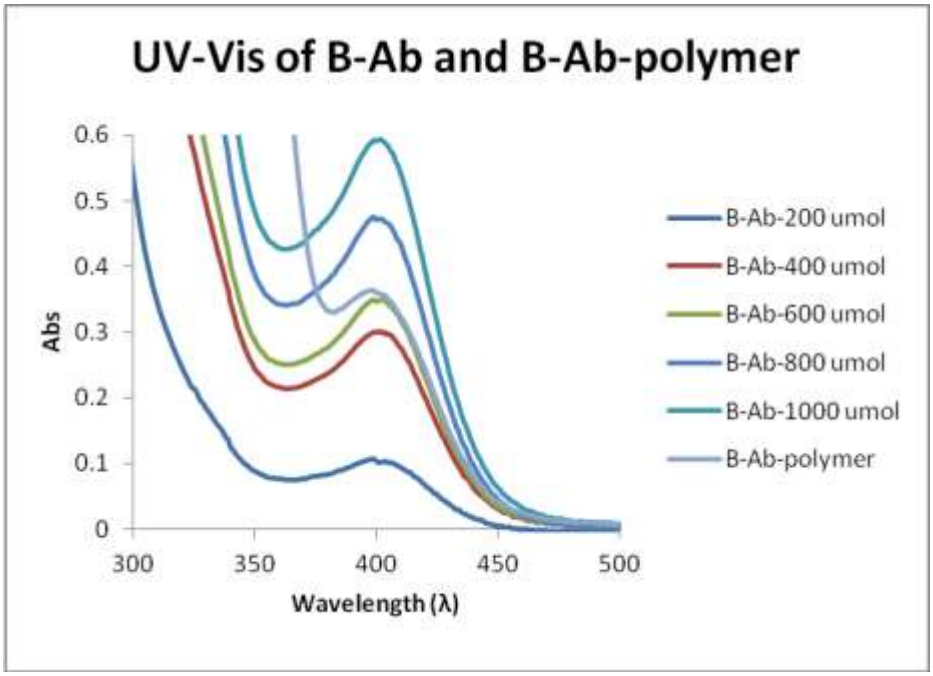

Figure 43. UV/vis absorbance at 400 nm of cyclic azobenzene and cyclic azobenzene incorporated polymer.

4.8.2 Conclusions

Carboxyl cyclic azobenzene analogue was successfully incorporated into the polymer poly (2-hydoxyethyl)methacrylate. Samples collected after 24 h were found to have approximately 9% of incorporation of cyclic azobenzene compared to samples collected after 10 h (percentage incorporation 6%). Future work involves establishing the time-dependence of incorporation of cyclic azobenzene into the polymer. In addition the changes of the surface morphology of thin polymer films upon illumination with light will be studied by confocal microscopy and/or atomic force microscopy.

4.9 Future Experiments

(A) Photoregulation of hybridization

Two unmodified 20-mer sequences, namely 3′-Dabsyl and 5′-FAM and seven modified 3′-Dabsyl 20-mer sequences with different incorporation of cyclic azobenzene at various locations will be used to study the photo-regulation of hybridization. 3′-Dabsyl and 5′-FAM act as a FRET pair in this experiment. The experiment involves illumination of solution containing modified 3′-Dabsyl and unmodified 5′-FAM sequences. It is hypothesized that in the *cis*- form of cyclic azobenzene, duplex is not formed, due to its non-planar nature. Therefore the fluorescence from the FAM is not quenched. However after illumination with light at 400 nm, the *cis*- form isomerizes to *trans*-form. Owing to the planar geometry of the *trans*- form, duplex formation will be induced. Due to the close proximity of Dabsyl and FAM in the duplex, the fluorescence from FAM is quenched by Dabsyl. The percentage fluorescence quenched from FAM will provide insight into the efficiency of photoregulation of hybridization by cyclic azobenzene.

(B) Photoregulation of peptide conformation

Incorporation of biscarboxyl cyclic azobenzene will be carried out using a conventional peptide synthesizer. The modified peptide will then be used study the effect of photoisomerization of cyclic azobenzene on peptide conformation and its biological function.

(C) Photoregulation of polymer structure and properties

In future, studies on the time-dependent incorporation of cyclic azobenzene into polymer are required to have an understanding on relationship between time and percentage incorporation. Incorporating cyclic azobenzene into polymers with different functionalities such as amino groups, will also provide insight into reactivity of cyclic azobenzene with different functional groups on the polymer. Confocal microscopy and/or atomic force microscopy will be employed to study the changes on the surface morphology of thin polymer films with incorporated cyclic azobenzene upon illumination with light at desired wavelength.

Chapter-5 Experimental

5.1 Instrumentation

^{1}H NMR spectra were measured at 300 or 600 MHz with a Bruker Avance 300 and 600 Digital NMR spectrometers with a 14.1 and 7.05 Tesla Ultrashield magnet, respectively. Tetramethylsilane was used as an internal standard; ^{13}C NMR spectra were measured at 150.9 MHz and ^{31} P at 121 MHz with the same spectrometer. *J* values and chemical shifts are given in ppm and Hz, respectively. The following deuterated solvents from C/D/N isotopes Inc. were used for the preparation of NMR samples. Dimethyl-d_6 sulfoxide with 0.05% tetramethylsilane (99.0 atom % D), deuterated chloroform (99.0 atom % D), and deuterated oxide (99.9 atom % D). Low and high resolution mass spectra were obtained with Kratos Concept IS high resolution mass spectrometer using electron impact or fast bombardment sources. interfaced with DART 32 bit acquisition system through a Sun Sparcstation 10 and Mach 3 software. UV/Vis spectra were recorded with a Biochrom Ultrospec 2100pro UV/Visible spectrophotometer. Chemicals were purchased from Aldrich or TCI America and used without further purification unless stated otherwise.

5.2 Crystal growth

Single crystals of cyclic azobenzene **142** and bromoazoxybenzene **145** were obtained by slow evaporation of corresponding solutions in absolute ethanol.

5.3 X-ray diffraction experiment

X-diffraction experiment was performed by Dr. Alan Lough at the University of Toronto. Diffraction data were collected on a Nonius Kappa-CCD diffractometer using monochromated Mo-Kα radiation and were measured using a combination of ϕ scans and ω scans with κ offsets, to fill the Ewald sphere. The data were processed using the Denzo-SMN package.[125, 126] Absorption corrections were carried out using SORTAV.[126] The structure was solved and refined using SHELXTL V6.1[1280.1] for full-matrix least-squares refinement that was based on F^2. All H atoms were included in calculated positions and allowed to refine in riding-motion approximation with U_{iso} tied to the carrier atom.

5.4 Chromatography

Desican 230-400 mesh silica gel 60 was used for flash chromatography. Thin layer chromatography was performed on Silicycle SilicaPlate F-254 TLC plates using the following solvent mixtures:

Solvent A: hexane-dichloromethane (50:50, v/v)

Solvent B: hexane-dichloromethane (40:60, v/v)

Solvent C: hexane-dichloromethane (20:80, v/v)

Solvent D: dichloromethane

Solvent E: methanol-dichloromethane (5:95, v/v)

Solvent F: methanol-dichloromethane (10:90, v/v)

Solvent G: methanol-dichloromethane-triethylamine (5:94:1, v/v)

Solvent H: hexane-dichloromethane-triethylamine (48:50:2, v/v)

Reverse phase high-performance liquid chromatography (HPLC) was carried out on a 4.6 x 150 mm Acclaim PA C18 3μ column: the column was eluted with water-acetonitrile mixtures at a flow rate of 0.80 ml/min. Ion-exchange high-performance liquid chromatography was carried out on a DNAPAc column.

5.5 Solvents and Chemicals

Benzene and toluene were dried by heating under reflux over sodium in the presence of benzophenone for 4 h and then distilled. *N*,*N*- Diisopropylamine, dimethylformamide, pyridine, and dichloromethane were dried by heating under reflux over calcium hydride for 4 h and then distilled. Chloroform was dried by heating under reflux over phosphorus pentoxide for 4 h and then distilled. All the distilled solvents were stored over activated 4 Å molecular sieves. All other reagents were purchased from Sigma-Aldrich or VWR Canlab without further purification prior to use unless stated otherwise.

Preparation of compounds

11, 12-Dihydrodibenzo[c, g] [1, 2] diazocine-5-oxide 140

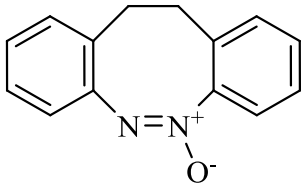

Triethylamine (22 ml, 0.16 mol) was added to methanol (100 ml) followed by addition of formic acid (5.7 ml, 0.15 mol). The final pH of the solution was adjusted to 9.5. 2,2'-Dinitrodibenzyl **137** (1.00 g, 3.67 mmol), followed by lead powder (3.50 g, 16.9 mol, 200 mesh) were added. After the reaction mixture was stirred vigorously at room temperature for 24 h, another portion of lead powder (3.00 g, 14.5 mmol) was added, and stirring was continued for another 24 h. The products were filtered and the filtrate was concentrated under reduced pressure. The residue was re-dissolved in dichloromethane (20 ml) and extracted with saturated aqueous sodium bicarbonate (3 x 10 ml). The organic layer was dried ($MgSO_4$) and concentrated under reduced pressure. The residue was purified by column chromatography on silica gel. The appropriate fractions, which were eluted with dichloromethane-hexane (40:60 v/v), were pooled and concentrated under reduced pressure to give the *title compound* as a pale yellow solid (505 mg, 61 %).

M.p. 167-169 °C (ethanol).

R_f (system B): 0.49

HR-MS (EI) found 224.09420, $C_{14}H_{12}N_2O$ required 224.09496

$\delta_H(CDCl_3)$: 2.88 (1 H, ddd, *J* = 5.9, 9.6 and 14.4), 2.98 (1 H, ddd, *J* = 5.2, 10.0, and 14.9), 3.22 (1 H, ddd, *J* = 5.1, 10.1, 14.6), 3.37(1 H, ddd, *J* = 5.9, 10.1, 15.0), 6.94(1 H, d, *J* = 7.8), 7.02 (2 H, d, *J* = 4.0), 7.04 (1 H, d, *J* =7.6), 7.10-7.20 (4 H, m).

$\delta_C(CDCl_3)$: 30.1, 31.2, 121.6, 127.2, 127.3, 127.8, 129.6, 130.3, 130.4, 131.5, 131.8, 146.0, 148.7.

2-Chloro-11,12-dihydrodibenzo[c,g][1,2]diazocine 143

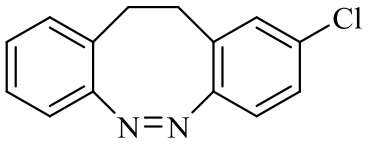

To a suspension of aluminum chloride (208 mg, 1.56 mmol) in carbon disulfide (3.0 ml), a solution of 11,12-dihydrodibenzo[c,g][1,2]diazocine-5-oxide **140** (350 mg, 1.56 mmol) in carbon disulfide (2.0 ml) was added drop-wise under nitrogen. The reaction mixture was heated under reflux for 5 h and then cooled and concentrated under reduced pressure. To the dark residue was added hydrochloric acid (0.1 *M*, 6 ml), and the mixture was extracted with diethyl ether (3×5 ml). The organic layers were washed first with water (2×20 ml) and then with saturated aqueous sodium bicarbonate (2×20 ml), dried ($MgSO_4$), and concentrated under reduced pressure. The residue was purified by column chromatography on silica gel. The appropriate fractions, which were eluted with dichloromethane-hexane (30:70v/v), were combined and concentrated under reduced pressure to give the *title compound* as a light yellow solid (30 mg, 8%).

M.p. 80–82°C (ethanol).

R_f (solvent C) 0.78.

HR-MS (EI) found 242.06156, $C_{14}H_{11}ClN_2$ required 242.06108.

$\delta_H(CDCl_3)$: 2.76 (2 H, m), 2.98 (2 H, br, m), 6.79 (1 H, d, *J* = 8.4), 6.85 (1 H, d, *J* = 7.8), 6.99 (1 H, d, *J* = 1.5), 7.00 and 7.01 (1 H), 7.06 (1 H, t, *J* = 7.5), 7.11 (1 H, dd, *J* = 1.9 and 8.4), 7.17 (1 H, t, *J* = 7.7).

$\delta_C(CDCl_3)$: 31.4, 31.7, 118.7, 120.4, 126.8, 126.9, 127.4, 127.6, 129.5, 129.7, 130.2, 132.2, 153.7, 155.3.

2-Bromo-11,12-dihydrodibenzo[c,g][1,2]diazocine 144

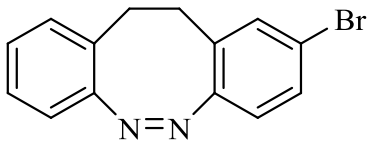

To a suspension of aluminum bromide (145 mg, 0.544 mmol) in carbon disulfide (3.0 mL) a solution of 11,12-dihydrodibenzo[c,g][1,2]diazocine-5-oxide **140** (100 mg, 0.446 mmol) in carbon disulfide (2.0 ml) was added drop-wise under nitrogen. The reaction mixture was heated under reflux for 5 h, and then cooled and concentrated under reduced pressure. The dark residue was then treated carefully with hydrochloric acid (0.1 *M*, 6 ml), and extracted with diethyl ether (3×5 ml). The ether layers were combined and washed successively with water (2×20 ml) and saturated aqueous sodium bicarbonate (2×20 ml). The organic layer was separated, dried ($MgSO_4$) and evaporated to dryness under reduced pressure. The residue was purified by column chromatography on silica gel. The appropriate fractions, which were eluted with dichloromethane-hexane (30:70 v/v), were combined and concentrated under reduced pressure to give the *title compound* as a light yellow solid (12 mg, 9%).

R_f (solvent C): 0.78

HR-MS (EI) found 286.01081, $C_{14}H_{11}BrN_2$ required 286.01056.

$\delta_H(CDCl_3)$: 2.76 (2 H, m), 2.99 (2 H, br, m), 6.73 (1 H, d, *J* = 8.4), 6.85 (1 H, d, *J* = 7.8), 7.02 (1 H, d, *J* = 7.5), 7.07 (1 H, t, *J* = 7.4), 7.15 (1 H, d, *J* = 1.6), 7.18 (1 H, t, *J* = 7.5), 7.26 (1 H, dd, *J* = 1.7 and 8.4).

$\delta_C(CDCl_3)$: 31.4, 31.6, 118.7, 120.3, 120.6, 127.0, 127.4, 127.5, 129.7, 129.8, 130.4, 132.4, 154.2, 155.3.

5,6,11,12-Tetrahydro-dibenzo[c,g][1,2]diazocine 141

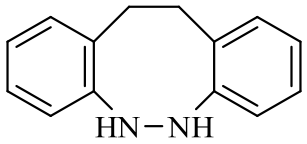

To a solution of triethylamine (2.1 ml, 15 mmol) in ethanol (10 ml) was added formic acid (0.54 ml, 15 mmol), and the final pH of the solution was adjusted to 7. To this solution was added first 2,2'-dinitrodibenzyl **137** (100 mg, 0.367 mmol) followed by zinc powder (200 mg, 3.06 mmol) over a period of 15 min under vigorous stirring. After the reaction mixture was heated under reflux for 5 h, the products were filtered and concentrated to dryness under reduced pressure. The residue was extracted with dichloromethane (20 ml). The organic layer was dried ($MgSO_4$) and evaporated under reduced pressure. The residue was purified by column chromatography on silica gel. The desired product was obtained upon evaporation of appropriate fractions, which were eluted with dichloromethane-hexane (35:75, v/v) as a light orange solid (55 mg, 71%).

R_f(solvent D): 0.70.

HR-MS (EI) found 210.11540, $C_{14}H_{14}N_2$ required 210.11570.

$\delta_H(CDCl_3)$: 3.28 (4 H, s), 5.56 (2 H, s), 6.74 (2 H, d, *J* = 7.9), 6.98 (2 H, t, *J* = 6.9), 7.13 (2 H, t, *J* = 7.9), 7.19 (2 H, d, *J* = 6.9).

$\delta_C(CDCl_3)$: 31.4, 117.7, 122.4, 126.6, 131.0, 133.4, 146.6.

Preparation of molybdenum dioxo dichloride(dmf)$_2$

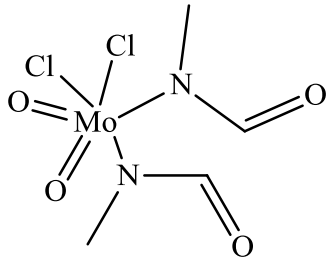

A stirred mixture of finely powdered molybdenum trioxide (MoO_3, 1.00 g, 6.85 mmol) and 10 ml of 6 M hydrochloric acid was heated under reflux until most of the MoO_3 was dissolved (about 2-3 h), then cooled to room temperature and filtered. To the filtrate was added freshly distilled dimethylformamide (3 ml) under stirring. The resulting white microcrystalline precipitate was collected by filtration, washed with acetone (2 ×10 ml) and dried under vacuum. The *title compound* was obtained as light blue powder (2.00 g, 93%).

11,12-Dihydrodibenzo[c,g][1,2]diazocine 142

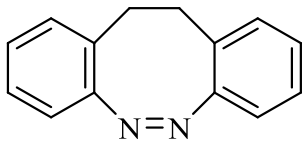

*Method A: deoxygenation of azoxybenzene **140** using triphenylphosphine and molybdenum dioxo dichloride(dmf)$_2$.* To a solution of 11,12-dihydrodibenzo[c,g][1,2] diazocine-5-oxide **140** (100 mg, 0.446 mmol) in dry tetrahydrofuran (5 ml) were added triphenylphosphine (585 mg, 2.23 mmol) and molybdenum dioxo dichloride $(dmf)_2$[123, 124] (20 mg, 5.6 mmol). The reaction mixture was heated under reflux for 3 h and then concentrated under reduced pressure. The residue was purified by column chromatography on silica gel. The appropriate fractions, which were eluted with dichloromethane-hexane (30:70 v/v), were combined and concentrated under reduced pressure to give 5,6-dihydrodibenzo[c,g][1,2]diazocine **142** as a light yellow solid (55 mg, 59%).

R_f (solvent A): 0.72.

HR-MS (EI) found: 208.10023, $C_{14}H_{12}N_2$ required 208.10005.

$\delta_H(CDCl_3)$: 2,75–2.83 (2 H, m), 2.97–3.05 (2 H, m), 6.85 (2 H, d, J = 7.8), 7.00 (2 H, t, J = 7.5), 7.03 (2 H, t, J = 7.3), 7.15 (2 H, J = 7.3).

$\delta_C(CDCl_3)$: 31.7, 118.7, 126.7, 127.1, 128.1, 129.6, 155.5

Method B: oxidation of hydrazine 141

To a solution of 5,6,11,12-tetrahydro-dibenzo[c,g][1,2]diazocine **141** (100 mg, 0.476 mmol) in methanol (1.5 ml), titanium (III) chloride (5 µl, prepared by diluting 1 ml of ~10 wt.% solution of $TiCl_3$ in 20-30 wt.% hydrochloric acid with 10 ml of methanol) and hydrobromic acid solution (5 µl, prepared by diluting 1 ml of 33% hydrobromic acid in acetic acid with 10 ml of methanol) were added using a Hamilton syringe at room temperature under nitrogen. Hydrogen peroxide solution (82 µl, 20% in water, 0.43 mmol) was then added and the reaction mixture was stirred at room temperature for 30 min. The volatiles were removed under reduced pressure and the solid residue was purified by column chromatography on silica gel. The appropriate fractions, which were eluted with dichloromethane-hexane (30:70 v/v), were combined and concentrated under reduced pressure to give the *title compound* as a light yellow solid (45 mg, 45%). NMR data are identical to those obtained by method A.

2-Bromo-11,12-dihydrodibenzo[c,g][1,2]diazocine-6-oxide 145

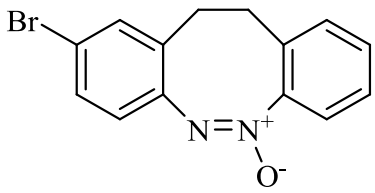

To a solution of azoxybenzene **140** (100 mg, 0.446 mmol) in acetic acid (1.0 ml), bromine (100 µl, 1.95 mmol) was added drop-wise. After the reaction mixture was heated at 50°C for 4 h, stirring was allowed to continue overnight at room temperature. The products were then diluted with cold water (50 ml). Sodium hydrogen sulfite (40% aqueous solution) was added drop-wise until the color changed from brown to pale yellow. The mixture was extracted with dichloromethane (3×30 ml).

The organic layers were combined and washed with water (2×25 ml) and saturated bicarbonate solution (2×25 ml). The organic layer was dried ($MgSO_4$) and concentrated under reduced pressure. The residue was purified by column chromatography on silica gel. The desired product was obtained upon evaporation of appropriate fractions, which were eluted with dichloromethane-hexane (40:60 v/v), as a light brown solid (94.5 mg, 70%).

M.p. 143–146°C (ethanol).

R_f (solvent C): 0.54.

HR-MS (EI) found 302.00508, $C_{14}H_{11}BrN_2O$ required 302.00547.

$\delta_H(CDCl_3)$: 2.84 (1 H, ddd, *J* = 5.9, 9.6, and 14.8), 2.98 (1 H, ddd, *J* = 5.1, 9.9 and 14.8), 3.21 (1 H, ddd, *J* = 5.1, 10.1, and 14.8), 3.36 (1 H, ddd, *J* = 5.9, 9.9, and 15.0), 6.82 (1 H, d, *J* = 8.4), 7.07 (1 H, d, *J* = 7.5), 7.16–7.22 (3 H, m), 7.24–7.26 (2 H, m).

$\delta_C(CDCl_3)$: 30.1, 30.9, 120.5, 121.7, 123.5, 128.1, 129.6, 130.3, 130.6, 131.1, 133.2, 134.1, 145.0, 148.7.

2-Bromo-11,12-dihydrodibenzo[c,g][1,2]diazocine 144

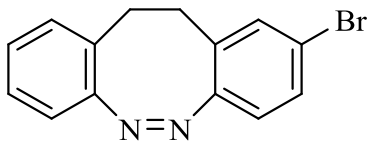

To a solution of bromo azoxybenzene **145** (500 mg, 1.65 mmol) in dry benzene, was added phosphorus trichloride (2.3 ml, 0.026 mmol) slowly and the reaction mixture was heated under reflux for 4 h. The reaction mixture was then evaporated under reduced pressure.

To the dark residue, hydrochloric acid (0.1 *M*) was added, followed by extraction with diethyl ether (2×10 ml). The organic layers were washed with sodium bicarbonate (2×10 ml) twice and the organic layers were dried ($MgSO_4$) and evaporated to dryness under reduced pressure. The residue was purified by column chromatography on silica gel. The desired product was obtained upon evaporation of appropriate fractions, which were eluted with dichloromethane-hexane (30:70 v/v), as a pale yellow solid (421 mg, 89%).

R_f (solvent B): 0.78.

HR-MS (EI) found 286.01081, $C_{14}H_{11}BrN_2$ required 286.01056.

$\delta_H(CDCl_3)$: 2.76 (2 H, m), 2.99 (2 H, br, m), 6.73 (1 H, d, *J* = 8.4), 6.85 (1 H, d, *J* = 7.8), 7.02 (1 H, d, *J* = 7.5), 7.07 (1 H, t, *J* = 7.4), 7.15 (1 H, d, *J* = 1.6), 7.18 (1 H, t, *J* = 7.5), 7.26 (1 H, dd, *J* = 1.7 and 8.4).

$\delta_C(CDCl_3)$: 31.4, 31.6, 118.7, 120.3, 120.6, 127.0, 127.4, 127.5, 129.7, 129.8, 130.4, 132.4, 154.2, 155.3.

2-Cyano-11,12-dihydrodibenzo[c,g][1,2]diazocine-6-oxide 146

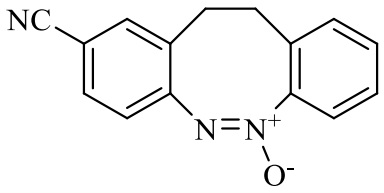

To a solution of 2-bromo-11,12-dihydrodibenzo[c,g][1,2] diazocine-6-oxide **145** (100 mg, 0.330 mmol) in dry *N*,*N*-dimethyl formamide (3.0 ml), copper (I) cyanide (40 mg, 0.447 mmol) was added. After the reaction mixture was heated under reflux overnight, the products were cooled to room temperature, followed by addition of ethylenediamine (10% aqueous solution, 15 ml) the mixture was extracted with dichloromethane (2×20 ml). The organic layer was separated and successively washed with sodium cyanide (10% aqueous solution, 10 ml) and water (3×20 ml). The organic layer was dried ($MgSO_4$) and concentrated under reduced pressure. The residue was purified by column chromatography on silica gel. The desired product was obtained upon evaporation of appropriate fractions, which were eluted with dichloromethane-hexane (60:40 v/v) as a pale yellow solid (62 mg, 75%).

M.p. 178–181°C (ethanol).

R_f (solvent C): 0.32.

HR-MS (EI) found 249.08949, $C_{15}H_{11}N_3O$ required 249.09021.

$\delta_H(CDCl_3)$: 2.94 (1 H, ddd, *J* = 5.3, 10.0, and 14.8), 3.02 (1 H, ddd, *J* = 4.8, 10.1, and 14.8), 3.26 (1 H, ddd, *J* = 4.6, 10.3, and 14.7), 3.40 (1 H, ddd, *J* = 5.2, 10.0, 14.8), 7.05 (1 H, d, *J* = 8.2), 7.07 (1 H, d, *J* = 7.5), 7.17 (1 H, d, *J* = 7.6), 7.22 (1 H, t, *J* = 7.4), 7.25 (1 H, d, *J* = 7.4), 7.35 (1 H, s), 7.43 (1 H, d, *J* = 8.1).

$\delta_C(CDCl_3)$: 29.9, 30.7, 111.0, 118.1, 121.6, 122.8, 128.3, 129.8, 130.7, 131.0, 131.3, 133.8, 134.2, 148.6, 149.5.

5,6,11,12-Tetrahydrodibenzo[c,g][1,2]diazocine-2-carbonitrile 147

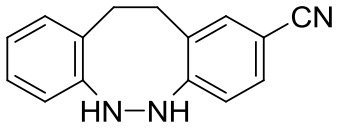

To a solution of 2-cyano-11,12-dihydrodibenzo [c,g][1,2]diazocine-6-oxide **146** (100 mg, 0.401 mmol) in methanol (3.0 ml), hydrazine hydrate (0.5 ml, 16 mmol) and aluminum powder (200 mg) were added. After the reaction mixture was heated under reflux for 24 h, the products were filtered through a thin layer of celite and washed with dichloromethane (10 ml). The filtrate and washing were combined and concentrated under reduced pressure. The residue was purified by column chromatography on silica gel. The desired product was obtained upon evaporation of appropriate fractions, which were eluted with ethyl acetate-hexane (20:80 v/v), as a pale yellow solid (60 mg, 64%).

R_f (solvent D): 0.43.

HR-MS (EI) found 235.11045, $C_{15}H_{13}N_3$ required 235.11095.

$\delta_H(DMSO\text{-}d_6)$: 2.97–2.99 (2 H, m, br), 2.31–2.34 (2 H, m, br), 6.84 (1 H, dt, *J* = 1.0 and 7.3), 6.86 (1 H, d, *J* = 8.2), 6.87 (1 H, d, *J* = 7.3), 7.03 (1 H, dt, *J* = 1.2 and 7.4), 7.08 (1 H, d, *J* = 7.2), 7.26 (1 H, d, *J* = 4.3), 7.43 (1 H, dd, *J* = 1.9 and 8.3), 7.48 (1 H, d, *J* = 1.5), 7.93 (1 H, d, *J* = 4.3).

δ_C(DMSO-d_6): 30.2, 31.3, 101.0, 116.3, 118.4, 120.5, 121.9, 126.7, 130.7, 131.2, 132.5, 132.8, 134.6, 147.8, 153.3.

11,12-Dihydrodibenzo[c,g][1,2]diazocine-2-carbonitrile 148

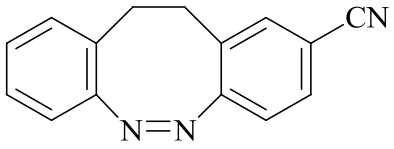

To a solution of 5,6,11,12-tetrahydrodibenzo[c,g][1,2] diazocine-2-carbonitrile **147** (110 mg, 0.468 mmol) in methanol (2 ml), titanium (III) chloride (5 µl, prepared by diluting 1 ml of ~10 wt.% solution of $TiCl_3$ in 20-30 wt.% hydrochloric acid with 10 ml of methanol) and hydrobromic acid solution (5 µl, prepared by diluting 1 ml of 33% hydrobromic acid in acetic acid with 10 ml of methanol) were added using a 10 µl Hamilton syringe at room temperature under nitrogen. After a solution of hydrogen peroxide (100 µl, 20% in water, 0.526 mmol) was added drop-wise at room temperature, the reaction mixture was stirred at room temperature for 15 min. The volatiles were removed under reduced pressure and the solid residue was purified by column chromatography on silica gel. The appropriate fractions, which were eluted with dichloromethane-hexane (55:45 v/v), were combined and concentrated under reduced pressure to give the *title compound* as a light yellow solid (85 mg, 78%).

R_f (solvent D): 0.60.

HR-MS (EI) found 233.09554, $C_{15}H_{11}N_3$ required 233.09530.

$\delta_H(CDCl_3)$: 2.78–2.87 (2 H, m), 3.00–3.07 (2 H, m), 6.87 (1 H, d, *J* = 7.7), 6.92 (1 H, d, *J* = 8.1), 7.01 (1 H, d, *J* = 7.5), 7.08 (1 H, dt, *J* = 1.2 and 7.5), 7.19 (1 H, t, *J* = 7.5), 7.32 (1 H, d, *J* = 1.2), 7.44 (1 H, dd, *J* = 1.4 and 8.0).

$\delta_C(CDCl_3)$: 31.9, 110.8, 118.2, 118.6, 119.5, 127.0, 127.2, 127.8, 129.9, 130.1, 130.7, 133.5, 155.3, 158.

11,12-Dihydrodibenzo[c,g][1,2]diazocine-2-carboxylic acid 149

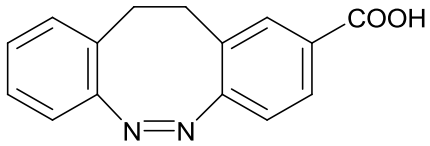

The carbonitrile **148** (100 mg, 0.429 mmol) was placed in a solution of potassium hydroxide (2.65 g) in ethanol (25 ml) and water (10 ml) and heated under reflux for 4 h. The solvents were removed under reduced pressure and the residue was treated with aqueous hydrochloric acid (6 *N*) until the mixture turned acidic (pH 4). The mixture was extracted with ethyl acetate (3×20 ml). The combined organic layers were washed with brine (2×10 ml), dried ($MgSO_4$), and concentrated under reduced pressure to give the crude carboxylic acid which was purified by column chromatography on silica gel. The appropriate fractions, which were eluted with dichloromethane-methanol (95:5 v/v), were combined and concentrated under reduced pressure to give the *title compound* as a light yellow solid (82 mg, 76%).

R_f (solvent E): 0.60.

HR-MS (EI) found 252.08979, $C_{15}H_{12}N_2O_2$ required 252.08988.

$\delta_H(CDCl_3)$: 2.83 (1 H, m), 2.89 (1 H, m), 3.04 (2 H, m), 6.87 (1 H, d, *J* = 7.8), 6.92 (1 H, d, *J* = 8.1), 7.00 (1 H, d, *J* = 7.6), 7.05 (1 H, t, *J* = 7.7), 7.17 (1 H, t, *J* = 7.5), 7.76 (1 H, d, *J* = 1.2), 7.87 (1 H, dd, *J* = 1.3 and 8.1).

$\delta_C(CDCl_3)$: 31.4, 31.5, 118.6, 118.8, 127.0, 127.4, 127.5, 127.6, 128.9, 129.9, 131.8, 155.4, 159.8, 169.9.

(*Z*)-*N*-((2*S*,3*S*)-1,3-Dihydroxybutan-2-yl)-11,12-dihydrodibenzo [c,g][1,2] diazocine-2-carboxamide 151

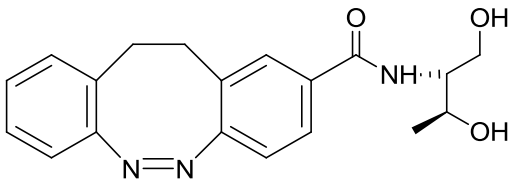

To a solution of 11,12-dihydrodibenzo[c,g][1,2]diazocine-2-carboxylic acid **149** (100 mg, 0.397 mmol) in dry *N*,*N*-dimethyl formamide (2.0 ml), D-threoninol **150** (35 mg, 0.33 mmol), *N*,*N*-dicyclohexylcarbodiimide (82 mg, 0.40 mmol) and *N*-hydroxysuccinamide (46 mg, 0.40 mmol) were added. After the reaction mixture was stirred for 5 h at room temperature under a nitrogen atmosphere, the precipitate was removed by filtration and the filtrate was evaporated under reduced pressure. The oily residue was purified by column chromatography on silica gel. Evaporation of appropriate fractions, which were eluted by dicholoromethane-methanol (95:5 v/v), gave the *title compound* as a pale yellow foam (105 mg, 93% based on D-threoninol).

R_f (solvent F): 0.7.

$[\alpha]_D^{20}$ = -12.8 (c = 0.10, methanol).

HRMS (EI) found 339.1569, $C_{19}H_{21}N_3O_3$ required 339.15829.

δ_H (DMSO-d_6): 1.01 (3 H, t, *J* = 6.1), 2.83-2.86 (2 H, m), 2.88-2.91 (2 H, m), 3.40-3.45 (1 H, m), 3.51-3.55 (1 H, m), 3.81-3.84 (1 H, m), 3.85-3.88 (1 H, m), 4.56-4.61 (2 H, m, br, OH, ex), 6.88 (1 H, d, *J* = 7.8), 6.92 (1 H, d, *J* = 8.1), 7.07 (1 H, t, *J* = 7.3), 7.10 (1 H, d, *J* = 7.2), 7.19 (1 H, dt, *J* = 7.19) (1 H, t, *J* = 7.2), 7.60 (1 H, d, *J* = 2.9), 7.66 (1 H, d, *J* = 8.1), 7.71 (1 H, d, *J* = 8.3, NH, ex).

δ_C (DMSO-d_6): 20.6 and 20.7, 31.2 and 31.4, 57.2, 60.7 and 60.9, 65.3, 118.6 and 118.7, 118.8, 126.5 and 126.6, 127.4, 127.8, 128.1, 128.5 and 128.6, 129.5 and 129.6, 130.4, 133.8, 155.6, 157.5, 166.1.

(*Z*)-*N*-((2*R*,3*S*)-1-(bis(4-methoxyphenyl)(phenyl)methoxy)-3-hydroxybutan-2-yl)-11,12-dihydrodibenzo[c,g][1,2]diazocine-2-carboxamide 152

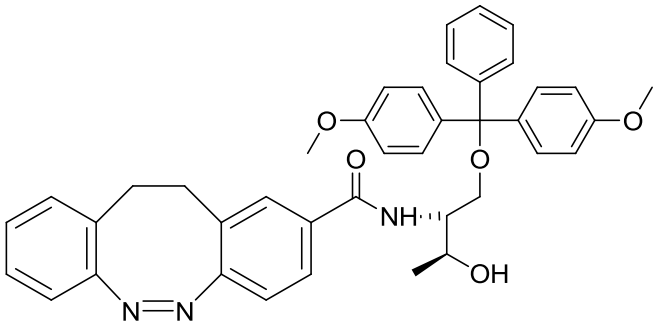

(*Z*)-*N*-((2*S*,3*S*)-1,3-Dihydroxybutan-2-yl)-11,12-dihydrodibenzo[c,g][1,2]diazocine-2-carboxamide **151** (700 mg, 2.06 mmol) was azeotroped with dry toluene (10 ml) and then dry pyridine (2 × 10 ml). To the reaction flask containing **151**, dry pyridine (20 ml) was added and the mixture was azeotroped to a volume of approximately 10 ml. To the solution, 4,4'-dimethoxytrityl chloride (840 mg, 2.47 mmol) was added under nitrogen. The reaction mixture was stirred at room temperature for 1 h and triethylamine (1 ml) was added. The products were poured into saturated aqueous sodium bicarbonate (40 ml) and extracted with dichloromethane (3× 30 ml).

The organic layers were combined, dried ($MgSO_4$) and evaporated to dryness to obtain an oily product. The oily residue was purified by column chromatography on silica gel. The desired product was obtained upon evaporation of appropriate fractions, which were eluted with methanol-dichloromethane (1:99 v/v), as a pale yellow foam (1.133 g, 86 %).

R_f (solvent G): 0.65

LRMS (ESI) found 640.30 ($M\text{-}H^+$), $C_{40}H_{30}N_3O_5$ required 641.29.

δ_H (DMSO-d_6): 0.974 (3 H, d, J = 6.0), 2.85-2.93 (5 H, m). 3.14-3.19 (1 H, m), 3.7 (6 H, d, J = 1.5), 3.9-4.0 (2 H, m), 4.52-4.55 (1 H, d, J = 3), 6.8-7.9 (20 H, m), 8.01-8.03 (1 H, m, NH, ex)

δ_C (DMSO-d_6): 20.7 and 31.1 and 31.4 and 55.3, and 55.4, 55.6 and 55.7 and 63.3 and 63.5, 65.6 and 65.6, 85.5, 113.5 and 118.7 and 118.7, 126.5, 126.9, 127.3, 127.8, 128.1, 128.1, 128.5, 128.6, 129.5, 129.6, 130.0, 130.1, 130.1, 130.3, 133.6 and 133.7, 136.1, 136.2, 136.3, 136.4, 145.5, 155.5, 157.5, 158.4, 166.0 and 166.1.

2-cyanoethyl-phosphodichloridite

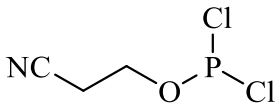

3-Hydroxypropionitrile (54.0 ml, 0.79 mol) and 1,1,1,3,3,3-hexamethyldisilazane (84.0 ml, 0.40 mol) were mixed and heated at 135 ^oC. After 2 h, the products were cooled to room temperature. Dry acetonitrile (500 ml) was added, and this solution was added dropwise to a solution of phosphorus trichloride (75.0 ml, 0.86 mol) in acetonitrile (800 ml) at -40 ^oC over a period of 2h. After the addition was complete, the reaction mixture was allowed to warm up to room temperature over a period of 2 h.

The products were then concentrated under reduced pressure. The viscous liquid was distilled under vacuum (90 ^{o}C/1 mmHg) to give the *title compound* as a colorless liquid (67.1 g, 98%).

δ_p [D_2O insert]: 178.3.

(2-cyanoethyl)-*N,N*-diisopropyl phosphochloridite

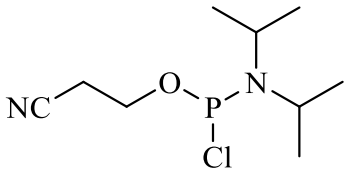

Dry diisopropylamine (40.75 ml, 0.29 mol) in dry diethyl ether (80 ml) was added dropwise to a solution of 2-cyanoethyl phosphodichloridite (25.0 g, 0.145 mol) in dry diethyl ether (350 ml) at -20 ^{o}C over a period of 2h. After the addition was complete, the reaction mixture was allowed to warm up to room temperature and stirring was continued for another 20 h. The products were filtered by cannular filtration and the filtrate was concentrated under reduced pressure. The viscous liquid was then distilled under vacuum (140 ^{o}C/1 mmHg) to give the *title compound* as a colorless liquid (31.4 g, 91%). δ_p [D_2O insert]: 177.7

(2*S*,3*R*)-4-dimethoxytrityl-3-((*Z*)-11,12-dihydrodibenzo[c,g][1,2]diazocine-2-carboxamido)butan-2-yl(2-cyanoethyl) diisopropylphosphoramidite 153

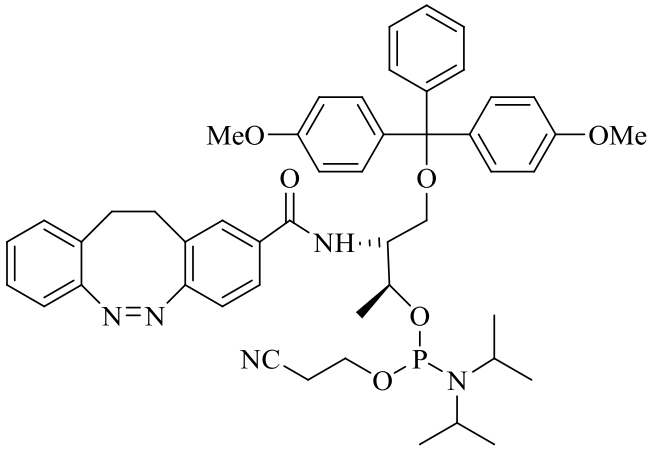

1-*O*-Dimethoxytrityl-3-hydroxybutan-2-yl)-11,12-dihydrodibenzo[c,g][1,2]diazocine-2-carboxamide **152** (572 mg, 0.892 mmol) was azeotroped with dry toluene (2×10 ml) and dissolved in dry tetrahydrofuran (5 ml), followed by addition of dry *N*,*N*-diisopropyl ethylamine (Hünigs base, DIPEA, 0.5 ml, 2.67 mmol), and (2-cyanoethyl)-*N*,*N*-diisopropyl phosphochloridite (314 mg, 1.33 mmol). The reaction mixture was stirred at room temperature for 30 min. Triethylamine was added and the products were evaporated under reduced pressure. The residue was purified by column chromatography on silica gel. The desired product was obtained upon evaporation of appropriate fractions, which were eluted with hexane-dichloromethane-triethylamine (28:70:2 v/v), as a pale yellow color glass (500 mg, 67%).

R_f (solvent H): 0.57

LRMS (ESI) found 876.40 [M^+Cl^-] $C_{49}H_{56}N_5O_6P$ required 876.37.

δ_H ($CDCl_3$): 1.14-1.28 (15 H, m), 2.30 (1 H, s), 2.56-2.57 (2 H, m), 2.66-2.67 (2 H, m), 2.80-2.85 (2 H, s), 3.01 (2 H, s), 3.18 -3.27 (2 H, m), 3.50 (3 H, s), 3.78 (6 H, s), 4.32-4.44 (2 H, m), 6.40-6.46 (1 H, m, NH ex), 6.79-7.50 (20 H, m).

δ_C($CDCl_3$): 10.9, 11.4, 14.1, 18.7, 19.7, 20.2, 20.2, 20.4, 20.7, 22.6, 24.3, 24.4, 24.5, 24.6, 24.7, 25.2, 29.0, 29.7, 31.4, 31.5, 31.6, 31.7, 34.5, 34.6, 36.0, 43.0, 43.1, 43.2, 46.1, 53.4, 54.4 and 54.48, 54.8, 55.1, 55.2, 57.7, 57.8, 58.1, 58.2, 62.7, 62.9, 69.0, 69.1, 86.1, 86.2, 113.1, 113.2, 117.6, 117.7, 118.6, 118.9, 125.0, 125.1, 125.2, 126.7, 126.8, 126.9, 127.3, 127.4, 127.5, 127.8, 127.9, 128.1, 128.2, 128.8, 128.9, 129.0, 129.1, 129.8, 130.0, 130.1, 133.2, 133.3, 135.9, 136.0, 144.7, 155.3, 155.4, 157.7, 158.4, 166.2.

δ_p [$CDCl_3$]: 148.19 and 148.22

4,4'-(ethane-1,2-diyl)dibenzonitrile 158

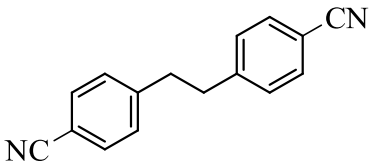

To a solution of anhydrous manganese chloride (202 mg, 1.6 mmol) in dry tetrahydrofuran (3 ml), naphthalene (45 mg, 0.33 mmol) and lithium metal (22.2 mg, 3.2 mmol) were added. The reaction mixture was stirred at room temperature for 1 h followed by addition of 4-(bromomethyl)benzonitrile **157** (250 mg, 1.275 mmol). Stirring was continued for 20 min at room temperature and then hydrochloric acid (3 *N*) was added until evolution of fume stopped. The products were extracted with ethyl acetate (2×15 ml). The organic layer was washed with saturated sodium bicarbonate (2×15 ml), dried ($MgSO_4$) and purified by column chromatography on silica gel.

The appropriate fractions, which were eluted with hexane-ethyl acetate (90:10 v/v), were combined and concentrated under reduced pressure to give the *title compound* as a light yellow solid (65 mg, 44 %).

R_f (solvent B): 0.63

HRMS (EI): found 232.10005, $C_{12}H_{12}N_2$ required 232.1000

δ_H ($CDCl_3$): 3.01 (4 H, s), 7.23 (4 H, d, J = 8.1), 7.58 (4 H, d, J = 8.4)

δ_C ($CDCl_3$): 37.2, 110.3, 118.8, 129.1, 129.2, 130.0, 132.3, 146.0

4,4'-(ethane-1,2-diyl)bis(3-nitrobenzonitrile) 159

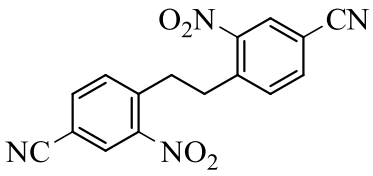

To a solution of 4,4'- (ethane-1,2-diyl) dibenzonitrile **158** (115 mg, 0.50 mmol) in sulfuric acid (2 ml), conc. nitric acid (2 ml) was added slowly at 0 °C. The reaction mixture was stirred at 0 °C for 1 h, followed by addition of cold water (10 ml) and then extracted with dichloromethane (2× 10 ml). The organic layers were combined, washed with saturated sodium bicarbonate, dried ($MgSO_4$), concentrated under reduced pressure, and purified by column chromatography on silica gel. The appropriate fractions, which were eluted with hexane-dichloromethane (60:40, v/v), were combined and concentrated under reduced pressure to give the *title compound* as a light yellow solid (115 mg, 72 %).

R_f (solvent B): 0.70

LRMS (FAB): found 391.0 [M + 3 Na^+] $C_{16}H_{10}N_4O_4$ required 391.0

δ_H ($CDCl_3$): 3.34 (2 H, s), 7.64 (1 H, d, J = 8.1), 7.81-7.90 (1 H, dd, $J_{1,2}$ = 1.5, $J_{1,3}$ = 8.1), 8.31 (1 H, s).

δ_C ($CDCl_3$): 34.3, 112.6, 116.7, 117.5, 128.8, 133.6, 136.2, 140.2.

5,6,11,12-tetrahydrodibenzo[c,g][1,2]diazocine-3,8-dicarbonitrile 160

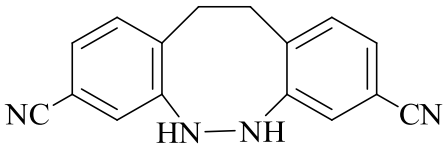

To a solution of triethylamine (2.1 ml, 0.015 mol) in ethanol (7 ml) was added formic acid (0.54 ml, 0.014 mol) and the final pH of the solution was adjusted to 7. To this solution was added 4,4'- (ethane-1,2-diyl)bis(3-nitrobenzonitrile) **159** (100 mg, 0.310 mmol) followed by zinc powder (200 mg, 3.05 mmol) over a period of 15 min under vigorous stirring. The reaction was stirred at room temperature for 5 h. The products were filtered, concentrated under reduced pressure. To the residue, saturated aqueous sodium bicarbonate (20 ml) was added and extracted with dichloromethane (2×25 ml). The organic layers were combined, dried ($MgSO_4$) and concentrated under reduced pressure. The residue was purified by column chromatography on silica gel. The appropriate fractions, which were eluted with dichloromethane-hexane (50:50 v/v), were pooled and concentrated under reduced pressure to give *title compound* as a pale yellow solid (60 mg, 74.2 %).

R_f (solvent C): 0.60

LRMS (EI): found 260.0 $C_{16}H_{12}N$**4** required 260.0

δ_H (DMSO-d_6): 3.11 (2 H, s), 7.18 (1 H, d, J = 1.5), 7.23- 7.31 (2 H, m), 7.67 (1 H, s, NH, ex).

δ_C (DMSO-d_6): 29.1, 109.4, 116.7, 119.6, 120.1, 130.3, 130.6, 147.6.

(Z)-11,12-dihydrodibenzo[c,g][1,2]diazocine-3,8-dicarbonitrile 161

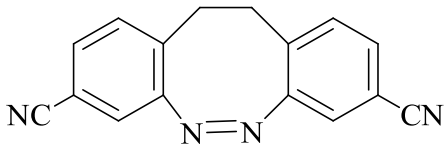

To a solution of 5,6,11,12-tetrahydrodibenzo[c,g][1,2]diazocine-3,8-dicarbonitrile **160** (50 mg, 0.192 mmol) in methanol (3 ml), titanium (III) chloride (25 µl, prepared by diluting 1 ml of ~10 wt.% solution of $TiCl_3$ in 20-30 wt.% hydrochloric acid with 10 ml of methanol) and hydrobromic acid solution (25 µl, prepared by diluting 1 ml of 33% hydrobromic acid in acetic acid with 10 ml of methanol) were added using a 50 µl Hamilton syringe at room temperature under nitrogen. After a solution of hydrogen peroxide (100 µl, 20% in water, 0.526 mmol) was added drop-wise at room temperature, the reaction mixture was stirred at room temperature for 15 min. The volatiles were removed under reduced pressure and the solid residue was purified by column chromatography on silica gel. The appropriate fractions, which were eluted with dichloromethane-hexane (30:70 v/v), were combined and concentrated under reduced pressure to give the *title compound* as a light yellow solid (45 mg, 90%).

R_f (solvent B): 0.65

HRMS (EI) found 258.09055, $C_{16}H_{10}N_4$ required 258.0905

δ_H ($CDCl_3$): 2.85- 3.12 (4 H, m), 7.13- 7.18 (4 H, m), 7.36-7.40 (2 H, dd, $J_{1,2}$ = 1.5, $J_{1,3}$ = 7.8).

δ_C ($CDCl_3$) 31.5, 111.6, 117.5, 121.0, 122.4, 130.8, 131.1, 132.9.

(Z)-11,12-dihydrodibenzo[c,g][1,2]diazocine-3,8-dicarboxylic acid 162

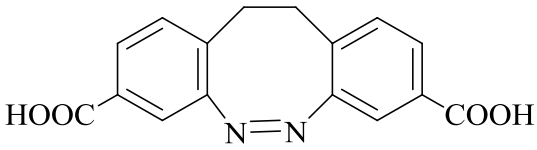

Dicarbonitrile **161** (30 mg, 0.115 mmol) was placed in a solution of potassium hydroxide (805 mg) in ethanol (7 ml) and water (3 ml) and heated under reflux for 4 h. Ethanol was removed under reduced pressure and the residue was treated with aqueous hydrochloric acid (6 *N*) until the mixture turned acidic (pH 4). The mixture was extracted with ethyl acetate (2×10 ml). The combined organic layers were washed with brine (2×15 ml), dried ($MgSO_4$), and concentrated under reduced pressure to give the crude carboxylic acid which was purified by column chromatography on silica gel. The appropriate fractions, which were eluted with dichloromethane-methanol (94:6 v/v), were combined and concentrated under reduced pressure to give the *title compound* as a light yellow solid (25mg, 73%).

R_f (solvent G): 0.52

δ_H(MeOD): 2.93-3.00 (2 H, m), 7.12 (1 H, d, J = 3.9), 7.43 (1 H, s), 7.66 (1 H, d, J = 3.9)

δ_C (MeOD): 30.8, 119.3, 127.9, 128.4, 129.5, 131.0, 132.0, 154.9.

Synthesis of 4,4'-(ethane-1,2-diyl)dibenzonitrile 158

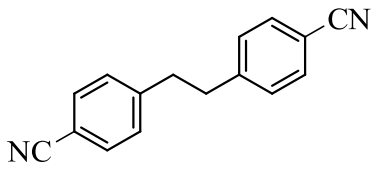

To a suspension of iron particles (200 mg) in water (5 ml), copper chloride (20 mg, 0.20 mmol) was added and stirred at room temperature for 10 min. To the reaction mixture was added 4-(bromomethyl) benzonitrile **157** (350 mg, 1.785 mmol). The reaction mixture was stirred at room temperature for 12 h. The products were filtered, and the filtrate was extracted with dichloromethane (2×10 ml). The organic layers were combined, dried ($MgSO_4$), evaporated to dryness under reduced pressure, and purified by column chromatography on silica gel. The appropriate fractions, which were eluted with dichloromethane were combined and concentrated under reduced pressure to give the *title compound* as a light yellow solid (150 mg, 72%).

R_f (solvent B): 0.63

HRMS (EI): found 232.10005, $C_{12}H_{12}N_2$ required 232.1000

δ_H ($CDCl_3$): 3.01 (4 H, s), 7.23 (4 H, d, J = 8.1), 7.58 (4 H, d, J = 8.4)

δ_C ($CDCl_3$): 37.2, 110.3, 118.8, 129.1, 129.2, 130.0, 132.3, 146.0

Preparation of Iron nanoparticles

To a solution of ferric chloride (615 mg, 3.78 mmol) in ethanol (15 ml) and water (5 ml) was added sodium dodecyl sulfate (200 mg), sodium borohydride (400 mg) in ethanol (10 ml) and deionised water (5 ml). The reaction mixture was stirred for 1-2 h after the appearance of black precipitate. The products were filtered and the solid was washed with ethanol (20 ml) and acetone (20 ml) to obtain the iron nanoparticles.

Synthesis of cyclic azobenzene incorporated poly(2-hydroxyethyl) methacrylate polymer 164

Poly (2-hydroxyethyl)methacrylate **163** (26.2 mg, 0.0013 mmol) and cyclic azobenzene carboxylic acid **149** (50 mg, 0.2 mmol) were dissolved in dry chloroform (5 ml), followed by addition of EDC (42.2 mg, 0.22 mmol) and DMAP (5 mg). The reaction was allowed to proceed for 24 h, and the products were extracted with water (10 ml) and chloroform (10 ml). The chloroform layer was dried ($MgSO_4$) and concentrated to dryness to obtain pale yellow solid.

References

1. Roger, L. P. A.; Knowler, J. T.; Leader, D. P. *The Biochemistry of Nucleic Acids,* Chapman and Hall. UK, **1992**, Ed. 11th, pp 1-3.

2. Dahm, R. *Hum. Genet*. **2008**, *122*, 565-581.

3. Garrett, H. R.; Grisham, M. G. *Biochemistry*, Mary Finch, Boston, USA, **2008**, Ed. 4th, pp 291-303.

4. Bloomfield, V. A.; Crothers, D. M.; Tinoco, I. *Nucleic Acids; Structures, Properties, and Function*. University Science Books, Sausalito, CA, **2000**, pp 1-2.

5. Ghosh, A.; Bansal, M. *Acta Crystallogr. D Biol. Crystallogr.* **2003**, *59*, 620-626.

6. Mauseth, J. D. *Botany: An Introduction to Plant Biology*, Jones and Barlett Publishers, UK, **2009**, Ed. 4th, pp 433-435.

7. Mayer, G.; Heckel, A. *Angew. Chem. Int. Ed*. **2006**, *45*, 4900-4921.

8. Edelson, R. L. *Sci. Am*. **1988**, *259*, 50-57.

9. Harper, S. M.; Neil, C. L.; Gardner, H. K. *Science* **2003**, 301, 1541-1544.

10. Carell, T.; Burgdorf, C. L.; Kundu, M. L.; Cichon, M. *Curr. Opin. Chem. Biol*. **2001**, *5*, 491-498.

11. Kaplan, J. H.; Forbush III, B.; Hoffman, F. J. *Biochemistry* **1978**, *17*, 1929-1935.

12. Givens, S. R.; Weber, W. F. J.; Jung, H. A.; Park, C. H. *Methods Enzymol*. **1998**, *291*, 1-29.

13. Martinek, K.; Varfolomeyev, S. D.; Berezin, V. I. *Eur. J. Biochem*. **1971**, *19*, 242-249.

14. Engels, J.; Schlaeger, E-J. *J. Med. Chem*. **1977**, *20*, 907-911.

15. Pillai, R. N. V. *Synthesis* **1980**, 1-26.

16. Pelliccioli, P. A.; Wirz, J. *Photochem. Photobiol. Sci.* **2002**, *1*, 441-458.

17. Corrie, T. E. J.; Barth, A.; Munasinghe, N. R. V.; Trentham, R. D.; Hutter, C. M. *J. Am. Chem. Soc*. **2003**, *125*, 8546-8554.

18. Adams, S. R.; Kao, J. Y. P. J.; Tsien, Y. R. *J. Am. Chem. Soc*. **1989**, *111*, 7957-7968.

19. Momotake, A.; Lindegger, N.; Niggli, E.; Barsotti, R. J.; Ellis-Davies, R. C. G. *Nat. Methods* **2006**, *3*, 35-40.

20. Walbert, S.; Pfleiderer, W.; Steiner, E. U. *Helv. Chim. Acta*. **2001**, *84*, 1601-1611.

21. Hagen, V.; Frings, S.; Wiesner, B.; Helm, S.; kaupp, U. B.; Bendig, J. *ChemBioChem*. **2003**, *4*, 434-442.

22. Fedoryak, O. D.; Dore, T. M. *Org.Lett.* **2002**, *4*, 3419-3422.

23. Conrad II, P. G.; Givens, S. R.; Weber, F. J.; Kandler, K. *Org. Lett*. **2000**, *2*, 1545-1547.

24. Lukeman, M.; Scaiano, C. J. *J. Am. Chem. Soc*. **2005**, *127*, 7698-7699.

25. i) Munck, S.; Bedner, P.; Bottaro, T.; Harz, H. *Eur. J. Neurosci.* **2004**, *19* 791-797. ii) Ming, G. L.; Song, H. J.; Berninger, B.; Holt, C. E.; Tessier-lavigna, M.; Poo, M. M, *Neuron* **1997**, *19*, 1225-1235.

26. Pollock, J.; Crawford, J. H.; Wootton, F. J.; Corrie, T. E. J.; Scott, H. R. *Neurosci. Lett.* **2003**, *338*, 143-146.

27. Hagen, V.; Dzeja, C.; Frings, S.; Bendig, J.; Krause, E.; Kaupp, U. B. *Biochemistry* **1996**, *35*, 7762-7771.

28. Salerno, C. P.; Magde, D.; Patron, A. P. *J. Org. Chem.* **2000**, *65*, 3971-3981.

29. Salerno, C. P.; Resat, M.; Magde, D.; Kraut, J. *J. Am. Chem. Soc.* **1997**, *119*, 3403-3404.

30. Allin, C.; Gerwert, K. *Biochemistry* **2001**, *40*, 3037-3046.

31. Schönleber, R. O.; Bendig, J.; Hagen, V.; Giese, B. *Bioorg. Med. Chem.* **2002**, *10*, 97-101.

32. Kim, J-S.; Raines, T. R. *Protein Sci*. **1993**, *2*, 348-356.

33. Hiraoka, T.; Hamachi, I. *Bioorg. Med. Chem. Lett*. **2003**, *13*, 13-15.

34. Wu, L.; Wang, Y.; Wu, J.; Lv, C.; Wang, J.; Tang, X. *Nucleic Acids Res*. **2013**, *41*, 677-686.

35. Deiters, A. *Curr. Opin. Chem. Biol*. **2009**, *13*, 678-686.

36. Monroe, W. T.; McQuain, M. M.; Chang, M. S.; Alexander, J. S.; Haselton, F. R. *J. Biol. Chem*. **1999**, *274*, 20895-20900.

37. Ando, H.; Furuta, T.; Tsien, R. Y.; Okamoto, H. *Nat. Gene*. **2001**, *28*, 317-325.

38. Shah, S.; Rangarajan, S.; Friedman, S. H. *Angew. Chem. Int. Ed*. **2005**, *44*, 1328-1332.

39. Mikat, V.; Heckal, A. *RNA* **2007**, *13*, 2341-2347.

40. Chaulk, S. G.; MacMillan, A. M. *Nucleic Acids Res*. **1998**, *26*, 3173-3178.

41. Kröck, L.; Heckel, A. *Angew. Chem. Int. Ed*. **2005**, *44*, 471-473.

42. Heckel, A.; Mayer, G. *J. Am. Chem. Soc*. **2005**, *127*, 822-823.

43. Wenter, P.; Furtig, B.; Hainard, A.; Schwalbe, H.; Pitsch, S. *Angew. Chem. Int. Ed*. **2005**, *44*, 2600-2603.

44. Hobartner, C.; Silverman, S. K. *Angew. Chem. Int. Ed*. **2005**, *44*, 7305-7309.

45. Xang, X. J.; Dmocchowski, I. J. *Org Lett*. **2005**, *7*, 279-282.

46. Ting, R.; Lermer, L.; Perrin, D. M. *J. Am. Chem. Soc*. **2005**, *126*, 12720-12721.

47. Okamoto, A.; Tanabe, K.; Inasaki, T.; Saito, I. *Angew. Chem. Int. Ed*. **2003**, *42*, 2502-2504.

48. Summerton, J.; Weller, D. *Antisense Nucleic Acids Drug Dev*. **1997**, *7*, 187-195.

49. Ouyang, X.; Shestopalov, L. A.; Sinha, S.; Zheng, G.; Pitt, C. L. W.; Li, W-H.; Olson, A. J.; Chen, J. K. *J. Am. Chem. Soc*. **2009**, *131*, 13255-13269.

50. Wang, Y.; Wu, L.; Wang, P.; Lv, C.; Yang, Z.; Tang, X. *Nucleic Acids Res*. **2012**, *40*, 11155-11162.

51. Dieters, A.; Garne, R. A.; Lusic, H.; Govan, J. M.; Dush, M.; Nascone-Yoder, N. M.; Yoder, J. A. *J. Am. Chem. Soc*. **2010**, *132*, 15644-15650.

52. Velasco, D.; Garcia-Amorós, J. *Beilstein J. Org. Chem*. **2012**, *8*, 1003-1017.

53. Krongauz, V.; Weiss, V.; Berkovic, G. *Chem. Rev*. **2000**, *100*, 1741-1753.

54. Irie, M. *Chem, Rev*. **2000**, *100*, 1.

55. Hug, H. D.; O'Donnell.; Hunter, K. J. *Photochem Photobiol*. **1980**, *32*, 841-848.

56. Willner, I.; Zahany, E.; Rubin, S. *J. Chem. Soc. Chem. Commun*. **1993**, 1753-1755.

57. Yokoyama, Y. *Chem. Rev*. **2000**, *100*, 1717-1739.

58. Willner, I.; Rubin, S.; Wonner, J.; Effenberger, F.; Bäuerle, P. *J. Am. Chem. Soc*. **1992**, *114*, 3150-3151.

59. Irie, M. *Chem. Rev*. **2000**, *100*, 1685-1716.

60. Feringa, L.B.; Deldenvan, A. R.; Koumura, N.; Geertsema, M. E. *Chem. Rev*. **2000**, *100*, 1789-1816.

61. Joshi, K. D.; Mitchell, J. M.; Bruce, D.; Lough, J. A.; Yan, H. *Tetrahedron* **2012**, 68, 8670-8676.

62. Griffiths, J. *Chem. Rev. Soc*. **1972**, *1*, 481-493.

63. Woolley, G. A.; Beharry, A. A. *Chem. Rev. Soc*. **2011**, *40*, 4422-4437.

64. Hartley, G. S. *Nature* **1937**, *140*, 281.

65. Delaire, J. A.; Nakatani, K. *Chem. Rev*. **2000**, *100*, 1817-1846.

66. Beharry, A. A.; Woolley, G. A. *Chem. Soc. Rev*. **2011**, *40*, 4422-4437.

67. Tang, X. J.; Dmochowski, I. J. *Mol. BioSyst*. **2007**, *3*, 100-110.

68. Asanuma, H.; Liang, X.; Nishioka, H.; Matsunaga, D.; Liu, M.; Komiyama, M. *Nat. Protoc.* **2007**, *2*, 203-212.

69. Mayer, G.; Heckel, A. *Angew. Chem. Int. Ed*. **2006**, *45*, 4900-4921.

70. Young, D. D.; Deiters, A. *Org. Biomol. Chem*. **2007**, *5*, 999-1005.

71. Rau, H. *Angew. Chem. Int. Ed*. **1973**, *12*, 224–235.

72. Dias, A. R.; Minas da Piedade, M. E.; Martinho Simoes, J. A.; Simoni, J. A.; Teixeira, C.; Diogo, H. P.; Meng-Yan, Y.; Pilcher, G. *J. Chem. Thermodyn*. **1992**, *24*, 439–447.

73. i) Fliegl, H.; Kohn, A.; Hattig, C.; Ahlrichs, R. *J. Am. Chem. Soc*. **2003**, *125*, 9821–9827; ii) Sudesh kumar, G. Neckers, C. D. *Chem. Rev*. **1989**, *89*, 1915-1925.

74. Tsuji, T.; Takeuchi, H.; Egawa, T.; Konaka, S. *J. Am. Chem. Soc*. **2001**, *123*, 6381–6387.

75. (i) Paudler, W. W.; Zeiler, A. G. *J. Org. Chem*. **1969**, *34*, 3237-3239. (ii) Siewertsen, R.; Neumann, H.; Buchheim-Stehn, B.; Herges, R.; Nather, C.; Renth, F.; Temps, F. *J. Am. Chem. Soc*. **2009**, *131*, 15594-15595.

76. Mitchell, G. R.; King, N. R. *Macromol. Symp*. **1999**, *137*, 155-165.

77. Hirano, M.; Yakabe, S.; Chikamori, H.; Clark, J. H.; Morimoto, T. J. *Chem. Soc*. **1998**, 770-771.

78. Gilbert, A. M.; Failli, A.; Shumsky, J.; Yang, Y.; Severin, A.; Singh, G.; Hu, W.; Keeney, D.; Petersen, P. J.; Katz, A. H. *J. Med. Chem*. **2006**, *49*, 6027–6036.

79. Noureldin, N. A.; Bellegarde, J. W. *Synthesis* **1999**, 939-942.

80. Brenzovich, W. E.; Houk, R. J. T.; Malubay, S. M. A.; Miranda, J. O.; Ross, K. M.; Abelt, C. J. *Dyes Pigments* **2002**, *52*, 101-114.

81. Len, C.; Hamon, F.; Djedaini-P, F.; Barbot, F. *Tetrahedron* **2009**, *65*, 10105-10123.

82. Khan, A.; Hecht, S. *Chem. - Eur. J*. **2006**, *12*, 4764-4774.

83. Badjic, J. D.; Kostic, N. M. J. *Mater. Chem*. **2001**, *11*, 408-418.

84. Dong, S. L.; Loweneck, M.; Schrader, T. E.; Schreier,W. J.; Zinth,W.; Moroder, L.; Renner, C. *Chem.- Eur. J*. **2006**, *12*, 1114-1120.

85. Lee, M. H.; Cho, B. K.; Yoon, J.; Kim, J. S. *Org. Lett*. **2007**, *9*, 4515-4518.

86. (i) Tsai, W. H.; Shiao, Y. J.; Lin, S. J.; Chiou, W. F.; Lin, L. C.; Yang, T. H.; Teng, C. M.; Wu, T. S.; Yang, L. M. *Bioorg. Med. Chem. Lett*. **2006**, *16*, 4440-4043; (ii) Lin, S. J.; Shiao, Y. J.; Chi, C.W.; Yang, L. M. *Bioorg. Med. Chem. Lett*. **2004**, *14*, 1173-1176.

87. Yamamura, M.; Kano, N.; Kawashima, T. *Inorg. Chem.* **2006**, *45*, 6497-6407.

88. Sanz, R.; Escribano, J.; Fernandez, Y.; Aguado, R.; Pedrosa, M. R.; Arnaiz, F. J. *Synlett* **2005**, 1389-1392.

89. Baigl, D.; Diguet, A.; Mani, K. N.; Geoffroy, M.; Sollogoub, M. *Chem. Eur. J*. **2010**, *16*, 11890-11896.

90. Baigl, D.; Estevez-Torres, A.; Crozatier, C.; Diguet, A.; Hara, T.; Saito, H.; Yoshikawa, K. *Proc. Natl. Acad. Sci. USA* **2009**, *106*, 12219-12223.

91. Nakatani, K.; Hayashi, G.; Hagihara, M. *Chem. Eur. J.* **2009**, *15*, 424-432.

92. Peng, T.; Dohno C.; Nakatani, K. *Angew. Chem. Int. Ed*. **2006**, *45*, 5623-5626.

93. Dohno, C.; Uno, S. N.; Nakatani, K.; *J. Am. Chem. Soc*. **2007**, *129*, 11898-11899.

94. Komiyama, M.; Asanuma, H.; Liang, X.; Nishioka, H.; Matsungs, D.; Liu, M. *Nat. Protoc.* **2007**, *2*, 203-212.

95. Liang, X.; Asanuma, H.; Kashida, H.; Takasu, A.; Sakamoto, T.; Kawai, G.; Komiyama, M. *J. Am. Chem. Soc*. **2003**, *125*, 16408-16415.

96. Liu, M.; Asanuma, H.; Komiyama, M. *J.Am. Chem. Soc*. **2006**, *128*, 1009-1015

97. Harbour, J. R.; Hair, M. L. *J. Phys. Chem*. **1979**, *83*, 648-652.

98. Rau, H.; Greiner, G.; Gauglitz, G.; Meier, H. *J. Phys. Chem*. **1990**, *94*, 6523.

99. Muri, M.; Schuermann, K. C.; De Cola, L.; Mayor, M. *Eur. J.Org. Chem*. **2009**, *15* 2562-2575.

100. Liu, L.; Yuan, S.; Fang, W.-H.; Zhang, Y. *J. Phys. Chem. A*. **2011**, *115*, 10027-10034.

101. Boeckmann, M.; Doltsinis, N. L.; Marx, D. *Angew. Chem., Int. Ed*. **2010**, *49*, 3382-3384.

102. Woolley, G. A.; Beharry, A. A.; Wong, L.; Tropepe, V. *Angew. Chem. Int. Ed*. **2011**, *50*, 1325-1327.

103. (i) Whitford, D. *Proteins: Structure and Function*, John Wiley and Sons Ltd, West Sussex, **2005**, pp 1-9. (ii) Bhagavan, N. V. *Medical Biochemistry*, Academic Press, California, USA, **2002**, Ed. 4th, pp 51-64.

104. Woolley, G. A.; Samanta, S.; Qin, C.; Lough, J. A. *Angew. Chen. Int. Ed*. **2012**, *51*, 6452-6455.

105. Emoto, A.; Uchida, E.; Fukuda, T. *Polymers* **2012**, *4*, 150-186.

106. Hillermeier, K. *Text. Res. J.* **1984**, *54*, 575-581.

107. Barrett, J. C.; Yager, G. K. *Polymer Nanostructures and their Applications*, American Scientific Publishers, **2006**, Vol. 1, pp 1-38.

108. Ambrosio, A.; Girardo, S.; Camposeo, A.; Pisignanao.; Maddalena, P. *Appl. Phys. Lett*. **2013**, *102*, 093102 (1-4).

109. Eisenbach, C. D. *Polymer* **1980**, *21*, 175-1179.

110. Ikeda, T.; Yu, Haifeng. *Adv. Mater*. **2011**, *23*, 2149-2180.

111. Hu, X.; Zhang, P. J.; Zhao, X. Y.; Li, L.; Tam, K. C.; Gam, L. H, *Polymers* **2004**, *45*, 6219-6225.

112. Gowda, S.; Gowda, D. C. *Synthesis* **2002**, 460-462.

113. Srinivasa, G. R.; Abiraj, K.; Gowda, D. C. *Tetrahedron Lett*. **2003**, *44*, 5835-5837.

114. Hwu, J. R.; Yau, C. S.; Tsay, S.-C.; Ho, T.-I. *Tetrahedron Lett*. **1997**, *38*, 9001-9004.

115. Gago, S.; Neves, P.; Monteiro, B.; Pessego, M.; Lopes, A. D.; Valente, A. A.; Paz, F. A. A.; Pillinger, M.; Moreira, J.; Silva, C. M.; Goncalves, I. S. *Eur. J. Inorg. Chem*. **2009**, 4528-4537.

116. Sanz, R.; Escribano, J.; Fern_andez, Y.; Aguado, R.; Pedrosa, M. R.; Arnaiz, F. J. *Synlett.* **2005**, 1389-1392.

117. Vozza, J. F. J. *Org. Chem*. **1969**, *34*, 3219-3220.

118. Ejsmont, K.; Dom_anski, A. A.; Kyzio1, J. B.; Zaleski, J. *Acta Crystallogr*. *A*. **2004**, C60, 368-370.

119. Spek, A. L. *Acta Crystallogr. D. Biol. Crystallogr*. **2009**, *65*, 148-155.

120. Friedman, L.; Shechter, H. *J. Org. Chem*. **1961**, *26*, 2522-2524.

121. Nanjundaswamy, H. M.; Pasha, M. A. *Synth. Commun*. **2005**, *35*, 2163-2168.

122. Drug, E.; Gozin, M. *J. Am. Chem. Soc*. **2007**, *129*, 13784-13785.

123. Merrified, R. B. *J. Am. Chem. Soc*. **1963**, *85*, 2149-2154.

124. Taghipoor, S.; Shekarriz, M.; Adib, M.; Biabani, T. J. *Chem. Res*. **2012**, 29-30.

125. Otwinowski, Z.; Minor, W. *Methods in Enzymology: Macromolecular Crystallography, Part A*; Carter, C. W., Sweet, R. M., Eds.; Academic: London, **1997**; Vol. *276*, pp 307-326.

126. Blessing, R. H. *Acta Crystallogr. A*. **1995**, *51*, 33-38.

127. Sheldrick, G. M. *Acta Crystallogr. A*. **2008**, *64*, 112-122.